

*Thesis
In Locked Case*

The composition and development of palag
AC SU no.M69 15565



Morgenstein, Maury
SOEST Library

THESIS

*OTO
Mor
Com
ms*

The Composition and Development of
Palagonite in Deep-sea Sediments
from the Atlantic and Pacific Oceans

by

Maury Morgenstein

B.A., Queens College, 1967

Abstract of Thesis

Submitted in partial fulfillment of the require-
ments for the degree of Masters of Science in
Geology in the Graduate School of Syracuse University,
August, 1969.

Approved _____

Date _____

ABSTRACT

During the alteration of basaltic glass to palagonite, Na, Al, Mg, Si, Mn and Ca are lost; K, Ti, Fe and O are added in the alteration product. The major differences between oceanic and terrigenous palagonites is the behavior of potassium. Potassium is usually depleted in the alteration material during terrigenous weathering, whereas it is enriched during the oceanic weathering (halmyrolysis). Palagonite commonly contains 2 to 3 times more H_2O^- and about 4 to 10 times more H_2O^+ than sideromelane (basaltic glass). The greater the hydration in palagonite the greater the degree of authigenic mineralization. Authigenic minerals present in deep-sea sediments which are derived from palagonite solution are: limonite, goethite, smectites, manganite, harmotome, phillipsite, intermediate zeolites of the phillipsite group and clinoptilolite.

Sea-water enters the basaltic glass through hair-channels which average 50 μ in length. As hair-channels become more numerous with increased hydration they form a 50 μ thick immobile product layer (solid solution border). The solid solution border eventually hydrates to a palagonite band which is 50 μ thick. Palagonitization proceeds as the hair-channels extend into the sideromelane. Most palagonite forms during diagenesis, although there is some syngenetic palagonitization. Syngenetic palagonitization occurs at high temperatures at the

time that volcanic exhalates enter the marine environment. Diagenetic palagonitization occurs after deposition of the original volcanic glasses and basalts. The configuration of the syngenetic palagonite is different in that it does not have the typical 50 u bands. Sea-water diffusion into mafic volcanic glass does not slow down as the hydrated region (palagonite) becomes thicker. Friedman and others (1966) diffusion constant for a quadratic rate formula can not be applied to palagonite formation. The rate formula used by Moore (1966) is also not applicable because it uses Friedman's diffusion constant. Rate formulas for palagonite formation were derived here by studying the geometry of the hair-channel sector, the solid solution border and the palagonite bands. The average total rate formula for palagonitization is:

$\sum R_p = (N-2)Q/T$ where: R_p = the rate of palagonitization, N=the number of palagonite bands, Q=the thickness of each band, and T=the age in years. For the first 50 u the rate formula is: $R_p = NQ/3T$. For the second and subsequent palagonite bands the rate formula is: $R_p = NQ/T$. When dealing with time in millions of years the expression $\sum R_p = (N-2)Q/T$ approaches the linear rate $R_p = NQ/T$. The rate formula for sideromelane hydration is:

$\sum R_h = (N+2)Q/T$, where R_h = the total rate of hydration. During diagenesis the first 50 u of oceanic palagonite form at an average rate of 0.97 ± 0.19 u/1,000 years. The first 50 u of fresh water palagonite to form during diagenesis does so at the rate of 2.62 u/1,000 years. The average rate of

palagonitization after the first 50 u have formed is:

2.91 ± 0.58 u/1,000 years. For fresh water palagonite the rate is 7.26 u/1,000 years. Manganese nodules dated by the palagonite hydration method show that the rate of manganese accretion decreases with time. An iron catalytic agent supplied through palagonitization is responsible for the accretion of an appreciable amount of submarine manganese nodules. The rate of manganese accretion observed is between 1.7 and 8.7 u/10³ years. This rate is dependent upon the rate of an iron catalyst evolution into the sediment and therefore, is dependent on the rate of palagonitization.

Diagenetic and syngenetic fracturing exist in sideromelane. Fracture assemblages produced are mostly tensile displacements which are similar to those described by Lachenbruch (1962) for mud cracks. Shear fractures occur during diagenesis and are produced by volume expansion due to the addition of sea-water into the alteration material. Micro-channel fractures (hair-channels) are also produced during diagenesis. Diagenetic and syngenetic fracturing provides conduits for sea-water entering into sideromelane. Since diagenetic fracturing is dependent upon stresses produced by hydration, there is a geometric increase of fracturing as time increases. This mode of fracturing provides increased volume of alteration material during time. Conchoidal contraction fractures are produced by differential contraction of the glass matrix and its phenocrysts during the quenching of a basaltic magma. Well

crystalized and exsolved palagioclase feldspar phenocrysts are not affected by hydration reactions and remain fresh throughout the process of palagonitization. Pyroxene laths such as pigeonite also remain fresh and unaffected during submarine weathering.

The Composition and Development of
Palagonite in Deep-sea Sediments
from the Atlantic and Pacific Oceans

by

Maury Morgenstein

B.A., Queens College, 1967

Thesis

Submitted in partial fulfillment of the requirements for the degree of Masters of Science in Geology in the Graduate School of Syracuse University, August, 1969.

Approved _____

Date _____

Table of Contents

	Page
I Introduction	1
Location of samples	3
II Chemistry of Palagonitization	4
Introduction	4
Method	4
Results	6
Electron Microprobe Petrology	11
Water diffusion in sideromelane	31
Discussion	54
III Fracture Analysis	57
Introduction	57
Classification of fractures	59
Discussion	69
Laboratory fracturing vs. Natural fracturing	75
IV Rate of Palagonitization	81
Introduction	81
Rate formula development	88
Derivation of the rate formula	90
Rate of palagonitization	95
Contribution of Palagonite to Marine Sediments	111
Palagonite dating tool	111
Authigenic Mineralization of deep-sea palagonites	121
V Conclusions	127
VI Acknowledgments	132
VII References	133
VIII Biographical data	137

Introduction

In the past century the term palagonite has often appeared in the geologic literature. However, the composition, mode of formation and overall geologic significance of palagonite have remained uncertain. The term was introduced by Van Waltershausen in 1845 (Bonatti, 1965) to distinguish a brown glassy material associated with pyroclastic rocks in eastern Sicily and Iceland. In 1926, Peacock, in a study of the petrology of Iceland, defined the nature of palagonite to be that of a highly hydrated volcanic glass. Fuller (1932), Denaeyer (1963) and Bonatti (1965) have concluded that palagonite is an alteration product of mafic volcanic glass (sideromelane). Palagonite alterations from sideromelane have been reported from world-wide localities, such as : in the Columbia River Basalt formation (Fuller, 1932), in the Quaternary basalts of Iceland (Peacock, 1926), in the Pacific Ocean (Murray and Renard, 1891; Nayudu, 1962; Arrhenius, 1963; and Morgenstein, 1967), and in hyaloclastites of Sicily (Rittman, 1958, as reported in Bonatti, 1965). Recently, Moore (1966) studied the rates of palagonite formation from submarine basalts adjacent to Hawaii, and suggested that palagonitization occurs during diagenesis. Bonatti (1965, p.1) concluded that, "The hydration which causes the formation of palagonite takes place at relatively high temperatures, that is mainly during effusion and cooling of the lava under water." An apparent contradiction exists in the literature concerning the time at

which mafic volcanic glass hydrates to palagonite. Arrhenius (1963, p. 698) emphasized this problem when he stated:

"The conditions determining the rate of decomposition and devitrification of volcanic glass in marine sediments are still obscure. While some minute glass shards in Mesozoic sediments are unaltered, some Quaternary deposits of ash and pumice have been entirely altered to montmorillonoid minerals or to phillipsite."

The purpose of this work is to define the time and rate of palagonite formation, the chemistry and geometry of glass hydration and the geologic significance of palagonitization. Chemical analyses were performed by wet chemical and electron microprobe examination. Petrographic thin section examination provided data of glass fracturing, mineral associations and the rate of palagonitization. Samples used for this study are mainly from the Atlantic and Pacific Oceans; however, reference is made to wide spread localities. A composite table (table 1) showing the location of each sample is found in this section. References are made to these samples as well as previously published samples in the following chapters.

Table 1
Location of Samples

Sample	Latitude	Longitude	Remarks
V22-227	30°23'N	47°14'W	Mid-Atlantic Ridge
A150-RD8	31°49'N	42°25'W	Mid-Atlantic Ridge
V16-SBT3	13°04'S	24°41'W	Mid-Atlantic Ridge
V25-12-T3	24°23'N	48°59'W	Mid-Atlantic Ridge
V25-12-T11	24°23'N	48°59'W	Mid-Atlantic Ridge
V25-13	24°47'W	50°26'W	Mid-Atlantic Ridge
RC8-D9	33°33'N	62°22'W	N. American Basin, Atlantic
V22-119	37°34'S	18°10'E	Argentine Sea Mt., S. Atlantic
RC10-110	16°32'S	156°04'W	South Pacific
V-16-130	59°22'S	132°46'W	South Pacific
V-16-127	54°30'S	163°19'W	South Pacific
5-9-16	*	Not available	North Central Pacific

* Sample supplied by Alpine Geophysical Associates, New Jersey.

CHEMISTRY OF PALAGONITIZATION

Introduction

Murray and Renard (1891) were the first to study the chemical composition of deep-sea basalts and their alteration products. At the time of their study, however, methods of analysis were not sufficiently accurate for examination of microscopic chemical changes of their samples. Recently, Moore (1966) used an electron microprobe for more complete analysis of palagonite and basaltic glass materials. However, he only studied six elements. In the present study, both electron microprobe and wet chemical analysis techniques were employed to study the chemical changes occurring during palagonitization. A comparison of previous and present analyses follows.

Method

Submarine basaltic glass and palagonite samples were cut into one inch diameter cylinders and the surface of each was polished carefully taking care not to contaminate the samples. They were then vacuum-coated with a layer of carbon a few hundred angstroms thick in order to make them conductive. During this process much of the free water was removed by the vacuum.

The samples were studied with a Philips Electron Microprobe by goniometrically scanning in search of all elements present, (from $27^{\circ}20'$ to $74^{\circ}20'$, at 200 counts/sec.), and by optically selecting areas of each sample and scanning them

individually for specific elements. No standards were used because none were available which would be representative of the types of material being studied. Purely qualitative analyses were accomplished by comparing peak height ratios of each element of one sample with the same element in another sample. Each element was run ten times and the counting rate for each was averaged. Wet chemical quantitative analyses were also performed. Total volatile analyses were accomplished by heating samples in silica glass tubing for one hour at 110°C (H₂O⁻) and then at 1500°C until the samples were liquified to draw off the remaining volatile gases (H₂O⁺). Samples were weighed before and at five minutes after each heat treatment in the hopes of eliminating the problem of reabsorption of volatile matter. There is, however, a slight increase in weight after heating due to the oxidation of iron present in the samples.

Results

Wet chemical analysis of a basaltic sample (A150-RD8) from the Mid-Atlantic Ridge is compared to previously published analyses in Table 2. On the basis of these analyses, the oceanic basalts studied from the Pacific and Atlantic are similar in composition but differ slightly from analyzed basalts of Iceland and Sicily. The largest variations occur in the elements calcium, potassium, sodium and iron.

Microprobe analyses of sample V22-227 from the Mid-Atlantic Ridge (Table 3) are compared in element percentage calculations (ratio analysis of fresh glass to alteration products) with those basaltic glasses and palagonites in Table 2. Chemical changes during the weathering of sideromelane to palagonite are shown in Tables 3 and 4. These analyses show that during the alteration of basaltic glass to palagonite Na, Al, Mg, Si, Mn and Ca are lost; K, Ti, Fe and O are added in the alteration product. Potassium and calcium show the largest variation during halmyrolysis.

Total volatile analysis (Table 5) indicates that palagonite contains 2 to 3 times more H₂O⁻ and about 4 to 10 times more H₂O⁺ than sideromelane. This indicates that palagonitization is a process of hydration of mafic volcanic glass (sideromelane). Observations show that the more hydrated the palagonite the greater the degree of alteration. The degree of alteration is measured by the extend of authigenic mineralization.

Table 2

Matched Chemical Analyses of Palagonite and Sideromelane in Weight %

Sample	A1	A2	B1	B2	C1	C2	D1	D2	E1	E2	F	*	F1	F2	F3	F4
SiO ₂	46.76	44.73	46.39	35.34	49.54	36.36	51.90	33.0	49.23	47.55	47.01	Na	1.9	1.9	0.7	0.8
Al ₂ O ₃	17.71	16.26	16.27	11.15	16.47	16.20	14.70	8.3	15.19	13.94	12.12	Ca	7.4	7.4	0.4	0.7
Fe ₂ O ₃	1.73	14.57	1.35	10.28	2.30	16.56	1.60	15.2	1.49	4.31	2.86	K	0.9	0.9	2.8	1.3
FeO	10.92	-	9.96	2.19	7.55	0.93	8.60	-	8.42	9.15	0.29		F5	F6	F7	F8
Mn ₂ O ₃	-	22.89	-	-	-	-	-	-	-	-	-	Na	0.4	1.2	0.4	0.9
MnO	0.44	-	tr.	0.22	0.19	1.25	-	0.1	0.15	0.21	0.17	Ca	0.5	0.3	0.4	0.7
MgO	10.37	2.23	9.77	6.52	7.91	4.86	8.70	5.0	8.46	6.15	12.61	K	3.0	3.5	3.5	1.7
CaO	11.56	1.88	13.00	7.01	11.43	6.77	10.40	7.0	11.01	10.85	8.98		F9	F10		
Na ₂ O	1.83	4.50	1.40	0.16	2.62	2.01	2.60	0.7	2.72	2.59	2.36	Na	0.5	0.4		
K ₂ O	0.17	4.20	0.15	0.19	0.30	0.94	2.40	0.3	0.13	0.20	0.72	Ca	1.2	0.5		
H ₂ O ⁺	-		0.15	8.90	0.95	0.31	0.20	9.3	0.82	2.15	0.66	K	2.7	3.3		
H ₂ O ⁻	-	9.56	0.10	15.50	0.27	6.26	0.16	18.3	0.13	0.43	0.41		* Electron			
TiO ₂	-	-	-	-	-	-	-	-	1.54	2.63	0.48		Microprobe			
P ₂ O ₅	-	-	-	-	-	-	-	-	0.13	0.24	0.27		F1 and F2, Transparent glass (Moore, 1966)			

(Dash = no determination)

- A South Pacific (Murray and Renard), 1=sideromelane, 2=palagonite
 B Iceland (Peacock, 1926), 1=sideromelane, 2=palagonite
 C Atlantic Ocean (Correns, 1930; reported in Bonatti, 1965), 1=sideromelane, 2=palagonite
 D Palagonia, Sicily (Hoppe, 1941; reported in Bonatti, 1965), 1=sideromelane, 2=palagonite
 E Mid-Atlantic Ridge (Analysis by F. Shido) E1 and E2 are fresh basalt, sample A150-RD8
 F Hawaii, East Rift Zone of Mouna Kea (Moore, 1966) sample 22, basalt

Hawaii, East Rift Zone.
 F3 thru F10, Palagonite
 Rind (Moore, 1966)
 Hawaii, East Rift Zone.

Table 3

Percent of Element or Oxide Within Sideromelane and Palagonite in Terrestrial and Oceanic Deposits

	A1	A2	B1	B2	C1	C2	D1	D2	*	
									G1	G2
SiO ₂	51.10	48.90	56.76	43.24	57.67	42.31	61.13	18.87	64.55	35.45
Al ₂ O ₃	52.10	47.90	59.33	40.67	50.41	49.59	63.92	36.08	48.81	51.19
Fe ₂ O ₃	10.62	89.38	11.61	88.39	12.19	87.81	9.52	90.48	36.12	63.88
FeO	--	--	81.98	18.02	89.04	10.96	--	--	--	--
MnO	--	--	trace	over 90%	13.19	86.81	--	--	64.58	35.42
MgO	74.37	25.63	59.97	40.03	61.94	38.06	63.50	36.50	63.96	36.04
CaO	86.01	13.99	64.96	35.04	62.80	77.20	59.77	40.23	88.83	11.17
Nu ₂ O	28.91	71.09	92.38	7.62	56.63	43.37	78.78	21.22	57.87	42.11
K ₂ O	7.00	93.00	42.86	57.14	24.19	75.81	64.91	35.09	9.73	90.27
Ti	--	--	--	--	--	--	--	--	35.46	64.54
O	--	--	--	--	--	--	--	--	38.46	61.54

All samples designated 1 are sideromelane, those numbered 2 are palagonite.

Data recalculated from Table 2. For SiO₂: A1 + A2 = 100%; D1 + D2 = 100%.

Samples A, C and G are Oceanic; B and D are Terrestrial.

* V22-227, Mid-Atlantic Ridge, microprobe analysis of elements; G1 = sideromelane, G2 = palagonite.

Dash = no determination.

Example of calculation: Table 2 reports 46.67% SiO₂ for A1, and 44.73% for A2.

The sum of A1 and A2 = 91.49, which is equivalent to 100% of SiO₂ in sample A.

There is 51.10% of SiO₂ in sample A1 of that 100%, and 48.90% of that total for A2. The calculations are made so that each matched sample may be compared for each element separately.

Table 4
 Element and Oxide Ratios In Oceanic and Terrestrial
 Samples. (Calculated from Table 3)

% Element X in Sideromelane/% Element X in Palagonite

Sample	OCEANIC			:	TERRESTRIAL	
	G1/G2*	A1/A2	C1/C2		B1/B2	D1/D2
SiO ₂	1.82	1.04	1.36		1.31	1.57
Al ₂ O ₃	0.95	1.08	1.01		1.45	1.77
Fe ₂ O ₃	0.56	0.11	0.14		0.13	0.10
FeO		-	8.12		4.54	-
MnO	1.82	-	0.15		1	-
MgO	1.77	2.90	1.62		1.49	1.74
CaO	7.95	6.17	1.68		1.85	1.48
Na ₂ O	1.37	0.40	1.30		12.12	4.91
K ₂ O	0.10	0.07	0.31		0.75	1.84
Ti	0.54	-	-		-	-
O	0.62	-	-		-	-

(Dash = no determination.)

Elements with ratios less than 2 are added to palagonite during the alteration of sideromelane to palagonite. Those elements with ratios greater than 2 are depleted in the alteration product (palagonite).

* Sample G is an element ratio. All other samples are oxides.

Table 5

Total Volatile Content in Samples From the Atlantic and Pacific Oceans

Sample %	Basalt			Sideromelane			Palagonite			H ₂ O ⁻	H ₂ O ⁺	Total
	H ₂ O ⁻	H ₂ O ⁺	Total	H ₂ O ⁻	H ₂ O ⁺	Total	H ₂ O ⁻	H ₂ O ⁺	Total			
V22-227 69 cm.	-	-	-	1.91	0.34	2.25	15.96	6.32	22.28	6.66	19.34	26.06 R.O.
RC10-82	0.26	0.19	0.45	3.24	1.62	4.85	11.96	8.40	20.36	-	-	-
A150-RD8	0.33	0.22	0.55	-	-	-	-	-	-	21.55	8.93	30.49 Y.O.
RC8-D9	-	-	-	-	-	-	9.76	-	Y	8.49	13.03	21.52 Y
RC10-110	-	-	-	-	-	-	7.75	17.33	25.09	-	-	-
5-9-16	1.08	1.62	2.69	0.89	0.89	1.78	30.34	16.55	46.81	-	-	-

Missing data is due to an insufficient quantity of sample for analysis.

H₂O⁻ was derived by heating samples to 110°C for one hour.

H₂O⁺ was derived by liquifing samples at 1500°C in silica glass tubing.

Y = yellow

B = light brown R.O. = reddish orange R = red Y.O. = yellowish orange

Microprobe Petrology: Observations and Results

In addition to microprobe analyses with a goniometer, a Norelco beamscan oscilloscope attachment was used for microchemical analysis of sideromelane and palagonite samples. The purpose of this section is to describe the process of palagonitization.

Interpretation of Cathode Ray Tube Photographs

Two different photograph displays are shown on the following plates. A Line Current Display (LCD) is similar to an electron microphotograph. Light areas in these displays are representative of light elements and dark areas are composed of heavy elements. Fractures are shown by black areas (those areas void of all elements). The Element Displays are fluorescent scans of individual elements and show their overall distribution for a specific area studied. The size and intensity of the individual displayed dots does not necessarily reflect the quantity of that element present in the sample. Light intensity reflects inherent element activity and oscilloscope gain settings.

Analysis of two samples are compared from the Mid-Atlantic Ridge (V22-227, see Table 2 for complete analysis) and from the Bellingshausen Basin, South Pacific (V16-130). The following section describes these microprobe photographs.

Description of Plates

Plate 1

An extensive fracture net in palagonite is best shown by

Plate 1

Electron Beam Scanning Photographs of palagonite in V22-227. The base of the photographs are 320 u long (magnification 400 diameters).

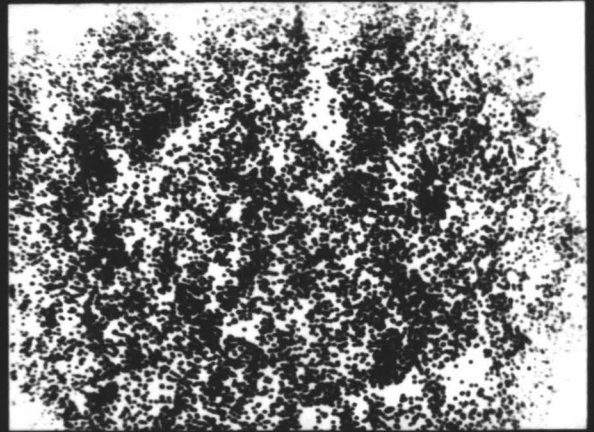
- A. Line Current Display showing the distribution of heavy and light elements.
- B. Oxygen display shows the concentration of oxygen in a cellular configuration.
- C. Potassium display depicts areas of palagonite. Areas void of potassium are sideromelane.

V22-227



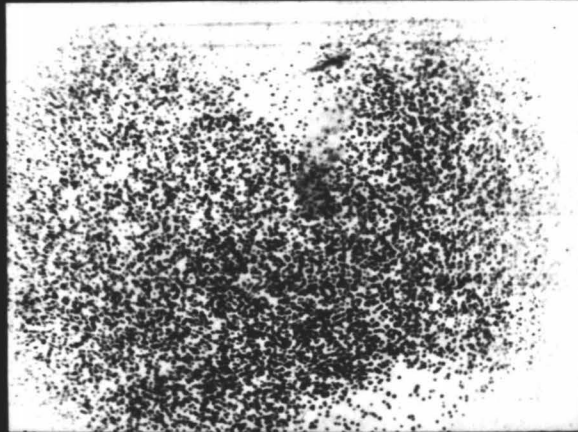
A

LCD



B

$O_{K\alpha}$



C

$K_{K\alpha}$

PLATE I

the Line Current Photograph of sample V22-227. The Oxygen display depicts the element voids in the fractures. Both potassium and oxygen are evenly distributed in the palagonite. The top central and lower right portions of the potassium display show that there is an absence of this element in these areas. These areas are sideromelane.

Plate 2

Two fractures in sideromelane with palagonite alterations along them are shown by the electron beam scanning photographs of sample V16-130. Palagonite is confined to the semicircular areas along the edge of the major fracture. Calcium is depleted in the palagonite and in the fractures, whereas, potassium is concentrated in these areas. An even concentration of potassium with a small distribution is shown in the relatively fresh sideromelane. This concentration does not approach the quantity of potassium in the palagonite. Palagonite takes the semicircular configuration because it has been displaced by some oblique strike slip motion along the major fracture. An apparent displacement of 150 u can be seen (see page 57 for a more detailed description of fracturing).

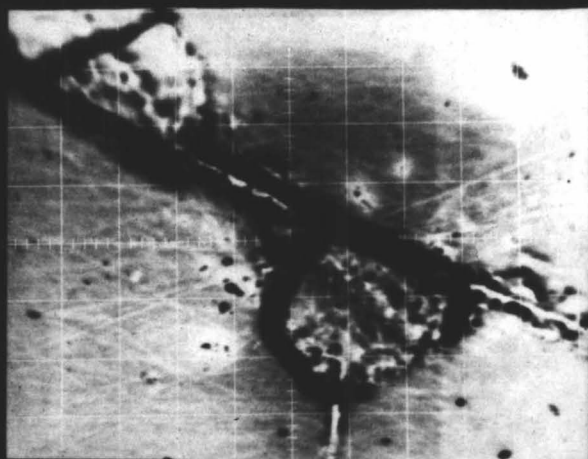
Plate 3

Two silica displays show the geometry of the fractures in V16-130. The 400 diameter magnification display depicts fractures at an acute angle. The upper right hand portion of this photograph is shown in more detail at a magnification of 2400 diameters. Relatively sharp boundaries can be seen at

Plate 2

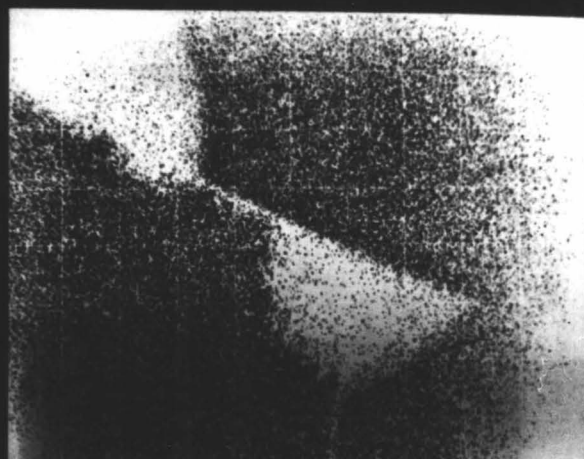
- A. Line current display showing fractures.
- B. Calcium display showing the distribution of sideromelane (areas rich in calcium are shown by the light display dots.)
- C. Potassium display showing the distribution of palagonite (areas rich in potassium are shown by the display dots). Palagonite is concentrated in the fractured areas.

V16-130



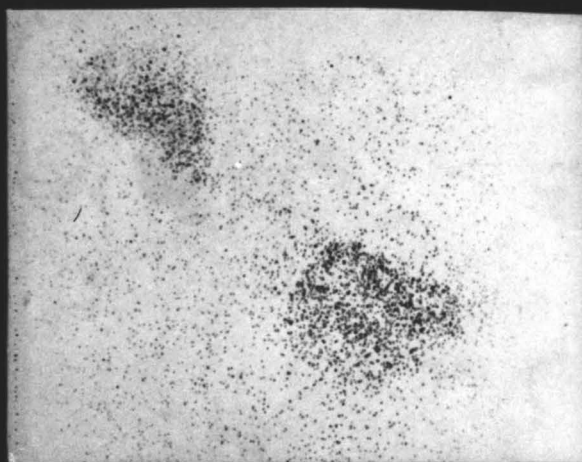
A

LCD



B

Ca
K α



C

K
K α

PLATE 2

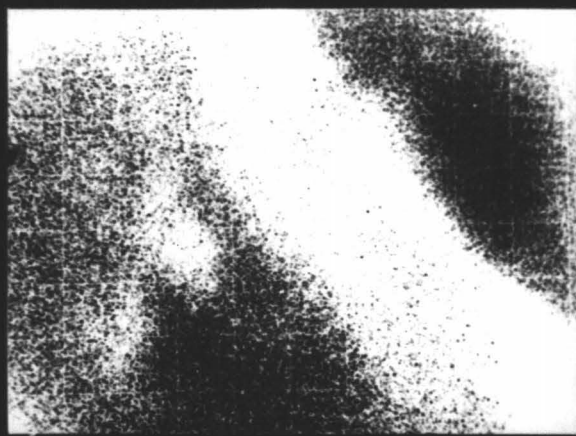
Plate 3

- A. Silica display at 400 diameters magnification shows areas of fracturing in the V16-130 sample.
- B. Silica display at 2400 diameters of magnification depicts the same fracture in more detail.
- C. Calcium display depicts areas of sideromelane.
- D. Potassium display showing areas of palagonite occurring along the path of a fracture.

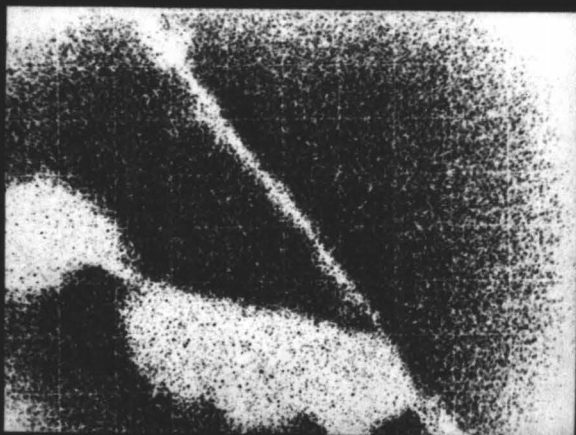
V16-130



A Si_{Kα} (400x)



B Si_{Kα} (2400x)



C Ca_{Kα}



D K_{Kα}

PLATE 3

either side of the fracture. A calcium and potassium display of 400 diameters again show the inverse relationship between these two elements. The calcium rich areas are sideromelane whereas the potassium concentrates in the palagonite. One fracture in the palagonite shows up in the silica and potassium displays.

Plate 4

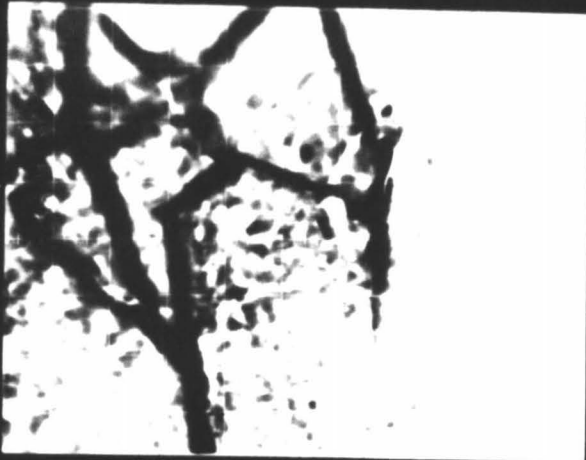
A fracture net with a calcic-plagioclase lath, palagonite and sideromelane is shown for sample V16-120. A diagrammatic outline map is drawn from the line current, Ca and K displays. Palagonitization has occurred around the feldspar lath while the feldspar remains fresh. The palagonite alterations occur in an old fracture which has been expanded. A sideromelane fragment, broken off from the walls of the fracture is altering to palagonite.

Plates 5 and 6

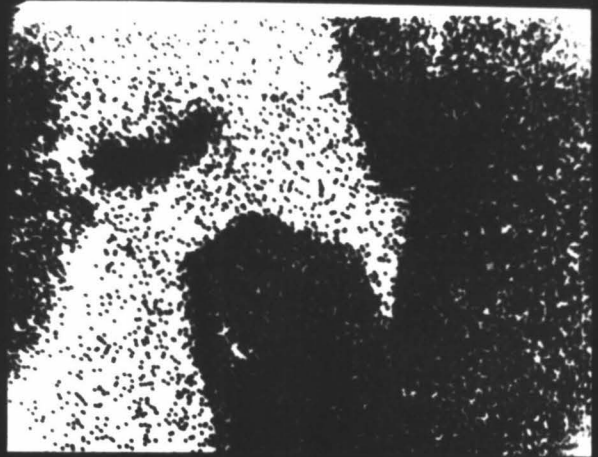
Electron beam scanning photographs of V16-130 show the distribution of seven elements in sideromelane and palagonite. Those elements gained (K, Ti, Fe) during the alteration of sideromelane to palagonite are shown in plate 5 and those lost (Mg, Si, Ca) are shown in plate 6. Aluminum is shown in plate 5, but it is doubtful whether its concentration changes very much during halmyrolysis as seen from its display here and from previous analyses. A mineral distribution diagram is shown on plate 6. In the lower central portion of the diagram there is a phenocryst containing iron, magnesium and silica. Optical work has determined that this is a pyroxene. Its chemical

Plate 4

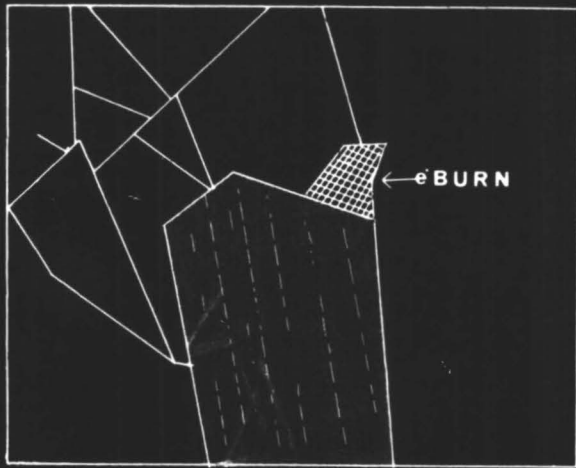
- A. Line current display showing light and heavy element distributions.
- B. Calcium display depicts the outline of a Ca-plagioclase feldspar and extent of sideromelane.
- C. Diagram shows the fracture assemblage and areas where the electron beam burnt a portion of the sample.
- D. Potassium display depicts areas of major fracturing which are rich in palagonite.
- E. A mineral map of the sample showing the distribution of palagonite, feldspar and glass (sideromelane).



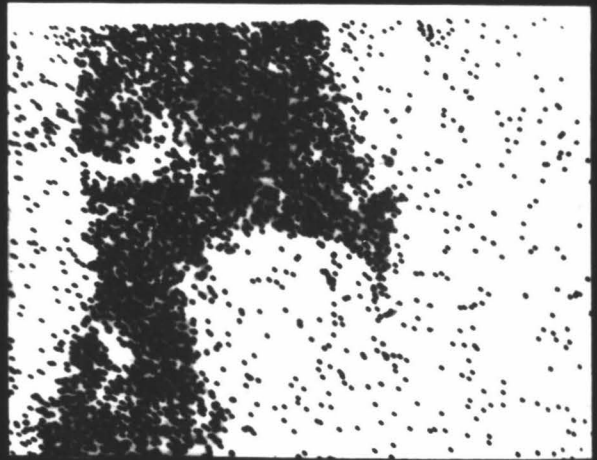
A LCD



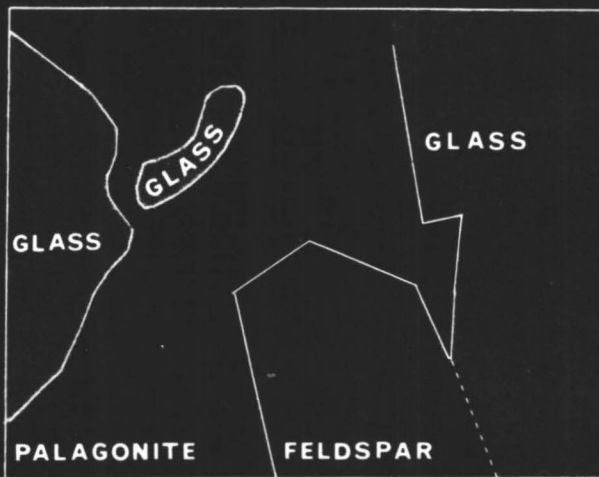
B Ca_{Kα}



C FRACTURE NET



D K_{Kα}



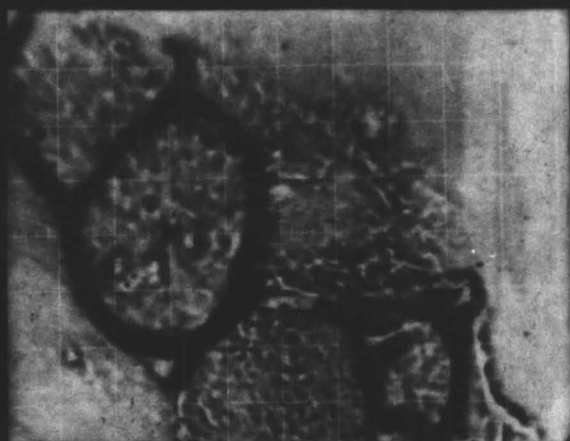
E

Plate 5

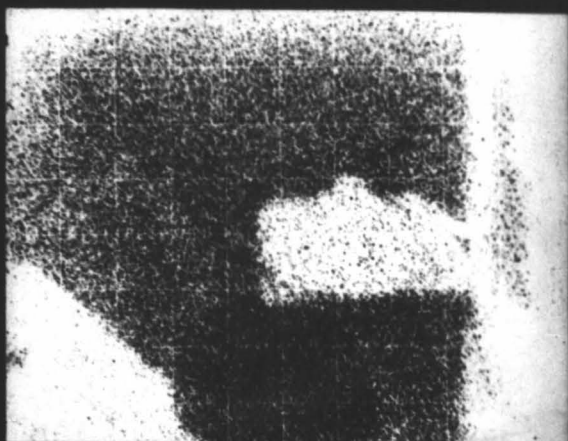
Elements added to palagonite during the hydration of sideromelane.

- A. Line current display depicting the geometry of the light and heavy elements.
- B. Iron display showing that iron is concentrated in the area of fracturing and in the pigeonite phenocryst.
- C. Potassium display shows the outline of the major fractures and the distribution of palagonite.
- D. Titanium display follows the potassium display in geometry. The titanium is localized in the palagonite.
- E. Aluminum display shows the relative decrease of aluminum in the pigeonite phenocryst and a rather even distribution in the glass and palagonite.

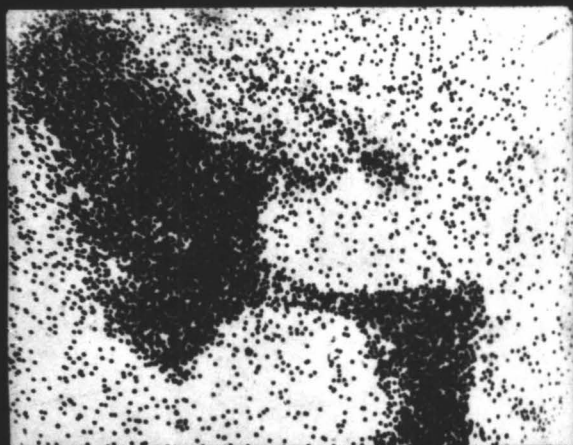
VI6-130



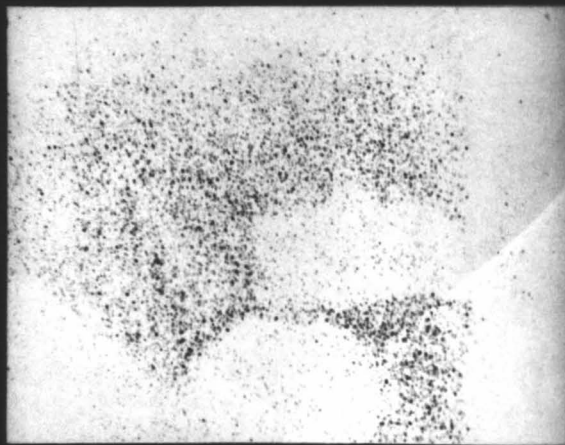
A LCD



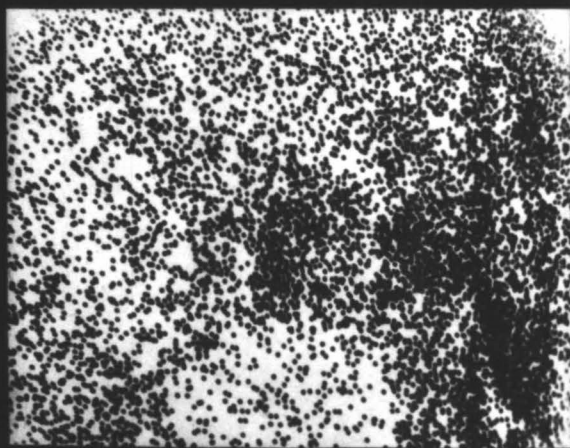
B Fe_{kα}



C K_{kα}



D Ti_{kα}



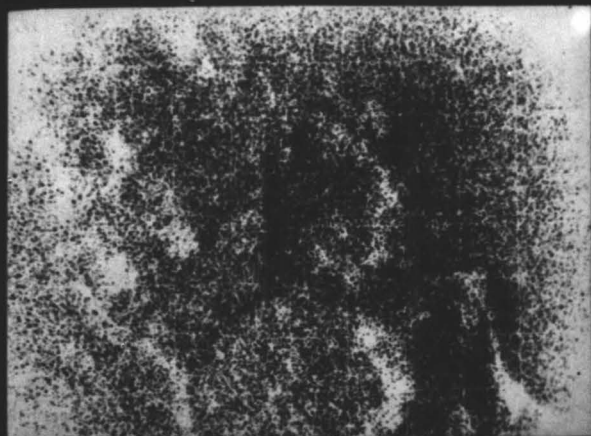
E Al_{kα}
PLATE 5

Plate 6

Elements lost during palagonitization in the alteration product (palagonite).

- A. Silica display shows the border outline of the glass (sideromelane), palagonite and pyroxene.
- B. Calcium display depicts the distribution of the sideromelane.
- C. Magnesium display shows the outline of the pigeonite phenocryst.
- D. A composite mineral diagram showing the distribution of glass, palagonite and pigeonite.

VI6-130



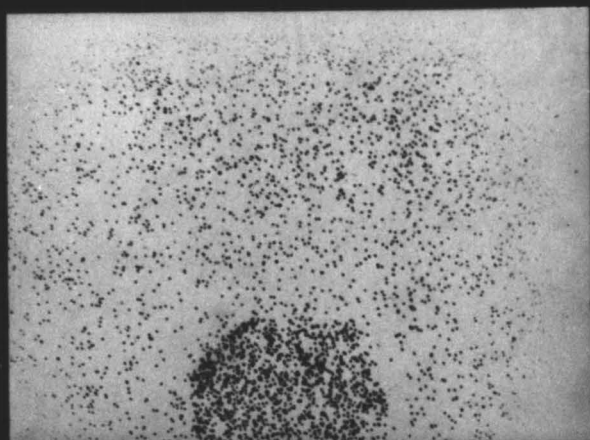
A

Si_{Kα}



B

Ca_{Kα}



C

Mg_{Kα}



D

PLATE 6

content is intermediate between clinoenstatite (MgSiO_3) and Clinohypersthene (FeSiO_3) suggesting that it is pigeonite. It is surrounded by palagonite and has retained its identity further suggesting that it is relatively stable, as is calcic-plagioclase, in halmyrolysis reactions.

Plates 7 and 8

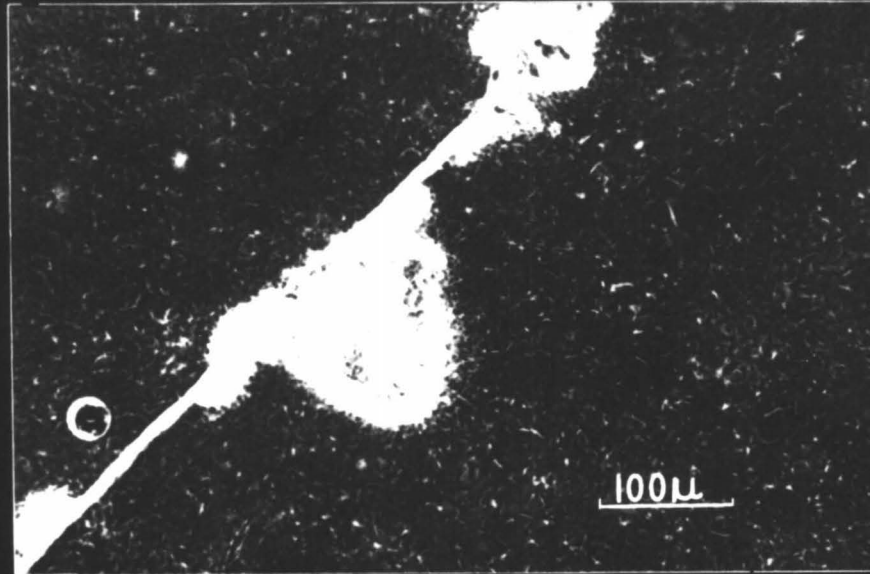
A comparison of the geometry of palagonite formation is shown by a photomicrograph of V22-227 and the Line Current Display of V16-130. Palagonitization occurs along a fracture in the sideromelane. Again, potassium and calcium show the largest variation in chemical behavior. Sodium is slightly depleted in the palagonite and it therefore behaves similar to calcium. The major fracture is clearly shown by the absence of silica along its path. Palagonite alteration occurs in two partially connected areas along the fracture. The lower concentration of calcium between these two areas of palagonite suggests that this intermediate area is in the process of hydration. Potassium concentration in the intermediate area is higher than recorded in the surrounding sideromelane.

In summary the cathode ray tube photographs confirm the results obtained by wet chemical analysis. The presence of calcium in the element display photographs is indicative of non-altered or slightly altered sideromelane. Calcium is inversely proportional to potassium, and therefore with increased potassium concentration calcium is depleted. Potassium rich areas are palagonite. The geometry of palagonitization is dependent

Plate 7

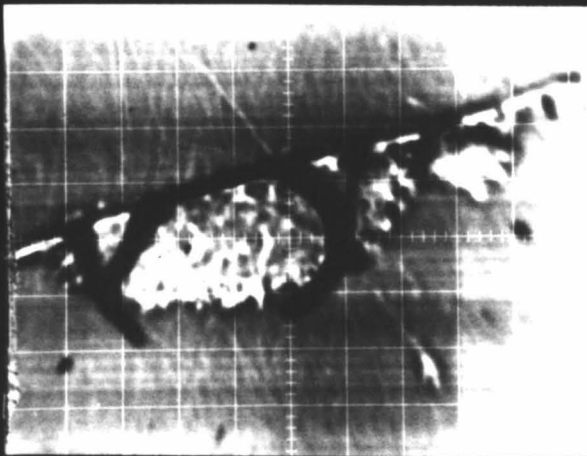
- A. Photomicrographs of V22-227 shows a fracture in sideromelane with palagonite alteration along the fracture. Plane polarized light. Scale as shown.
- B. Line current display of V16-130 shows a similar fracture in sideromelane and a similar palagonite concentration about the fracture. Sample V22-227 is from the Atlantic Ocean and V16-130 is from the Pacific.
- C. Silica display shows the major fractures more clearly. Silica is present in both the palagonite and the sideromelane.

V22-227



A

V16-130



B

LCD



C

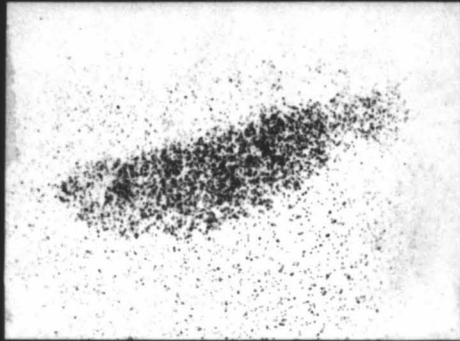
Si_{kα}

PLATE 7

Plate 8

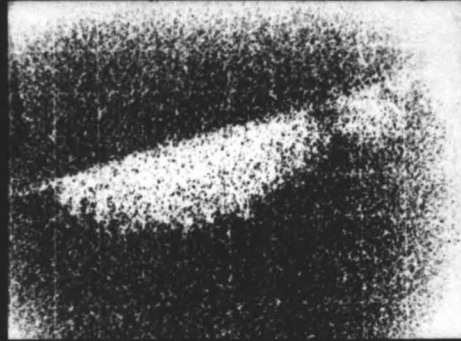
- A. Potassium display showing the concentration of palagonite.
- B. Calcium display depicting the concentration of sideromelane.
- C. Sodium display shows the relative decrease of this element in palagonite. The larger display dots are a function of oscilloscope gain settings.
- D. Titanium is concentrated in the palagonite.
- E. Aluminum shows a slight increase in concentration in the palagonite.
- F. Oxygen is also enriched in the palagonite.
- G. Iron follows the pattern of titanium and is concentrated in the palagonite.

V16-130



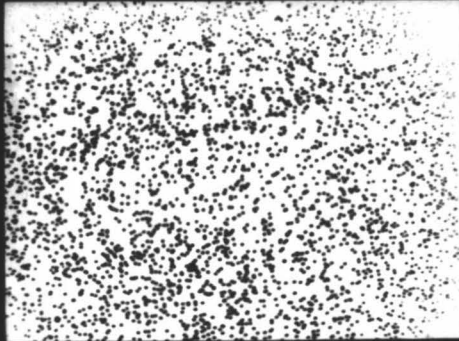
A

K_{Kα}



B

Ca_{Kα}



C

Na_{Kα}



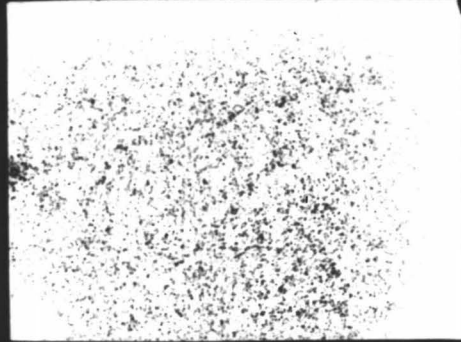
D

Ti_{Kα}



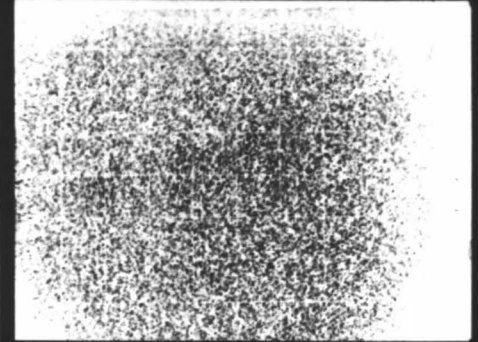
E

Al_{Kα}



F

O_{Kα}
PLATE 8



G

Fe_{Kα}

upon the configuration of the paths which water enters the fresh sideromelane. Plates 1 through 8 have shown that most of these major alterations occur along fractures.

A comparison of the results obtained by microprobe goniometer scanning, beam scanning photographs and wet chemical analysis show that the chemistry of palagonite formation is relatively constant in the Atlantic and Pacific Oceans. A major problem in the chemistry of palagonitization is the path in which the sea-water takes to hydrate the sideromelane. The following section discusses this problem.

Water Diffusion in Sideromelane

Sideromelane alters to palagonite by the process of hydration. This process of hydration is essentially a diffusion mechanism intermediate between solid-state reactions and pure liquid reactions. The mechanism of diffusion in solids has been extensively studied by use of thermodynamic calculations and through laboratory experiments on crystalline solids, as in Chapter 3, page 81. The thermodynamic equations for solid diffusion do not supply information concerning the path of the diffusing particles or the concentration of lattice defects. Knowledge of the concentration of lattice defects enables one to specify the atoms that are mobile as well as the frequency with which these atoms that are mobile are displaced during their travel through the solid. It is helpful to know this concentration in order to be able to follow the path of the diffusing particles. In solid-state reactions, the

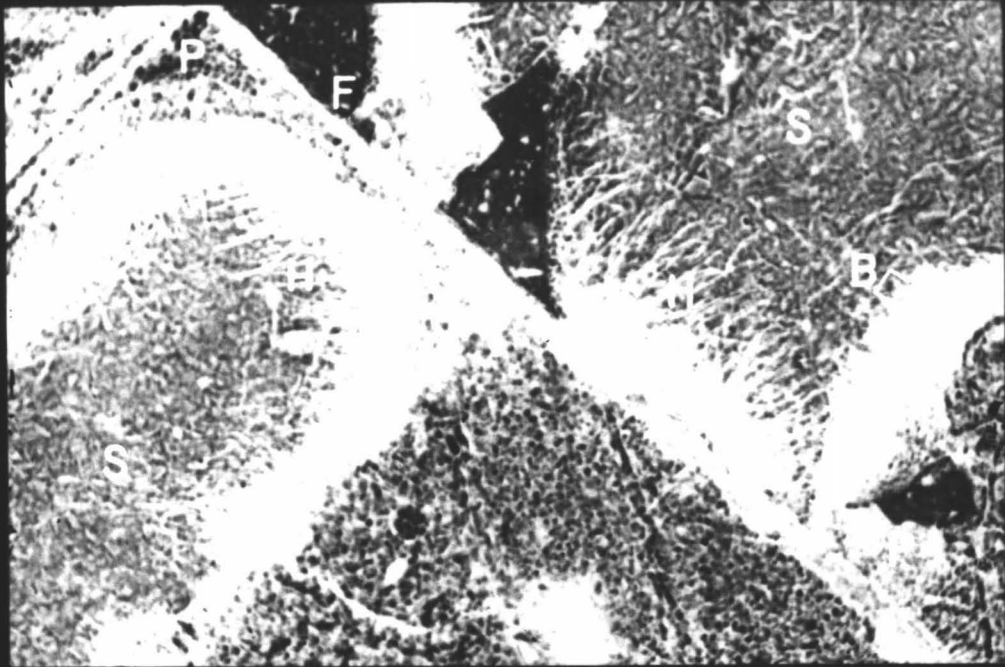
interaction between the solid depends on lattice defects, on the mobility of lattice units, and on the degree of contact between the reactants. (Jost, 1952) In fluid reactions, on the other hand, the reactant molecules are available to one another due to kinetic affects. (Op. cit.) In solid-state reactions an immobile product layer builds up at the interface of the reactants, and further reaction depends on diffusion of lattice units through this layer. (Op. cit.)

The process of hydration is somewhat different from the process of pure solid-state and fluid reactions. As diffusion proceeds there is an increase in the mobility of reactants due to increased kinetic affects. This concept has not been taken into account by present workers studying perlitization, (obsidian devitrification) or palagonitization. They wrongly assume that the rate of diffusion of water molecules into the glass lattice structure slows down as the depleted or hydrated regions become thicker. They base their assumptions on pure thermodynamic calculations for crystalline solids and apply these equations to amorphous glass hydration reactions.

For palagonite, an immobile product layer is built up during hydration. This layer is extensively hydrated and therefore the degree of lattice defects in the solid solution boundary area (immobile product layer) is considerably higher than in the unaltered glass. The rate of hydration is therefore dependent upon the slower rate of initial glass hydration (the point at which there is a minimum of lattice defects).

Plate 9

- A. Palagonite (P), sideromelane (s), hair-channels (H), solid solution border (g), and fractures (F) are indicated on the photograph. Two major fractures are shown at a right angle connection. Sample V22-227, plane polarized light. Scale as shown.
- B. Hair-channels growing from a major fracture. The dark area of the fracture is the solid solution border. The solid solution border is not fully developed. Sample V22-227, plane polarized light. Scale as shown.



A

100 μ



B

50 μ

Plate 9 shows the solid-solution boundary layer between palagonite and sideromelane. This layer has been divided into two sectors. The first is a solid-solution channel area (hereafter referred to as micro-channels or hair-channels) which defines the path of water into the glass structure. The density of the channels reflects the degree of lattice defects in the glass structure. The second part of the sector is a true immobile product layer and is referred to here as the solid solution border. It is composed of a high density of hair-channels and shows partial crystallization of some early authigenic minerals such as iron oxides (goethite and limonite) and smectites. The solid-solution border is more hydrated than the micro-channel area and thus diffusion of water into the solid solution border is more easily accomplished and also more rapid. The controlling rate of diffusion, however, is again represented by the rate of hair-channel development, and therefore, the overall diffusion rate in a linear direction is constant. A detailed description of the rate of palagonitization is found in chapter 3.

The exact configuration of the lattice defects in sideromelane is unknown. From microprobe analyses and microscopic observations the following assumptions can be made concerning the diffusion of water molecules into the glass lattice structure:

1. Lattice defects in sideromelane must be large enough to accommodate an entire water molecule because water molecules

diffuse into the glass lattice structure.

2. There is more potassium in palagonite than in the original sideromelane for oceanic palagonitization reactions. The potassium must therefore come from the sea-water. Potassium is the largest element in any measurable quantity in palagonitization reactions. Lattice defects in sideromelane must be at least as large as the diameter of potassium in order for this element to be accommodated in the lattice structure.

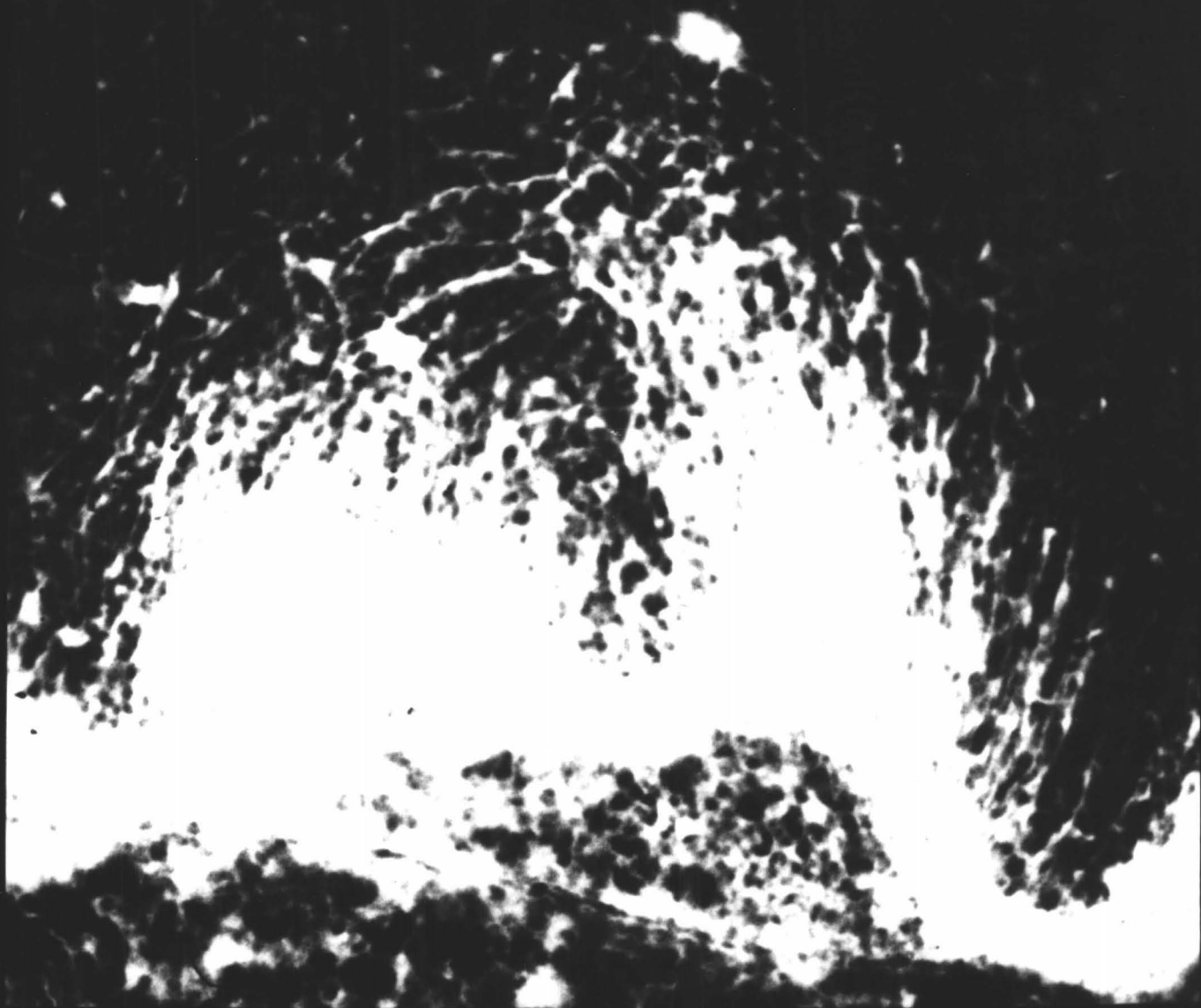
3. The path of the water molecules and potassium in sideromelane must be controlled by the configuration of lattice defects. Plate 10 shows the distribution of hair-channels at a palagonite - sideromelane boundary. These micro-channels grow perpendicular to the boundary toward the glass. They then curve and interconnect with each other. The individual paths of these channels reflect the geometry of some of the lattice defects in sideromelane.

4. Lattice defects must be a function of atomic spacing between large elements in the glass such as calcium or between silicate tetrahedra which are randomly orientated.

5. Marshall (1961) suggests that water molecules contained in glass are able to break the Si-O-Si, Al-O-Al, Si-O-Al cross bonds by adding hydroxyl groups to an Si or Al atom. In this case, the glass structure would partially break down (hydrate) if some small quantity of meteoric water were to be included in the glass structure either during cooling or before quenching of the basaltic melt. Therefore, the sidero-

Plate 10

Hair-channels, solid solution border, zeolites and palagonite filled fractures, and sideromelane are shown on the photograph. The hair-channels are interconnecting with each other. This photograph is an enlargement of figure B in plate 26, page 108. Sample V22-227, plane polarized light, .. Scale as shown.



|----- 50 μ -----|

PLATE 10

melane is partially hydrated, and both large voids and a high degree of kinetic movements exist. Thus, the glass structure can accept new sea-water during diagenesis without much difficulty. A difference in initial water contact might also explain why some glasses of basaltic composition do not alter to palagonite after extensive geologic time whereas some alter rapidly during diagenesis. Marshall (1961) estimates that a 15% initial water content in basaltic glass is the minimum requirement to initiate authigenic mineralization. In acidic glasses he suggests that initial water contents of about 20 to 25% may be required because the Si-O and Al-O bonds are more numerous.

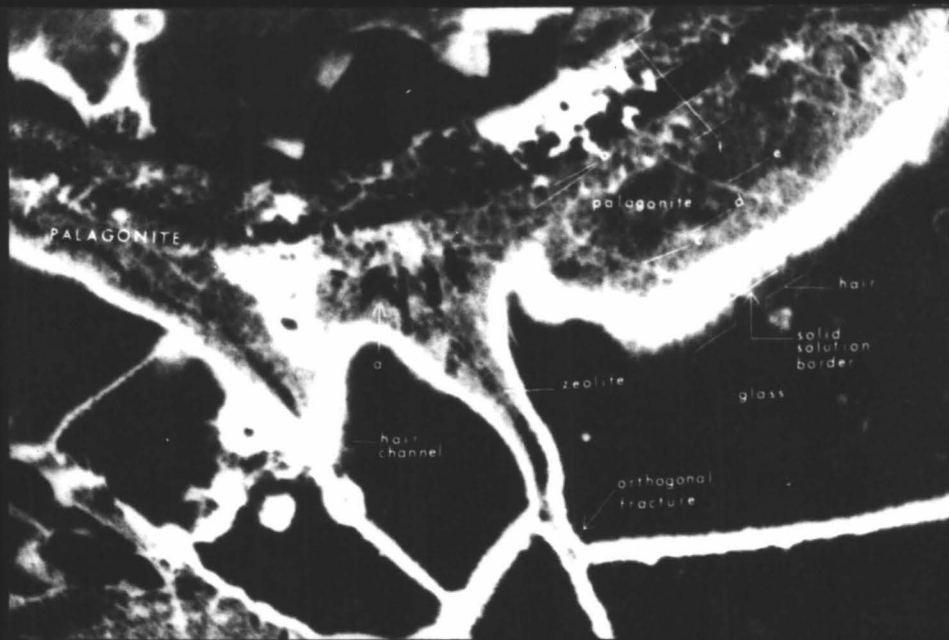
A composite picture of the alteration sequence described previously is shown on plate 11. Both fresh sideromelane and palagonite show the intricate structure which accompany the alteration reactions. Well defined fracture assemblages are interconnected at right angles. Palagonitization occurs along these fractures as well as at a large palagonite-sideromelane border. (Northern portion of photograph.) Remnant glass and palagonite boundaries are observed stage by stage in the alteration material. A major fracture (in detail) shows progressive authigenic mineralization where zeolites occupy the center of the fracture and define the original width of the displacement. Smectites and goethite are crystallized from the palagonite and are intermixed with palagonite in the remaining portions of the fracture. On either side of the fracture a

Plate 11

- A. Palagonite, glass, solid solution border, hair-channels and fractures are labeled on the photograph.
- a. Represents a zeolitized paleochannel border.
 - b. A palagonitized paleochannel border.
 - c, d, e, Stages of palagonite paleochannel border formation.
 - f. Palagonite banding.

Sample V22-227, plane polarized light. Scale as shown.

- B. An enlargement photograph of figure A (above). The details of the process of sideromelane solution are shown. The central zeolite channel (labeled zeolite in figure A) marks the position of the original fracture. Progressive stages of palagonitization can be observed. The hair-channel sector and the solid solution border zone are located between the palagonite and the sideromelane. Sample V22-227, plane polarized light. Scale as shown.



A

100 μ



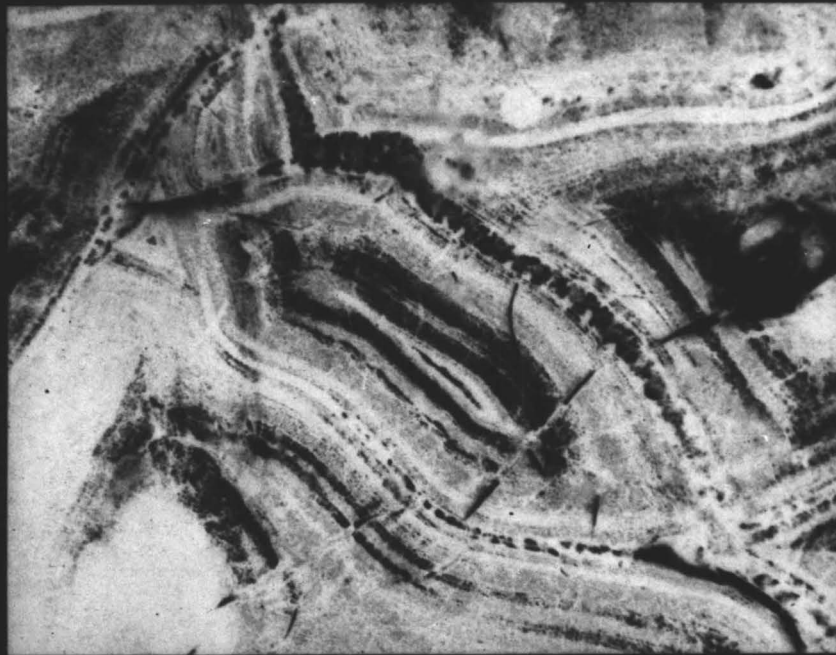
B

100 μ

solid solution border and hair channeled sector separate the sideromelane from the alteration material (palagonite). The fact that a series of alteration stages of palagonitization can be recognized suggests very strongly that it is diagenesis that is the process responsible for the development of palagonite and not syngeneses as is thought to be the case by many students of submarine volcanism. Rapid palagonitization during syngenetic quenching of submarine lava would necessitate a general homogeneity of the alteration material (palagonite) because there could not be sufficient time to develop a series of stages (each 50 u thick) as is found in typical palagonite banding. These palagonite bands (plate 12) represent stage by stage alteration of palagonite and are geometric reflections of the thickness of the solid solution border and hair-channelled sector. Equal palagonite configuration on either side of the fractures show correlations in both the exact width of banding and degree of authigenic mineralization (type and quantity of authigenic minerals). This suggests that hydration (sea-water diffusion) proceeds at a constant rate on all sides of a fracture. The fractures, of course, act as conduits for sea-water entering the glass and probably also define the path of removal of ions from the glass into the sea-water or sediment. Plate 13 shows these fractures in the sideromelane. Hair-channels and solid solution borders are commonly perpendicular to the fractures. They have their outlets (mouths) usually at a large palagonite-sideromelane border. In the

Plate 12

- A. Photograph shows cellular palagonite configuration with typical banding and fracturing. The fractures are mostly filled with zeolite fragments and smectites. Sample V25-12-T11, crossed nicols, gypsum plate. Scale as shown.
- B. Photograph of a palagonite cell during the alteration of sideromelane. The glass is located in the center of the cell (upper left portion of the photograph). Typical palagonite banding is observed. The fractures connect at right angles and are filled with zeolites and smectites. Sample V25-12-T3, partially crossed nicols, gypsum plate. Scale as shown.



A

500 μ



B

300 μ

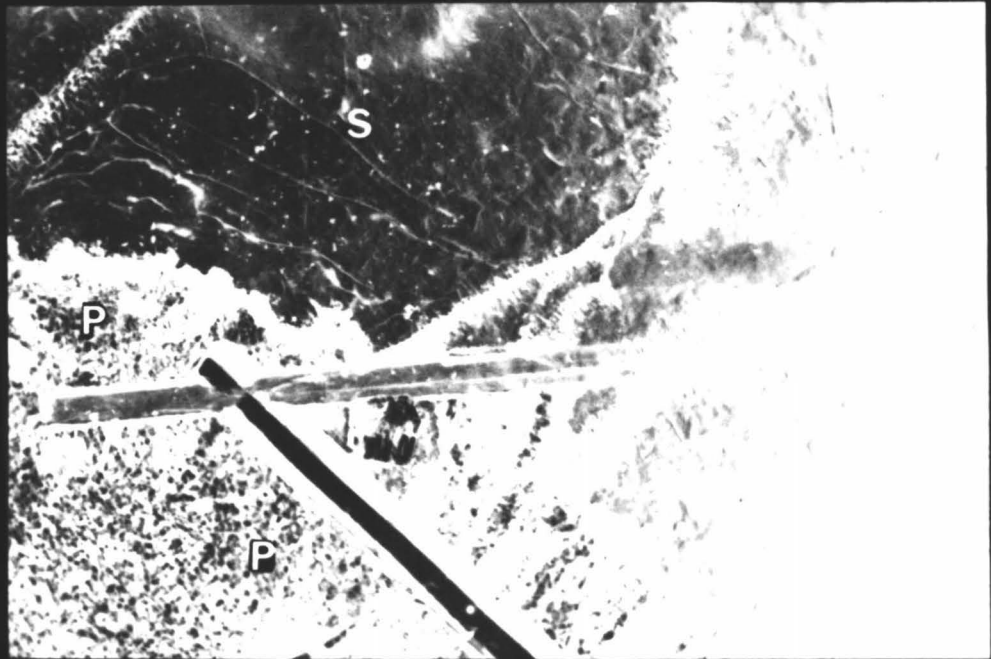
Plate 13

- A. Sideromelane with feldspar and pyroxene phenocrysts. Fractures are extensive in the sideromelane but do not extend into the phenocrysts. Hair-channels occur along these fractures. Sample V16-130, plane polarized light. Scale as shown.
- B. Sideromelane (S) and palagonite (P) with extensive fracturing in the sideromelane. Feldspar phenocrysts extend from the sideromelane into the palagonite. Hair-channels occur along the fractures and at the sideromelane - palagonite boundary. Sample V16-130, plane polarized light. Scale as shown.



A

200 μ



B

200 μ

photographs here, calcic-plagioclase laths extend from the sideromelane into the palagonite and do not show any alterations. Palagonitization proceeds around both feldspar and pyroxene phenocrysts. (plates 13, 14, 15). Feldspars showing exsolution features, commonly contain glass inclusions in the crystals (plate 16). These inclusions are sometimes altered to palagonite, but the original feldspar lath always remains fresh. Most of the fractures occurring in the sideromelane do not penetrate the feldspar laths, but stop at the feldspar-glass interface. In several cases the feldspars are fractured. They are mostly located in a palagonite matrix where large volume increases (due to hydration) probably initiate rupture. In several instances displacements in the feldspars can be shown to correlate with displacements in the palagonite in both direction and magnitude. Nevertheless, feldspars do not enter into the chemical reactions during palagonitization or during authigenic mineralization. The absence of phenocryst reactants during halmycolysis must play an important role in the overall availability of ions entering into authigenic chemical reactions. Authigenic mineralogy sometimes differs between magmas of different composition as shown by zeolites found by Morgenstein (1967) in the South Pacific and Iijuma and Harada (1969), in Hawaii. In sediments from the South Atlantic Ocean clinoptiolite was recognized as a major authigenic mineral product from the alteration of palagonite (Core V22-119). This zeolite has not been reported by either of the

Plate 14

- A. and B. Fresh feldspar phenocrysts in sideromelane. There are extensive fractures in the sideromelane, feldspars and in the palagonite. Both photographs are of V16-130. (Plane polarized light; scale as shown.)

Plate 15

- A. Sideromelane (S) and palagonite (P) with fresh feldspar laths in the palagonite. Palagonite banding is prominent. Sample V16-130, plane polarized light. Scale as shown.
- B. Exsolved feldspar in sideromelane. Some fracturing is present in the sideromelane but it is not extensive. Sample V22-227, plane polarized light. Scale as shown.



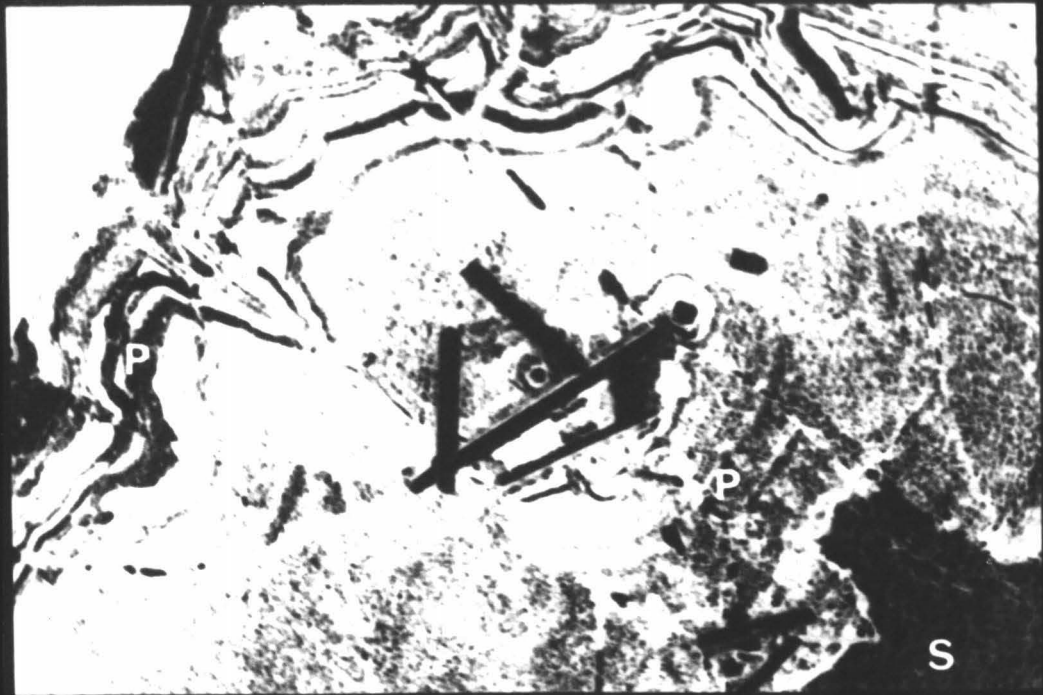
A

200 μ



B

300 μ



A

500 μ



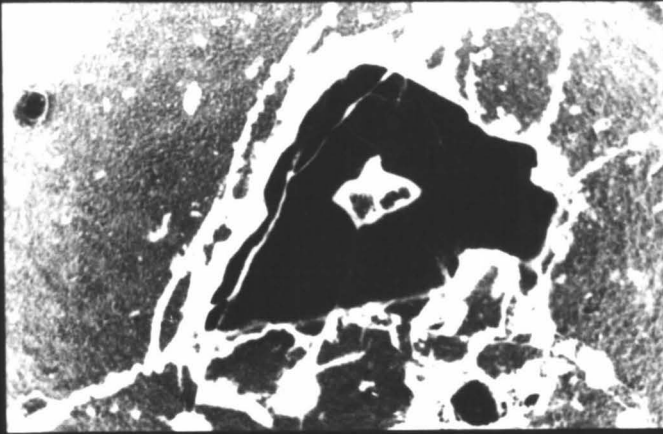
B

100 μ

PLATE 15

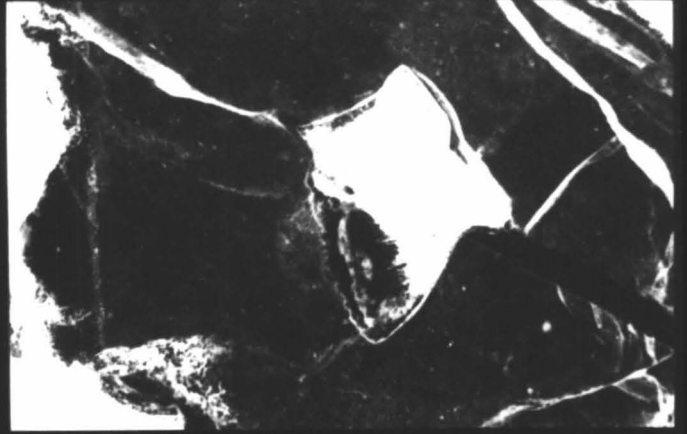
Plate 16

- A. Feldspar phenocryst in a sideromelane groundmass. The central portion of the feldspar contains a glass center which is under hydration. Sample V22-227, plane polarized light. Scale as shown.
- B. Feldspar phenocryst of figure A, showing the central glass inclusion in more detail. Sample V22-227, plane polarized light. Scale as shown.
- C. Feldspar phenocryst, with unusual symmetry, in sideromelane groundmass. Upper central portion of the phenocryst shows an altering sideromelane sphere. Sample V22-227, plane polarized light. Scale as shown.



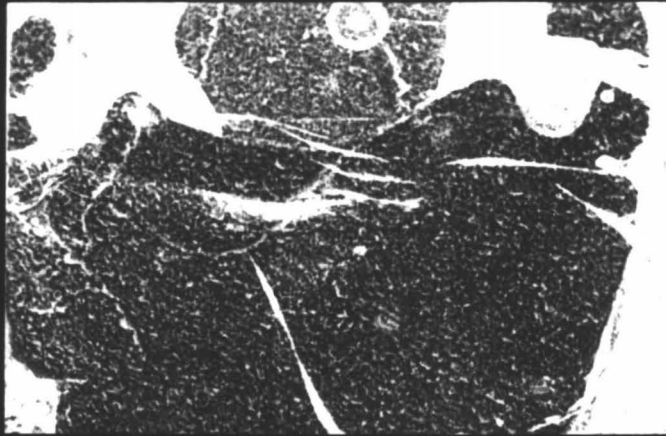
A

200 μ



B

100 μ



C

100 μ

PLATE 16

authors mentioned above. It is assumed that both the original magma chemistry, and the quantity and variety of phenocrysts which were crystallized out of the melt before quenching differs among these areas. The removal of major ions such as calcium, magnesium, and iron could very well affect the overall composition of the reactant- sideromelane. This would in turn affect the composition of palagonite and resulting authigenic minerals. However, these differences are mostly reflected in the authigenic mineralogy of the zeolite suite and not in the production of smectites or iron oxides. The major differences in authigenic mineralogy and thus lava composition occur mostly between oceanic and terrestrial source areas.

Discussion

The present investigation demonstrates that the chemistry of halmyrolysis of sideromelane in the Atlantic and Pacific Oceans is relatively constant and that the most marked deviations in chemical behavior during palagonitization occur between terrigenous weathering and oceanic weathering. In terrestrial decomposition of sideromelane (Table 4, page 9) sodium shows the largest change during hydration reactions. Potassium is the least affected in the alkali metal group (the periodic group which is most active during hydration). In Oceanic materials, potassium is enriched in the palagonite and calcium is depleted. Sodium shows little variation, but is in part lost during hydration. Moore (1966), reports that in Hawaiian samples during the replacement of basaltic glass

genous and oceanic hydration reactions is the decrease of potassium in the terrigenous decomposition product and an increase in the oceanic palagonites.

by palagonite, Na, Ca and Mn are lost, and K, Ti and Fe are gained. Moore's findings support the results obtained by microprobe analysis in this study. In addition to Moore's findings it is noted here that Si, and Mg are also lost, and O and in part Al are gained during palagonitization.

Moore (1966) suggests that the resultant chemical zoning in palagonites resemble ancient metamorphosed basalt pillows. He states that the zoning in these metamorphosed rocks are due to palagonitization which occurred prior to metamorphism. Miyrashero (verbal communication) suggests that the major difference between palagonites of terrigenous and oceanic origin is the quantity of potassium in the alteration product. He believes that potassium rich metamorphosed basaltic suits of old geosynclinal deposits originated as oceanic palagonites and that those suites depleted in potassium are possibly of terrigenous origin. If Miyrashero's tentative conclusions are further supported, there exists a method by which the origin of certain metamorphosed geosynclinal suites can be determined.

In laterites of east-central Puerto Rico, Briggs (1960) reported the relative increase of Al_2O_3 , Fe_2O_3 , TiO_2 , and H_2O , and a decrease in FeO , MnO , P_2O_5 , MgO , CaO , NaO and SiO_2 . Potassium oxide decreased slightly during lateritization. These lateritic soils were derived from a basaltic-andesite lava. These alteration reactions are similar to those described earlier for palagonites of terrigenous origin and support Miyrashero's contention that a major difference between terri-

FRACTURE ANALYSIS

Introduction

A study of the origin and distribution of fractures in basaltic glass was undertaken for the primary purpose of determining whether the fractures are of syngenetic or diagenetic origin. The overall affect of fracturing on the rate of sideromelane hydration was also investigated. The process of sideromelane solution to palagonite depends upon the length of exposure of glass surface area for sea-water interaction.

Lachenbruch (1962), Neal (1966), Tomkins (1966) and others have studied fracturing in semi-homogenous materials and have developed geometrical assemblages (figure 1) based upon experimentation and field observations of mud cracks. Lachenbruch (1962, p. 40) has developed the following classification of fracture patterns occuring in semi-homogenous materials:

Polygonal System

I Orthogonal Fractures

A. Random

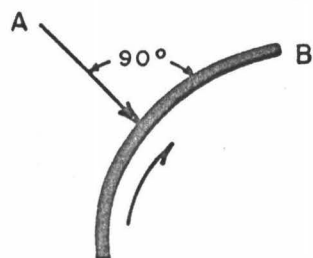
1. Regular
2. Irregular

B. Orientated

II Non-orthogonal Fractures

The new cracks in an area of rupture will follow randomly distributed zones of weakness (Lachenbruch, 1962). When the crack curves, the tangential stress component is greater on the convex side (Lachenbruch, 1962). Secondary fractures will form perpendicular to the greatest tension (the horizontal

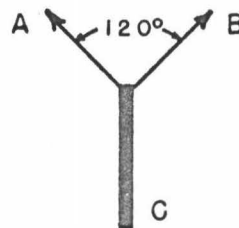
Figure 1
Polygonal System of Fracturing



Orthogonal Intersection

A is a secondary crack.

B is a primary crack.



Non-orthogonal Intersection

A and B are simultaneous

branches from crack C.

From data supplied by Lachenbruch, 1962.

tension is least in the direction perpendicular to the fractures at the time of failure), and will intersect the primary fractures at right angles. In "random" systems the initial and secondary fractures are not directionally oriented.

"Nonorthogonal" connections develop when one fracture splits into two (approximately 120° apart) during its propagation (Lachenbruch, 1962), (figure 1).

Griffith (1924), developed criteria which explain the propagation of fractures. He suggested that small cracks will generate into longer fractures because they are subjected to relatively higher stress concentrations at their terminus. In explaining the fractures of glasses, Griffith postulated that fracture occurs because of the presence of small cracks normal to the tensile stress.

Classification of Fracturing in Sideromelane

Several diagnostic varieties of fracturing were noted in the samples of sideromelane studied from the Atlantic and Pacific Oceans. The following classification is based upon observations of these samples and theories developed by the previously mentioned authors.

Classification of Fractures

1. Contraction Fractures: Produced during the initial cooling of the lava, (plate 17, and figure 1, page 58.)
 - A. Orthogonal Connections: Primary and secondary fracturing.
 - B. Nonorthogonal Connections: Primary fracturing.
2. Conchoidal Contraction Fractures: Produced by differential contraction arising from the differences in density of sideromelane and its phenocrysts. Syngenetic in origin. This variety of fracturing was first recognized by Nasedkin (1963), (plate 18).
3. Expansion Fractures: Produced by the increase in volume as the glass is hydrated. Orthogonal and nonorthogonal connections are represented with the former being more prevalent. These fractures are diagenetic in origin, (plate 19).

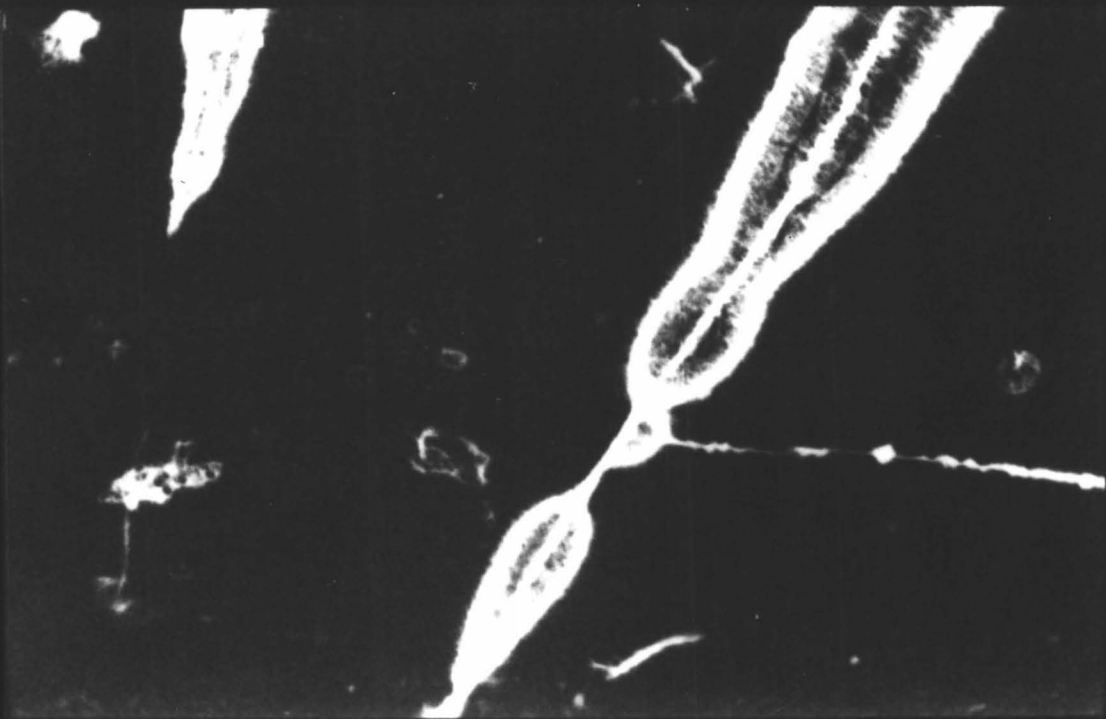
Plate 17

- A. A contraction fracture showing an orthogonal connection. Zeolites of the phillipsite group fill the fracture. Palagonite banding is prominent in the contraction cells. Sample V25-12-T3, crossed nicols, gypsum plate. Scale as shown.
- B. Contraction fractures with palagonite alterations along them. Solid solution border and hair-channel sector can be observed at the boundary between the palagonite and the sideromelane. Sample V22-227, plane polarized light. Scale as shown.



A

200 μ



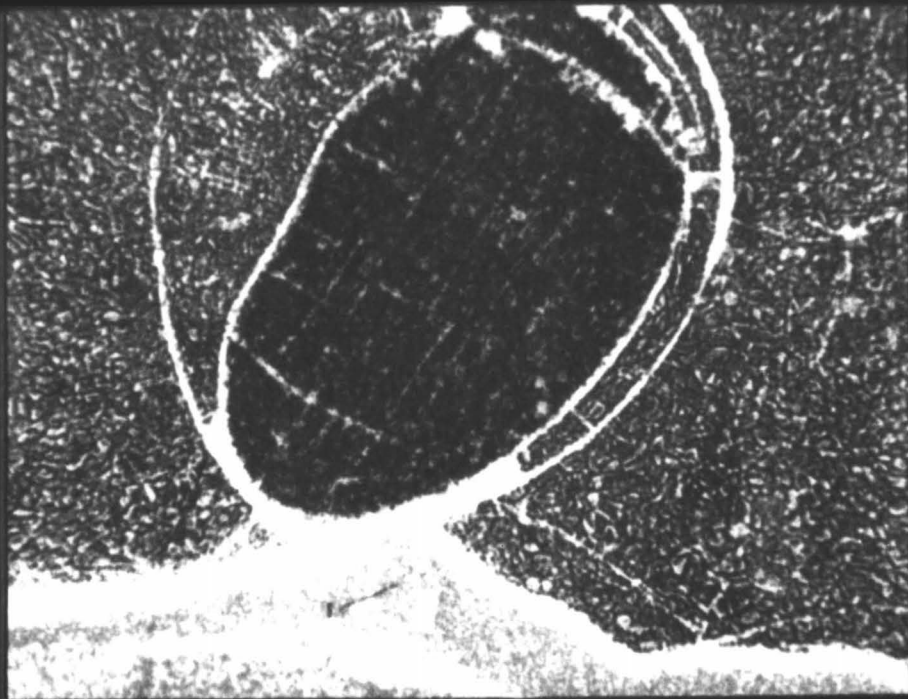
B

200 μ

PLATE 17

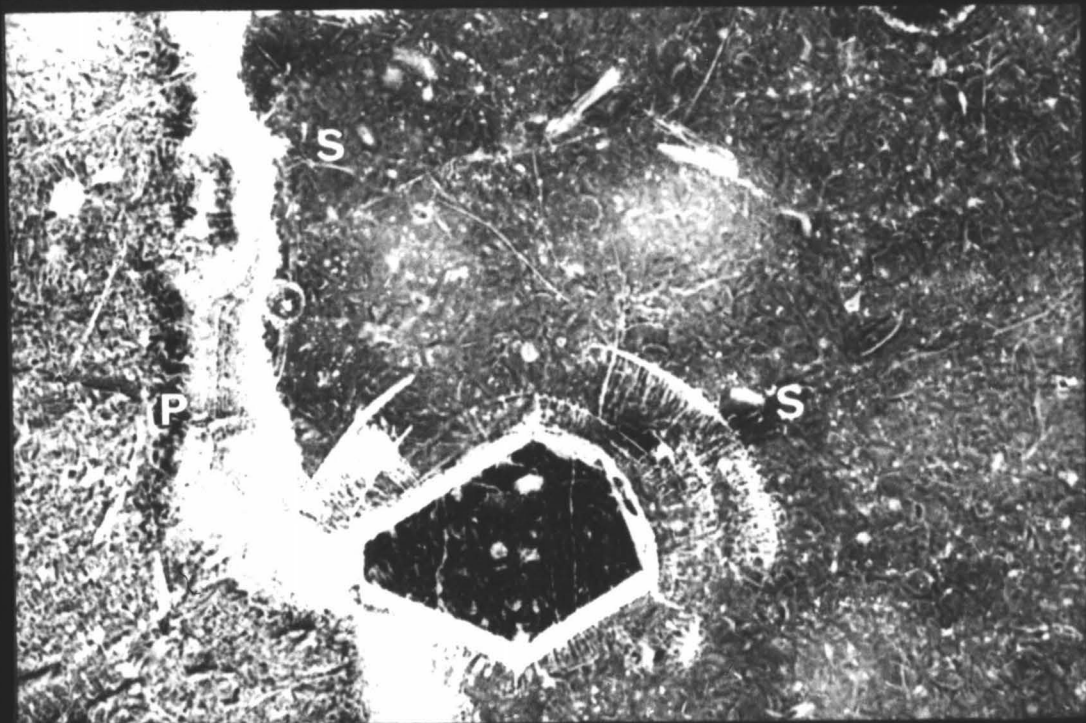
Plate 18

- A. Conchoidal contraction fractures around a feldspar phenocryst. The lower portion of the photograph is palagonite. A solid solution border and hair-channels are observed between the palagonite and the sideromelane. Alterations proceed along the conchoidal fractures. Fractures extending from the phenocryst to the conchoidal fracture are connected orthogonally and form after the conchoidal contraction fractures. Sample V25-12-T3, plane polarized light. Scale as shown.
- B. Conchoidal contraction fractures circumscribing a pyroxene phenocryst. Secondary fractures are orthogonal to the syngenetic conchoidal contraction fractures. Palagonite (P) and sideromelane (S) are separated by hair-channels and a solid solution border. Sample V22-227, plane polarized light. Scale as shown.



A

200 μ

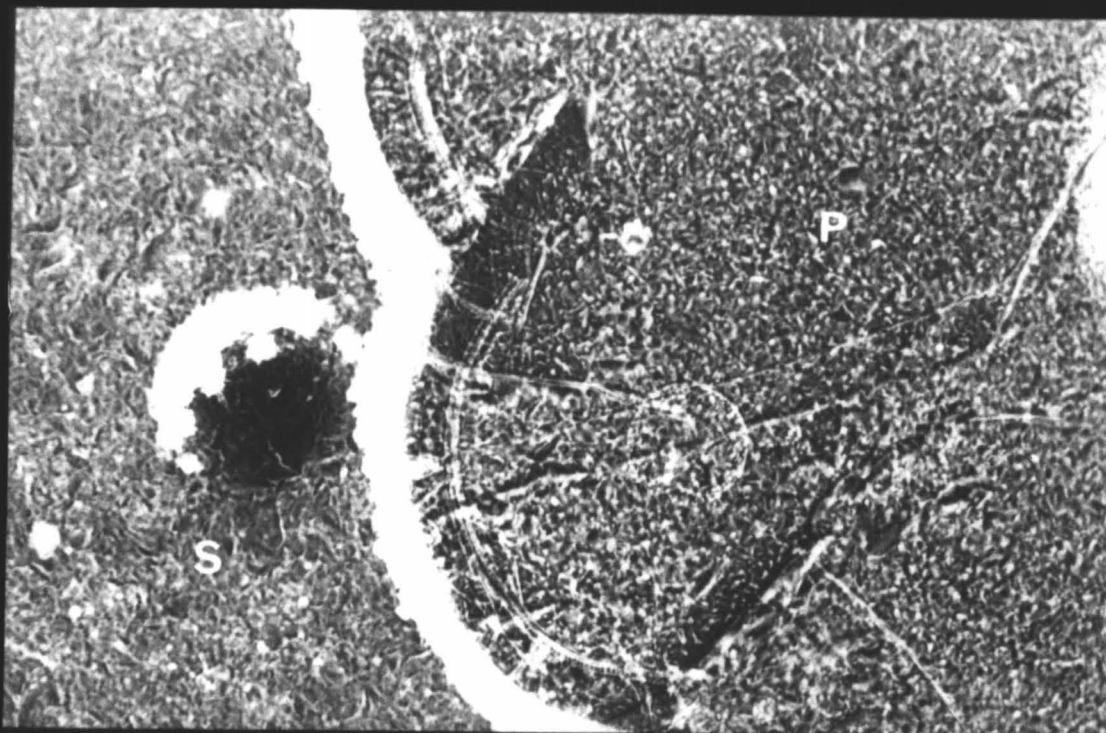


B

200 μ

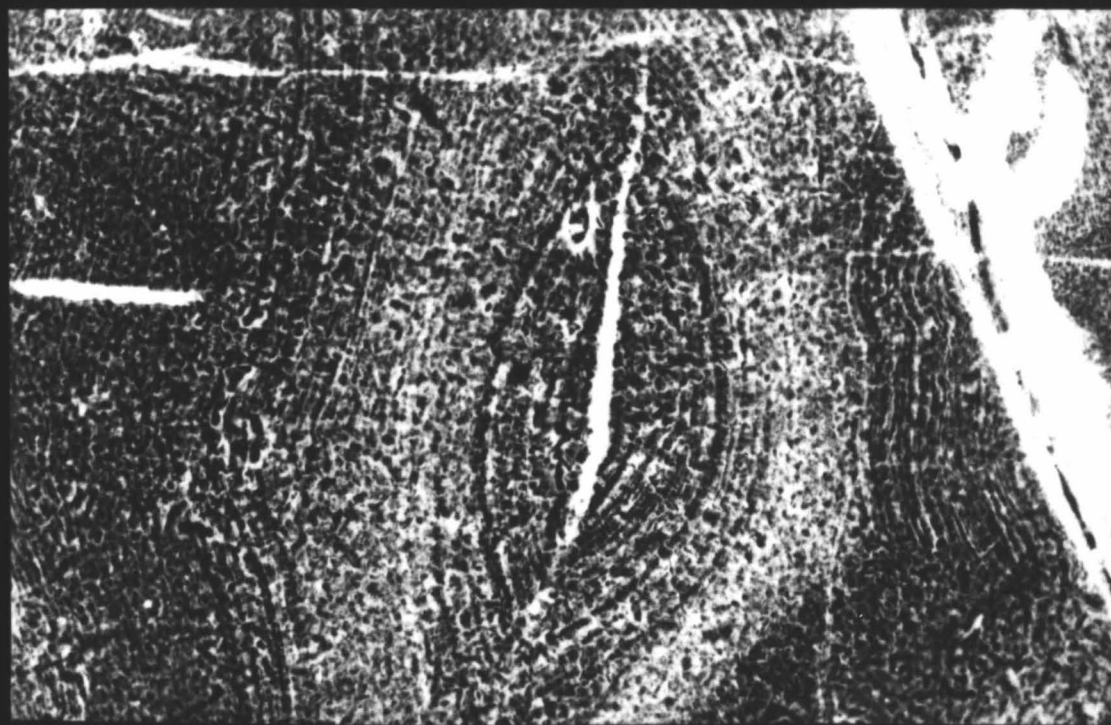
Plate 19

- A. Expansion fractures at the sideromelane (S) and palagonite (P) border. Secondary expansion fractures form at right angles to the primary expansion fractures. Sample V22-227, plane polarized light. Scale as shown.
- B. Expansion fractures in palagonite. Palagonite banding is observable around the fractures. Sample V22-227, plane polarized light. Scale as shown.



A

200 μ



B

200 μ

PLATE 19

4. Channel Microfractures: Produced during diagenesis by the expansion of the glass by hydration. These channels occur at the contact of the sideromelane and palagonite and grow at right angles to the contact. They are initiated by hydration of the glass and are propagated according to the Griffith (1924) criteria for fracturing. These microfractures have not been previously recognized. (plate 20)
5. Shear Fractures: Diagenetically propagated by the increase of volume during hydration. They develop as a release of stresses produced during palagonitization. Most of the shears are dependent upon the anisotropy of contraction and expansion fractures whereas some are geometrically controlled by the Mohr-Coulomb criteria for fracturing. For the latter case, movements are usually oblique and occur at acute dihedral angles to the greatest principal stress. Shear fractures have not been pre-

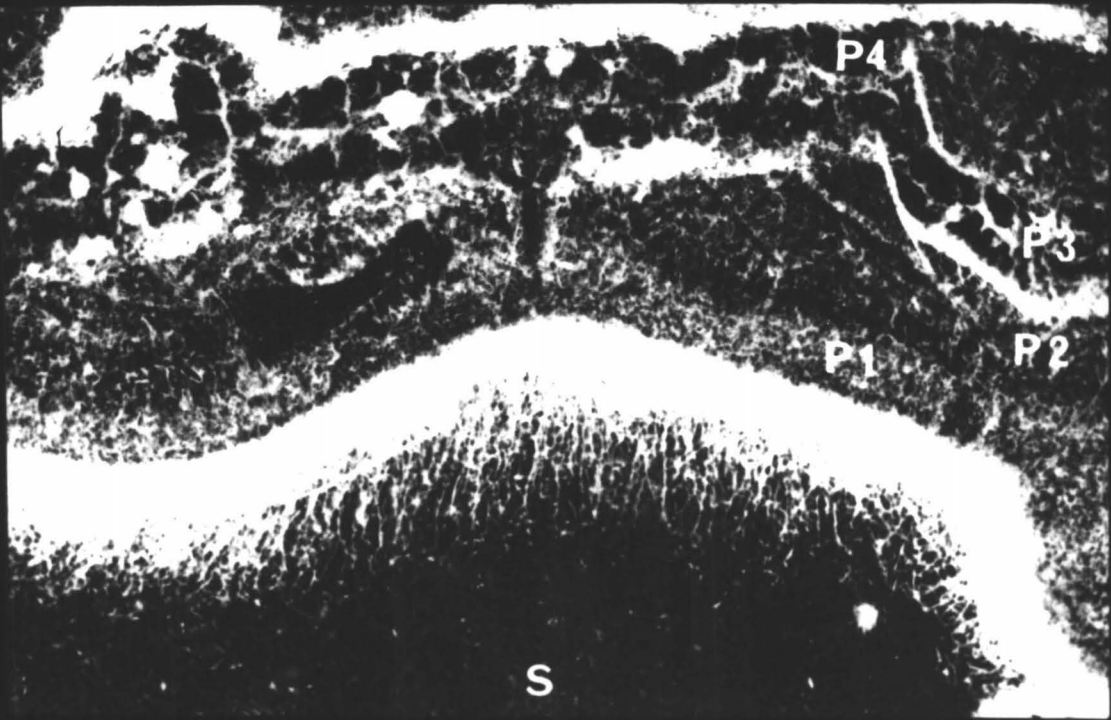
Plate 20

- A. Hair-channels growing from a major fracture.
Sample V22-227, plane polarized light.
Scale as shown.
- B. Hair-channels growing in sideromelane (S)
are separated from the first palagonite band
(P1) by a solid solution border. Other
palagonite bands are marked P2, P3, and P4.
The average thickness of each band is 50 u.
The average thickness of the solid solution
border and the average length of the hair-
channels are 50 u. Sample V22-227, plane
polarized light. Scale as shown.



A

50 μ



B

100 μ

PLATE 20

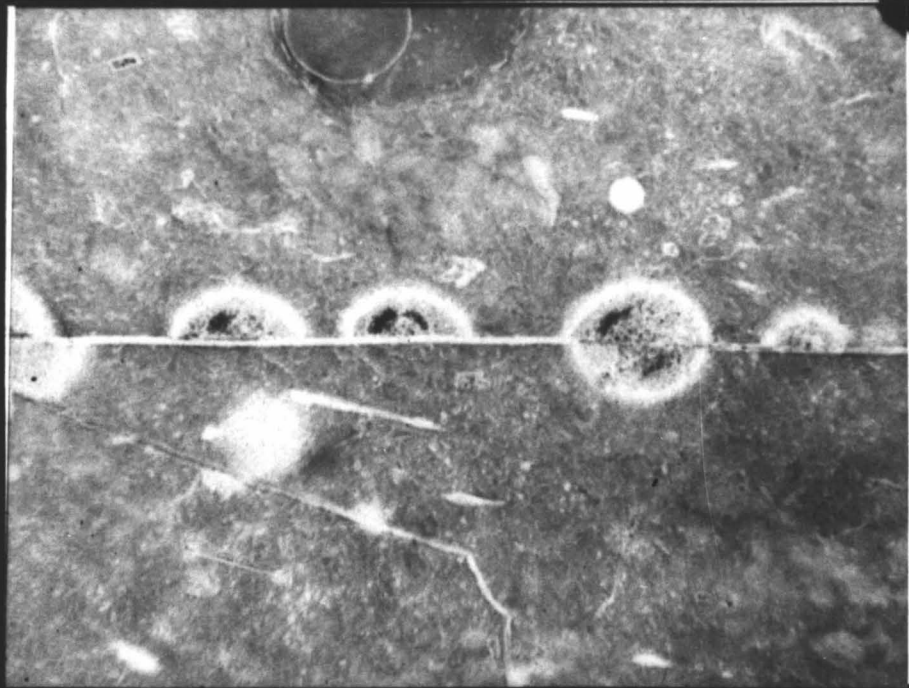
viously recognized in sideromelane and palagonite. (plate 21).

Discussion of Fracturing

In all cases, contraction fracturing occurs in response to syngenetic cooling of glass. Glass cooling is analogous to a shortening process since contraction reduces the surface area. Tensile fractures are in themselves a lengthening mechanism which develops in response to local shortening. The degree of shortening is dependent upon the localized contraction cells which develop for the most part as irregular orthogonal nets; and rarely as regular orthogonal or nonorthogonal configurations. The cooling of a basaltic lava on the sea floor causes fracturing and in itself increases the possibilities for extensive palagonitization (assuming that fracturing develops from contraction). During the transportation of the magma from its chamber to the surface, partial crystallization of rimmed calcioplagioclase feldspars and clinopyroxenes develop. Most of the phenocrysts show extensive exsolution features and in themselves are density stratified. (Plates 14, 15, 16) Stratification is due to Ca enrichment in the central portions of the phenocrysts. The phenocrysts are of higher density than the glass matrix and during cooling contraction fractures develop parallel to the phenocryst border outline. These fractures are due to differential density contraction. Many secondary orthogonal intersections develop in a radial

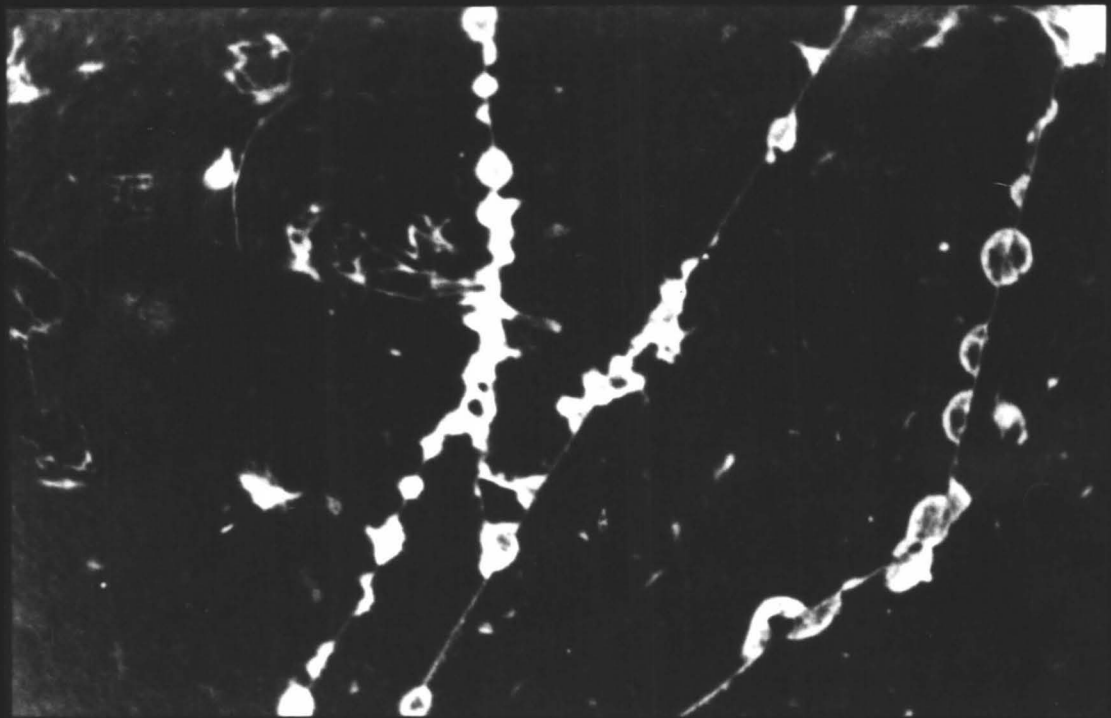
Plate 21

- A. Shear fractures with palagonite alterations along them. Sample V22-227, crossed nicols, gypsum plate. Scale as shown.
- B. Shear fractures with palagonite alterations. Apparent displacements can be seen in the areas of the palagonite alterations. Most movements seem to be oblique. Sample V22-227, plane polarized light. Scale as shown.



A

200 μ



B

400 μ

PLATE 21

splay from the phenocrysts to the concentric outer glass fractures (see plate 18). These secondary orthogonal connections may or may not be syngenetic; however, they have occurred after the primary concentric fracturing. One of the first to notice this variety of fracturing in volcanic glass was Nasedkin (1963) who found spherical cracking between zones of dissimilar density and suggested that these cracks were due to stresses built up between these zones. Using an electron microscope at a magnification of 11,000 diameters he also noted channels and channel-pores which did not exceed 200 A° in length. These microchannels are the paths which water takes during solid-solution-hydration. While studying devitrification of glass in tektites, Barnes and Russell (1966) also noted hair-channels developing concentrically from the central glass bubbles containing water vapor into the philippinite glass. In tektites, the zonation of micro-channels seems to be 20 u thick. (Barnes and Russell, 1966). In sideromelane these channel-fractures develop at an average of 50 microns in length (45 to 55 micron range) and are several microns wide. In cross-section they are conical, with their smallest end toward the glass and their largest toward the hydrated palagonite. Little doubt exists but that these micro-channels first develop chemically as channel pores during solid solution hydration and continue their evolution into larger and more conical features by a fracturing mechanism in which the fractures are propagated because they are subjected to rela-

tively higher stress concentrations at their terminus. Undoubtedly, the water filling the channel-fractures aids in developing differential stress concentrations by changing the pore pressure and thus aids in the overall fracture propagation. The concept of channel-fracture growth supports the contention that much of the palagonite observed in marine sediments is of diagenetic origin. Data further supporting this supposition come from observations of expansion fractures in sideromelane and palagonite samples. It has been well established in the proceeding chapter that sideromelane alters to palagonite through the process of hydration. As hydration proceeds there is an increase in volume. Two varieties of fracturing occur in response to this volume increase. One, expansion fractures, are tensile displacements whose configurations are similar to those described for contraction fracturing (orthogonal and non-orthogonal connections). The orientation of the stress field is however just the reverse - that is, the direction of the applied stresses differ in sign from positive to negative. Expansion fractures are oriented normal to syngenetic contraction fractures because the anisotropy of the syngenetic fractures control the stress configurations by controlling the direction of palagonitization. Syngenetic fractures act as conduits for sea-water entering the glass.

The second variety of fracturing which develops in response to volume increases is shear fracturing. Shears develop as an expression of lengthening, in response to differential

stresses exhibited through localized increases in volume. Most shearing shows measurable oblique displacements (apparent displacements) which develop sporadically, supporting the notion that a stress build up is necessary before movement can occur along previous fractures. (Plate 21) All of the shearing is localized phenomena which depends upon differential stress build ups in various contraction cells of sideromelane during its alteration to palagonite. The fact that shearing develops, again supports the supposition that diagenetic alterations are responsible for differential localized stresses and that these increases in volume are proportional to the surface area of fracturing.

Continuous increases in volume are resolved by tensile and shear displacements which geometrically supply more water for further palagonitization; thereby increasing the volume in a similar geometric progression. This volume increase controls further fracturing. The rate of palagonite formation in a three dimensional cell must therefore be proportional to the rate of induction of water through fracture assemblages. Since the fractures develop geometrically, the rate of supply of sea-water must also be geometric. If cellular configurations are not the case, and only one surface area is present for water diffusion, then palagonitization will proceed at a constant linear rate. The following chapter is devoted to the analysis of the rate of palagonitization.

Laboratory Fracturing Vs. Natural Fracturing

A series of experiments were performed to study the geometry of syngenetic fracturing in glass. Samples of fresh basaltic glass from the Mid-Atlantic Ridge were placed in silica tubing and heated to 1500°C, all volatile matter was drawn off and then the samples were cooled in dry air for five minutes. Both the basaltic glass and the glass tubing fractured during cooling. When laboratory fracture patterns of silica glass and basaltic glass are compared with those patterns produced during natural fracturing in basaltic glass little differences were noted. The overall fracture patterns are similar in that there is orthogonal and non-orthogonal connections. Orthogonal connections are however more numerous. Microchannels (hair-channels) are numerous in naturally fractured basaltic glass but are not present at all in laboratory fractured glass of either basaltic or rhyolitic composition. Plate 22 compares the typical fracture assemblage in natural glass (figure A) with that produced synthetically (figure B). Orthogonal connecting fractures are observed in both photographs. The experimental glass photograph shows typical contraction cells, and some non-orthogonal connections between fractures. The most striking difference between the two photographs is however the absence of hair-channels, in the lower photograph, and the extensive hair-channel network in the upper photograph. This indicates that hair-channels

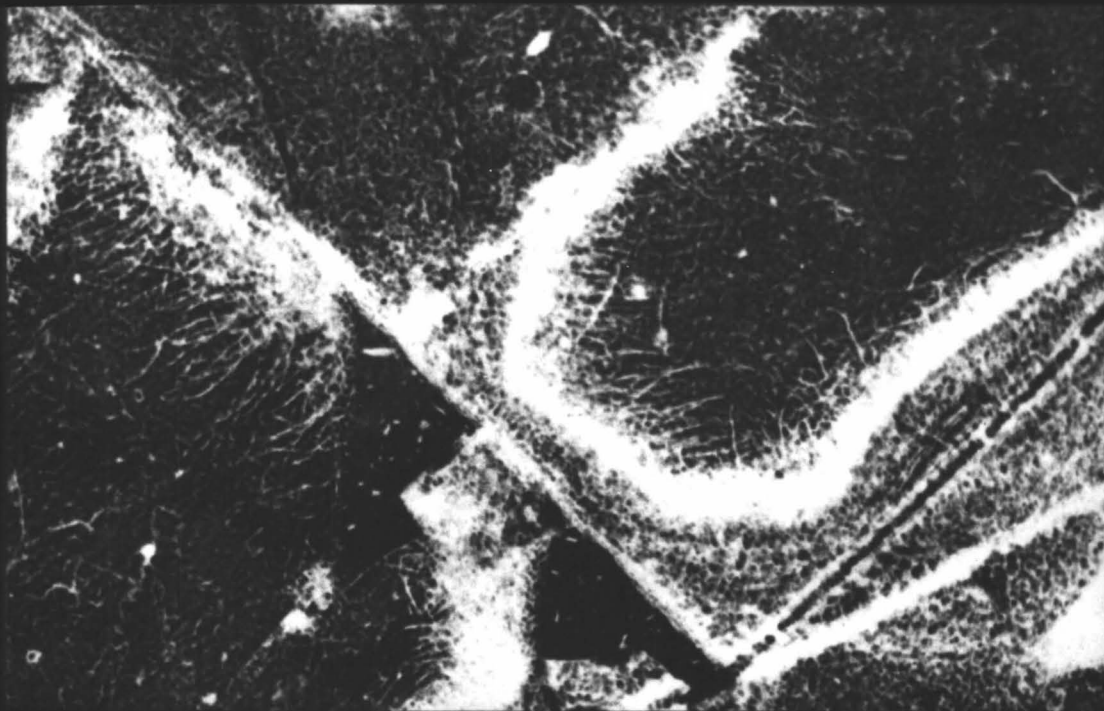
are diagenetic features and are not associated with syngenetic fracturing. Hair-channelling, when present, is always associated with palagonitization. It is logically concluded from this that banded palagonites (palagonites associated with hair-channels) are for the most part diagenetically formed. Some palagonite without typical banding may be formed during syngensis.

It was also noted that shear-fractures did not occur during laboratory experiments, but are numerous in naturally fractured glass. Shear fractures are therefore diagenetic in origin.

A photograph (Plate 23) of V22-227 is shown as a negative. White areas are palagonite. Dark areas are either fresh basaltic glass, or pyroxene and feldspar phenocrysts. Typical fracture assemblages are shown in this photograph. Most of the sideromelane cells are polygonal in outline. Differences in fracture width are easily noted. The wider the fractures the older they are. Feldspar and pyroxene phenocrysts remain unaltered, although several laths are fractured. Detailed photographs of selected areas of this thin section are shown throughout the text.

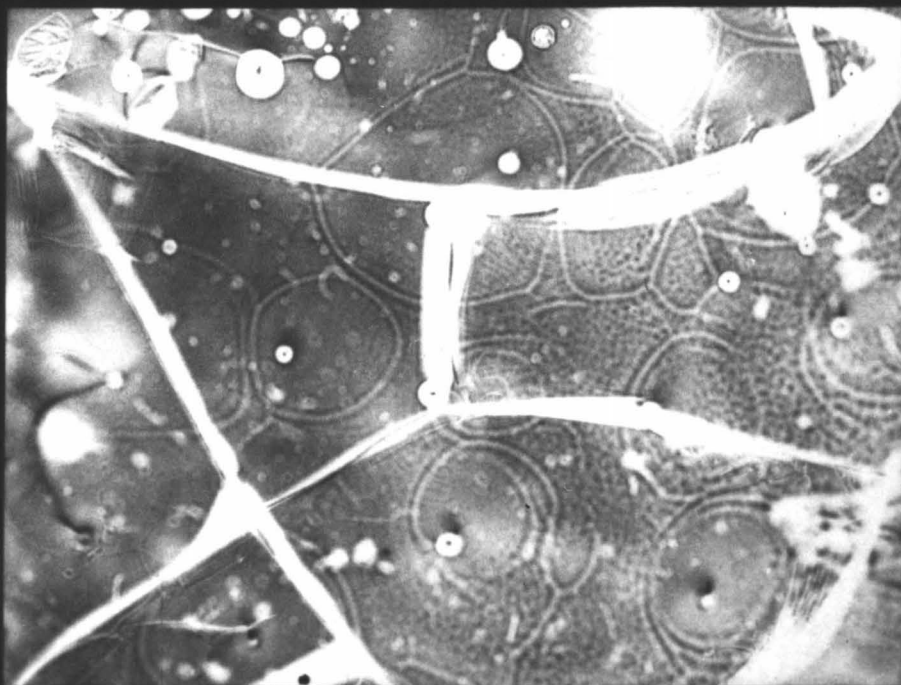
Plate 22

- A. Orthogonally connected fractures with palagonite banding, solid solution border and hair-channels. Sample V22-227, plane polarized light. Scale as shown.
- B. Laboratory fractured sideromelane with orthogonal and non-orthogonal fractures. Contraction cells in the sideromelane are also observable. Plane polarized light. Scale as shown.



A

100 μ



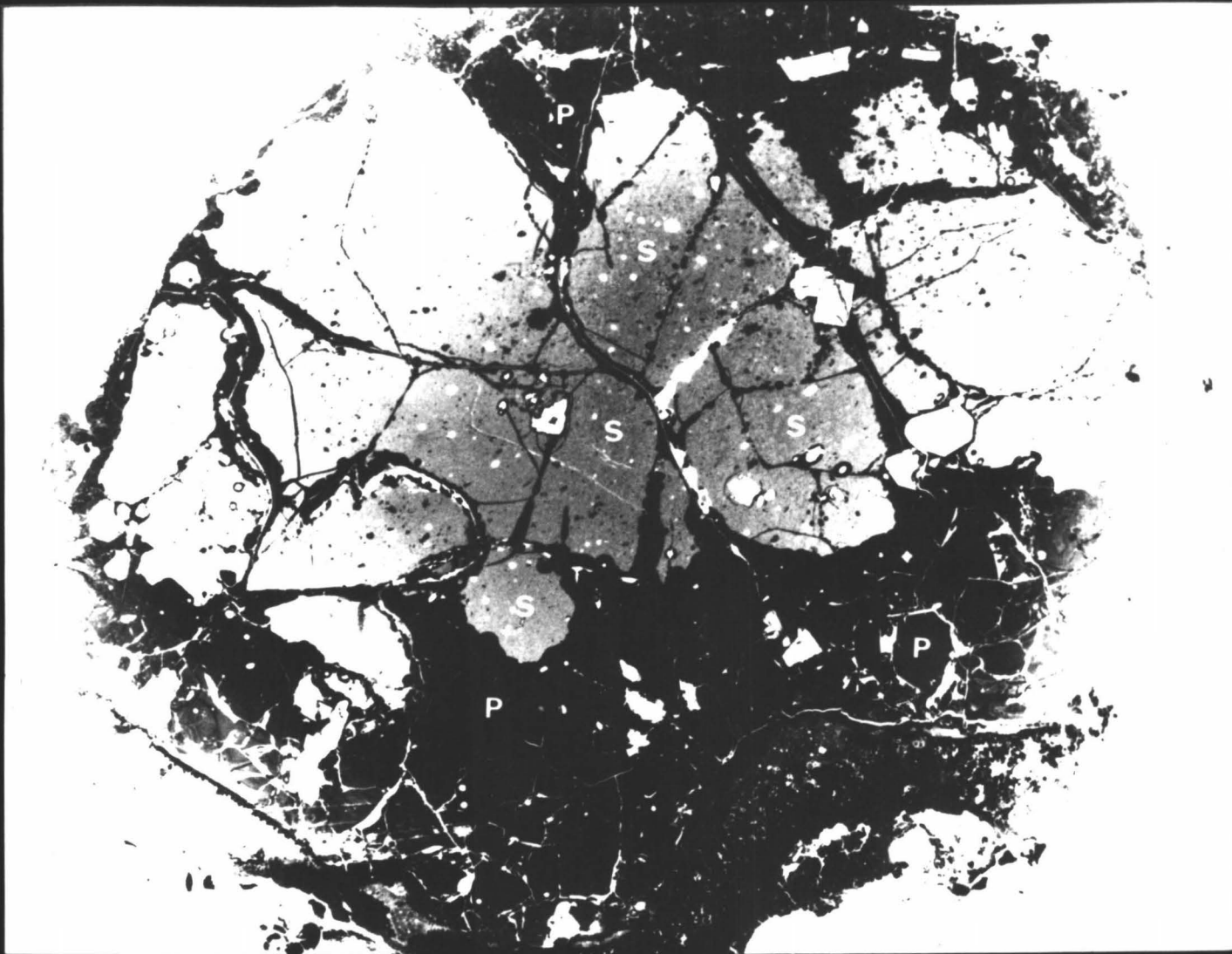
B

650 μ

PLATE 22

Plate 23

Photograph made from thin section negative shows typical sideromelane (S) cells with polygonal outlines, fracture assemblages and palagonite (P). Feldspar and pyroxene phenocrysts are abundant. Sample V22-227. Scale as shown.



1500 μ

PLATE 23

RATE OF PALAGONITIZATION OF SUBMARINE BASALTIC GLASS

Introduction

The rate of alteration of volcanic glass has been studied by several authors: Friedman and others (1966), Marshall (1961), Bonatti (1965), and Moore (1966). These authors used hydration curves for volcanic glass in hydrous and anhydrous environments and have attempted to define the limits of alteration by thermodynamic calculations of the diffusion coefficient of water molecules into glass structure for perlite formation, and by dating sideromelane through the use of reported manganese accumulation rates^t in deep-sea sediments. As a consequence two schools of thought have developed concerning the rate of palagonitization.

Marshall (1966) suggests that perlite forms at a rate of 2-5u/100 million years at temperatures less than 50°C.^{tt} (See figure 2) At higher temperatures^{ttt} (in the order of 200°C to 500°C) perlitization occurs in the order of 100 u/several hours to 1,000 years. Obviously, conclusions based upon Marshall's estimate suggest that the bulk of perlite is syngenetic and that diagenetic perlite occurs only in very minor quantities during long exposure through many Periods of geologic time.

t Moore used rates of manganese accumulation from Bender, and others (1966) which range from 2-3u/10³ yrs.

tt Marshall (1961) estimated that the diffusion coefficient at 20°C is similar in all natural glasses, and that it is of the order of 10⁻¹⁰ cm²/10⁶ yrs.

ttt The behavior of the diffusion coefficient as a function of temperature is shown by the equation: $D = D_0 e^{-E/RT}$

D = diffusion coefficient

D₀ = temp. independent part of the diffusion coefficient.

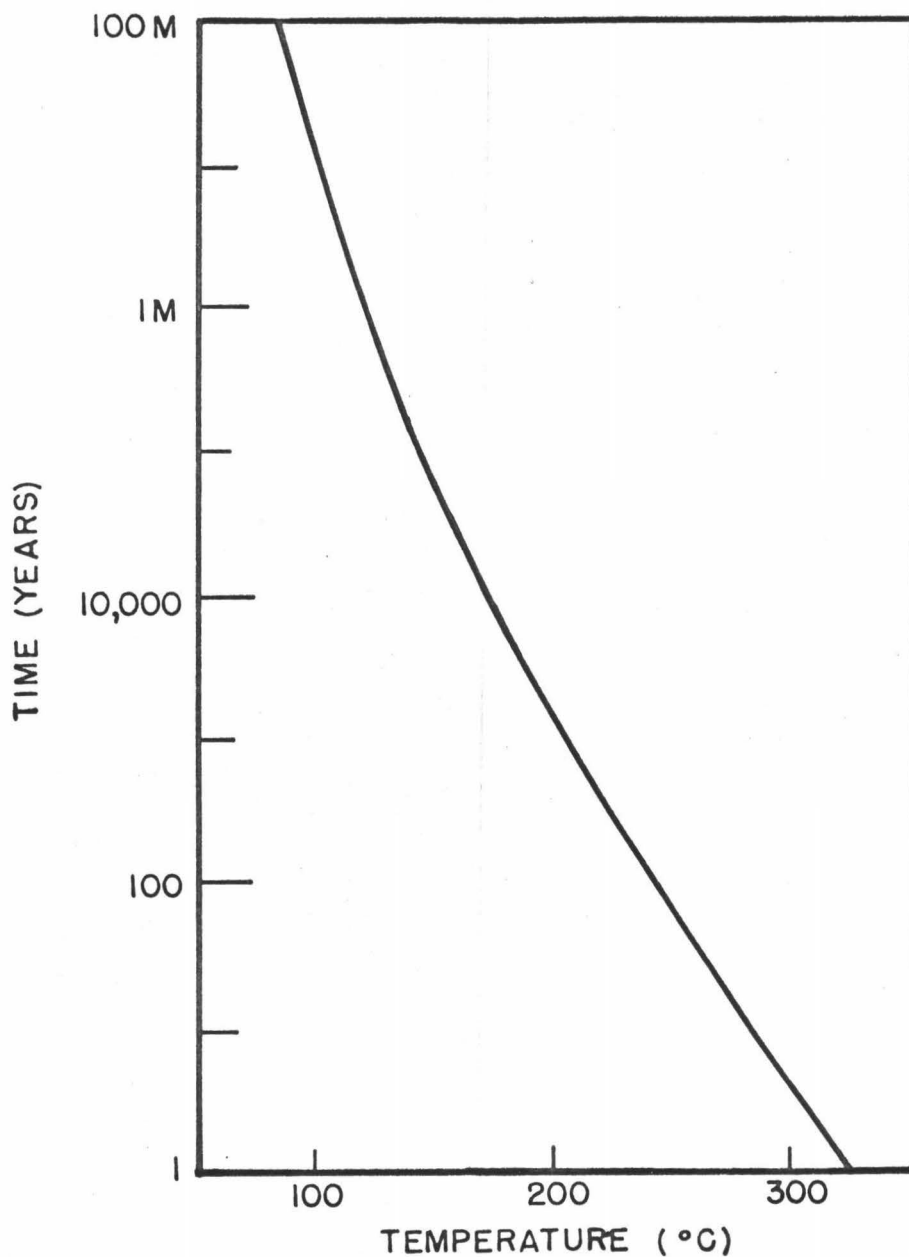


Figure 2

Time required for the hydrothermal reconstruction of perlite to a depth of 100 microns as a function of temperature. (After Marshall, 1961)

Bonatti (op. cit.) strongly supports Marshall's estimates and concludes that palagonite is a syngenetic product of sideromelane. He states: ". . . Underwater cooling of lavas is rapid. . . and palagonite is not a secondary product of sideromelane, but is formed directly during the interaction of hot lava with water." (Bonatti, 1965, p.9). Fuller (1932), Nayudu (1962), Silvestri (1963) and Bonatti (op. cit.) suggest that the only way palagonite may form as a secondary product

(diagenetically) is when it undergoes prolonged hydrothermal action connected with volcanic episodes.

In opposition to Marshall and Bonatti (1965), Friedman and others (1966) have developed strong evidence to show diagenetic perlite is the rule rather than the exception. They have recalculated the diffusion coefficient^t and have suggested that perlite forms in the order of 20 μ /40,000 years (μ /2,000 years) at 20°C.

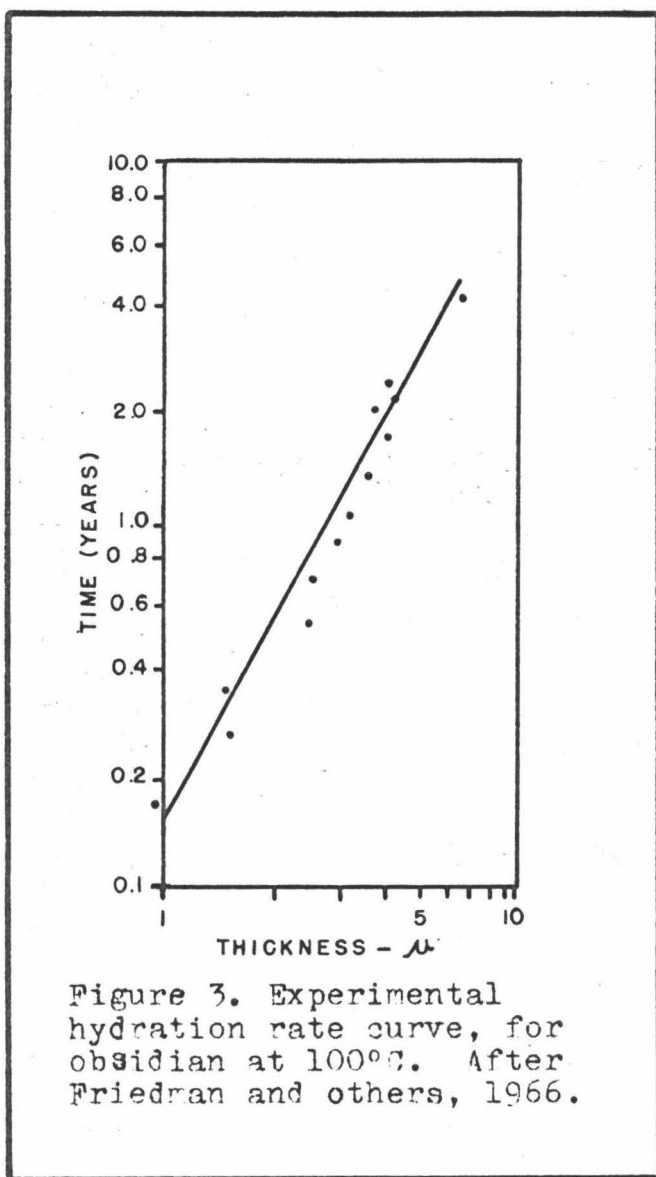


Figure 3. Experimental hydration rate curve, for obsidian at 100°C. After Friedman and others, 1966.

^t Their diffusion coefficient is $5 \times 10^{-5} \text{ cm}^2/10^6$ years at 20°C.

"Marshall assumed that the diffusion coefficient is independent of the concentration of water in glass. Our observation on the optical properties of perlite rims and obsidian cores appear to contradict this assumption" (Friedman and others, op. cit.)

Ross and Smith(1955) have concluded from a study of obsidian devitrification that perlite forms by secondary hydration after the emplacement of the original glass (obsidian).

Michels (1967) in a discussion of the historical development of this new dating tool for archeologists has reported several problems which affect the application of his (obsidian to perlite) alteration system to the (sideromelane to palagonite) system which we are most interested in. Michels states:

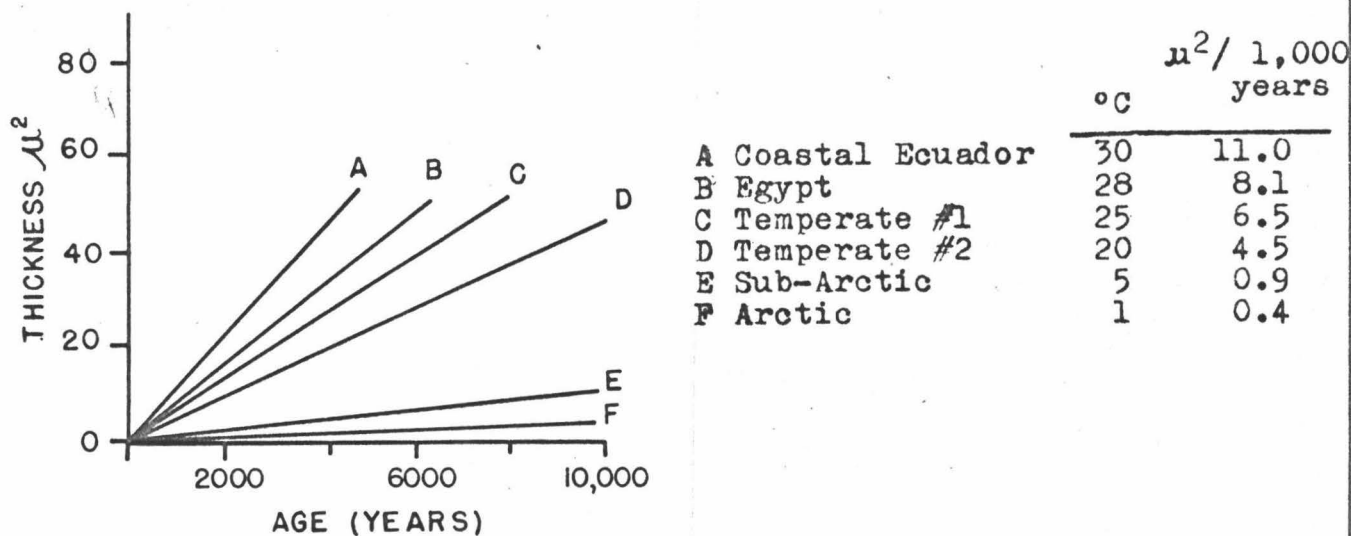


Figure 4. Hydration rate curves for obsidian artifacts of known age formed under different climatic conditions. After Friedman and others, 1966, p.324.

"It was discovered that the primary determinant of hydration rate is atmospheric or soil temperature, and since this is variable around the globe, separate rates of hydration would have to be established for each microenvironment. Different kinds of obsidian proved to have different rates of hydration under identical temperature regimes; and archeological application of the technique uncovered wide-ranging patterns of artifact reuse among prehistoric communities, which can interfere with dating unless compensated for." (Michels, op. cit., p. 211-212).

The archeologists undoubtedly have extensive problems due to reuse of artifacts. This, however, is not their basic problem, for the stringent temperature factors in hydration dating are much more numerous and critical. Glasses of different compositions give slightly different rates and therefore perlite formation rates cannot be extrapolated into palagonite hydration rates. For the most part, archeologists are dealing with terrestrial hydration which is slower than in oceanic or fresh water environments at similar temperatures.^t Secondly, mafic glasses alter at much faster rates than rhyolitic glasses because of the differences in the atomic bonding and the availability of large cations to provide atomic spaces for the water molecules to diffuse by solid solution.

The practicality and the reproducibility of the obsidian dating tool is however a major factor in the usefulness and validity of a new palagonite-sideromelane dating tool. Meighan and others (1968) have made carbon-14 dates and hydration analyses on obsidian tools from the Morret archeological site in Colima, Mexico. They assumed a linear rate of hydration

^t Friedman and others, 1966, state that the diffusion coefficient is dependent on the concentration of water in the glass. It must be assumed that the quantity of water in glass is dependent upon its environment of deposition. Bonatti (1965) states that in anhydrous environments hydration is minimal.

(years/microns). (Table 6) Friedman and Evans (1968) in a discussion of Mieghan's paper pointed out that hydration proceeds in a quadratic rate rather than a linear one, and they recalculated Mieghan's rate using the formula: Thickness² equals k time (microns²/year). Averaging the time span for the site, (C-14) values indicated 2050 years. Mieghan's hydration analysis indicated 1320 years and Friedman's recalculation showed 3,188 years. If the C-14 dates are valid, Mieghan's estimates are more correct. Archaeological data appear to support Mieghan's findings. (Mieghan, *AND OTHERS*, 1968a, and 1968b). Friedman's rate formula therefore, does not seem to be valid for this site. Friedman and Evans (1968) suggested using a $20 \text{ u}^2/1,000$ years rate for the Morret site. Based on their calculations in (1966) this indicates that the effective temperature for Colima, Mexico was greater than 30°C . It is interesting to note that the highest effective temperature published by Friedman and others (1966) is 30°C , and according to their calculations this yields a rate of $11 \text{ u}^2/1,000$ years. Friedman's temperature data does not support his rate formula and therefore, his results are not valid for the Morret site. Mieghan, on the other hand, is using a rate formula which is genetically consistent with both archeological and C-14 dates.

At least one other author has made a significant contribution to the palagonite dating problem. Moore (1966) has dated palagonite by hydration and has developed a rate formula

based upon manganese accumulation rates. Moore reports: "The thickness of palagonite as a function of time (T) in Kiloyears (Ky) may be defined by: $S = \sqrt{CT}$, where S is the thickness in microns, and C is a constant. The value of C ranges from 480 to 2,000 μ^2/Ky for Hawaiian submarine basaltic glass." (Moore, 1966, p. 163). His rate formula is based upon Friedman and others (1966), however the use of a constant manganese accumulation rate to date the age of the pyroclastics is somewhat uncertain. Much evidence is now available to show that manganese accumulation rates are not constant as reported by Bender and others (1966). (Bender, oral communication) Some manganese accumulation rates are, however, dependent upon palagonite hydration rates (Morgenstein and Felsher, in preparation).

Both Moore (1966) and Friedman and others (1966) use a quadratic rate formula for hydration rim dating. The significance of the quadratic formula lies in the belief that water diffuses into the glass structure at an increasingly slower pace as the thickness of the alteration layer increases. Friedman and others (1966) believe that this rate of diffusion is reproduced every 20 μ in the perlite structure. We have seen in chapter 1 that the rate of palagonitization does not proceed in the manner described by Moore (1966) and Friedman and others (1966). Again, the theory behind a linear rate for sea-water hydration in sideromelane is based upon the concept that as hydration proceeds, the material which has been

hydrated will pass water onto the areas which are undergoing alteration without any difficulty due to the short distance of transport. The solid solution border is more hydrated than the hair-channel sector and this area contains a greater content of water than the sideromelane. As palagonite becomes older it increases its water content, and thus, it is easier for water to travel through the alteration material as time increases. The rate, however, of palagonitization is dependent upon the slower rate of hydration at the hair-channel sector. Thus, Mieghan and others (1968a and 1968b) are using a more correct rate formula than Friedman and Evans, 1968, because it is linear and not quadratic.

Rate Formula Development

Rate formulas for the devitrification of sideromelane are developed by studying the geometry of palagonite formation. The rate of palagonitization does not equal the rate of sideromelane devitrification, nor is it a quadratic expression as suggested by Friedman and others (1966), and Friedman and Evans (1968). The diagram below (figure 5) is a sketch of sideromelane glass altering to palagonite using hypothetical numbers for the ease of calculation and clarity. Ten stages of palagonitization and twelve stages of hydration are shown. For the first two years of hydration (T1 and T2) the sample does not produce any palagonite. In the first year a 0.1 u band of hair-channels forms. In the second year this band of hair-channels is replaced by a band (0.1 u thick) of solid

Table 6

Morret Site, Colima Mexico Meighan, 1968 ^{tt} (u/years)													Deviation from C-14 in years	
Pit	Level	No. of C-14 Date	C-14 Yrs. Ago	No. Obsidian Readings	Av. hydra- tion u	Rate * yrs/u	Age yrs. ago u/time	Friedman and Evans, ^{ttt} (u ² /yrs)				Yrs. Ago	Meighan	Friedma
								Hydration u ²	Rate u ² /1,000yrs	Rate yr/u ²	Yrs. Ago			
2	120-160	1	1950	2	6.1	320	1952	37.21	13.9	72	2,678	+2	+728	
3	100-120	4	1500	8	5.8	260	1508	33.64	22.42	44.5	1,497	+8	-3	
3	140-160	1	1600	11	5.8	260	1508	33.64	20.10	49.5	1,671	-92	+71	
4	160-200	1	2025	3	6.5	310	2015	42.25	20.86	46	1,944	-10	-81	
7	220-280	3	2180	1	8.0	270	2160	64.00	29.35	34	2,176	-20	-4	
Span	120-280	16 ^t	750 _{BC} -1300 _{AD}	115	3.7-8.8	---	330BC- 990AD	13.69- 77.44	20.0	684BP- 50	3872BP	+310BP -420BP	+16 -1,154	
		---	668BP- 2718BP	---	---	---	978BP- 2,298BP	---	---	---	680BP** 3850BP	---	---	
	Duration of site in yrs.		2050 yrs.	---	---	---	1,320yrs.	---	---	---	3,188 yrs	-730	+1138	

^t Meighan and others, 1968, table 2, page 1073

^{tt} Meighan, 1968, table 1, page 1070

^{ttt} Friedman and Evans, 1968, Discussion, pages 813-814

* To nearest 10 years - the average hydration - rate to the nearest year is 284 years/u

** Dates reported in literature; recalculated

solution border and a new 0.1 u thick band of hair-channels is formed. During the third year of hydration (the first year of palagonitization) a 0.1 u band of palagonite replaced the solid solution border. A new solid solution border replaces the old hair-channel sector and a new hair-channel sector is formed. In the second year of palagonitization there is 0.2 u of palagonite (two bands) and the further development of a new solid solution border and hair-channel sector. As time continues the rate of palagonite production remains constant.

Derivation of the Rate Formulas

All data used in the derivation of the rate formulas are from the simplified model in figure 5.

Terms Defined

N = Number of palagonite bands
 Q = Thickness of each band
 T = Age in years
 R_p = Rate of palagonitization
 R_h = Rate of hydration

Rate 1 For the 1st State or Fraction of State of Palagonitization

$$R_p = NQ/3T \quad (I)$$

$$\text{lim. 1} = N < 1$$

example: $R_p = NQ/3T$
 = one stage (.1u thickness)/3 (one year)
 = (1) (.1u)/3 years
 = .1u / 3 years
 Time/u = 30 years/u

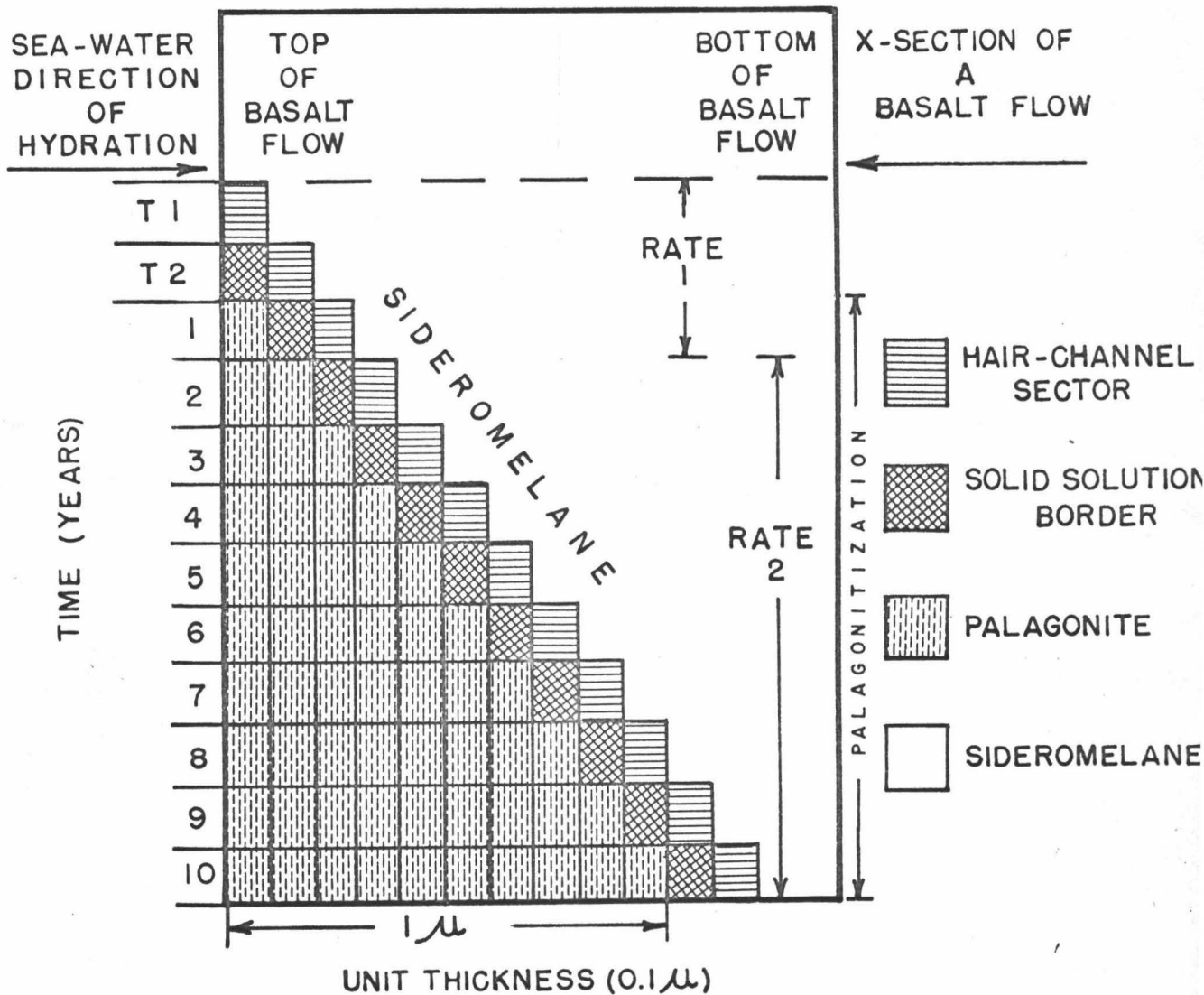


Figure 5. Staged formation of palagonite by the development of hair-channels and solid solution border. T 1 and T 2 represent a total of two years of hydration. Numbers 1 through 10 represent years of palagonitization.

Rate 2 For the Second and Subsequent Stages

(II)

$$R_p = NQ/T$$

lim. $N > 1$

example: 1. (for two years)

$$R_p = (2) (.1u)/2 \text{ years}$$

$$= .2 / 2 \text{ years}$$

$$= .1u / \text{years}$$

$$\text{Time}/u = 10 \text{ years}/u$$

example: 2. (for 10 years)

$$R_p = (10) (.1u)/10 \text{ years}$$

$$= 1u / 10 \text{ years}$$

$$\text{Time}/u = 10 \text{ years} / u$$

Rate 1 + Rate 2 Total Rate of Palagonitization

(III)

$$\Sigma R_p = (N-2)Q/T$$

example: 1. (for 10 years)

$$\Sigma R_p = (N-2)Q/T$$

$$= (10-2)(.1u)/10 \text{ years}$$

$$= 8 (.1u)/10 \text{ years}$$

$$= .8u / 10 \text{ years}$$

$$= .4u / 5 \text{ years}$$

$$\text{Time}/u = 12.5 \text{ years}/u$$

example: 2. (for 50 years)

$$\Sigma R_p = (N-2)Q/T$$

$$= (50-2)(.1u)/50 \text{ years}$$

$$= 4.8u/50 \text{ years}$$

$$\text{Time}/u = 10.4 \text{ years}/u$$

example: 3. (Time = 10^6 years)

$$\Sigma R_p = (10^6 - 2)(.1u)/10^6 \text{ years}$$

$$\text{Time}/u = 10^2/10^6 \text{ years}/u$$

Dealing with time in millions of years the expression

$$\Sigma R_p = (N-2)Q/T \text{ approaches the linear rate } R_p = NQ/T.$$

Rate of Hydration Measured from Palagonite Thickness

$$R_h = (N + 2) Q/T$$

example: 1. (one year)

$$\begin{aligned} \Sigma R_h &= (1+2)(.1u)/1 \text{ year} \\ &= 3(.1u)/1 \text{ year} \\ &= .3 u/\text{year} \\ \text{Time}/u &= 3.33 \text{ years}/u \end{aligned}$$

example: 2. (10 years)

$$\begin{aligned} \Sigma R_h &= (10 + 2)(.1u)/10 \text{ years} \\ &= 12(.1u)/10 \text{ years} \\ &= 1.2u/10 \text{ years} \\ &= 0.12u/\text{year} \\ \text{Time}/u &= 7.5 \text{ years}/u \end{aligned}$$

In summary, three palagonitization rate formulas are derived and one rate formula for hydration is formulated. The first formula (I) is only applicable to the first stage of palagonite formation. The second formula (II) applies to the palagonite rate after but not including the first stage of palagonitization. The third formula (III) averages the entire rate of palagonitization from the first stage to N number of stages.

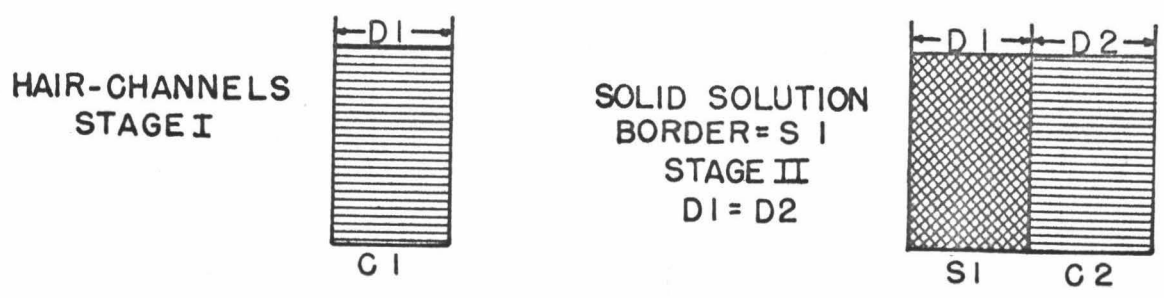
Two different rates for palagonitization exist even though there is a constant rate for hydration of glass. (Figure 5) Friedman's formula states that the thickness squared per time is the actual rate of hydration in obsidian glasses and that this rate is equal to the rate of perlite formation, for one band of thickness. He states:

"Many natural perlites have shell thickness of about 20u. Using our hydration rate equation for the diffusion coefficient determined from (a graph of the activation energy of hydration), we find that at 22°C it would

take about 40,000 years for a 20u thick hydrated surface to form an obsidian. After that period of time we believe that the stress would be so great that a crack would form at the interface between the hydrated and unhydrated glass and the process of hydration would start again. In 200,000 years, then, five 20-u shells, or a total thickness of 100 u of hydrated material, might be formed. This would mean that the obsidian piece would have been reduced by twice 100 u or by 0.2mm; if the greatest distance between cracks in the original obsidian was 0.2mm then the obsidian in our own hypothetical model would have been replaced by perlite in 200,000 years." Friedman and others, 1966, p. 326.

Friedman recognizes banding in perlite and attributes the bands to the tensile fractures developed at right angles to the palagonite growth surface. This is the second point where Friedman's model differs from the model proposed here. According to the Mohr-Coulomb criteria for fracturing, extension fractures will develop parallel to the greatest principal stresses. The greatest principal stresses are acting perpendicular to the axis of the banding and therefore the bands cannot be products of stress release by fracturing. The bands are an expression of the multiple stage development during hydration and are of constant thickness because the rate of hydration is constant. When the hydration rate changes the band thickness also changes. The time it takes for one stage of hydration to travel the distance, D_1 , of one band-width equals the time it takes for the second stage of hydration to travel the same distance. Therefore, the banding observed in perlite is not fracturing but rather due to differences in the

FIGURE 6
HAIR-CHANNEL AND SOLID SOLUTION BORDER DEVELOPMENT



amount of hydration. The observed banding is a measure of the degree of diagenetic crystallization of smectites, iron oxides and zeolites. The degree of crystallization is a function of ion migration. Ions migrate much more easily in a hydrated environment than in one which is not. In the above sketch (figure 6) S_1 has taken the place of C_1 , and C_2 developed during the time of the transfer of hair-channels (C_1) to a solid solution boarder (S_1). Since the rate of glass hydration is a function of the thickness of the hydrated glass bands, it follows that the rate of hydration between two chemically different glasses should have different banding widths. This is in fact what is observed between obsidian and sideromelane. Perlite is banded at approximately 20 u (Friedman and others 1966) whereas palagonite has bands averaging about 50 u in width. From this information we would expect that palagonitization is more rapid than perlite formation under similar environmental conditions. This is confirmed in the following section.

Of further interest, is the rate of zeolitization, or the rates of limonite and smectite formation. These rates will be dependent upon the rate of hydration which is defined by the

formula: $R_h = (N+2)Q/T$.

Rate of Palagonitization

The following discussion concerns the rate of palagonitization in marine and lacustrine environments. Table 7 reports the vital information for those samples studied for rate evaluation. The best available data for an age date for marine samples containing palagonite comes from sample A150-RD8, taken on the flank of the Mid-Atlantic Ridge (130 Km East of the axis of the Ridge) in water depths of 3700 meters. Saito, and others (1966) have dated the A150-RD8 dredge sample and found it to be early to Mid-Miocene based upon diagnostic foraminifera (*Globoquadrina dehescens*) within the sideromelane fractures (Plate 24). They have concluded that the basaltic glass was emplaced after the deposition of the Lower to Mid-Miocene sediments. Late Miocene and younger sediments coat the outer portion of the A150-RD8 dredge samples but are not associated with the interstitial fractures. A general age date based upon these findings suggests that the sample is 15 ± 3 My. old. Forty-two millimeters of palagonite was measured on the sample and represents the amount of palagonite formed since the emplacement of the volcanic flow. (Figure 7) A crust of 30 mm of manganese occurs above the palagonite and acts as a deterrent to submarine erosion. Using a general rate formula for palagonitization $\Sigma R_p = (N-2)Q/T$, the rate of palagonite formation is:

$$\begin{aligned} \Sigma R_p &= (840-2) 50u/15my \\ &= 4.19u/1,500 \text{ years} \\ &= 2.79u/1,000 \text{ years} \\ \text{Time}/u &= 358.2 \text{ years}/u \end{aligned}$$

Table 7

Thickness of Palagonite and Manganese in Samples Studied

Sample	Palagonite thickness u	Manganese in u
A150-RD8 ^t	42,000	30,000
Lake Motosu, Japan ^{tt}	9	-
V22-227	12,000	7,000
V16-130	5,000	10,000
V16-130	4,000	11,000
RC8-D9	5,375	4,500
RC10-110	6,000	-
V25-12-T3	3,500	750
V25-12-T11	6,000	2,000
V25-13	4,000	50
V16-SBT3, Manganese Nodules	2,000	6,000
" " "	3,500	5,000
" " "	3,500	4,000
" " "	2,500	6,000
" " "	3,000	5,000
" " "	2,000	5,000
" " "	2,000	5,000
" " "	1,500	4,000
" " "	3,500	5,000
5-9-16	750	-

t Age of A150-RD8 is 15⁺ 3 million years. (Saito and others, 1966)

tt Age of the Japan sample is 1,101 years (Tsuya, 1938 as reported in Moore, 1966)

Plate 24

Sample A150-RD8, showing extensive fracturing in palagonite. Foraminifera, zeolites, limonite and smectites fill the fractures. There is a manganese coating on the weathered outer surface of the sample. Scale as shown.

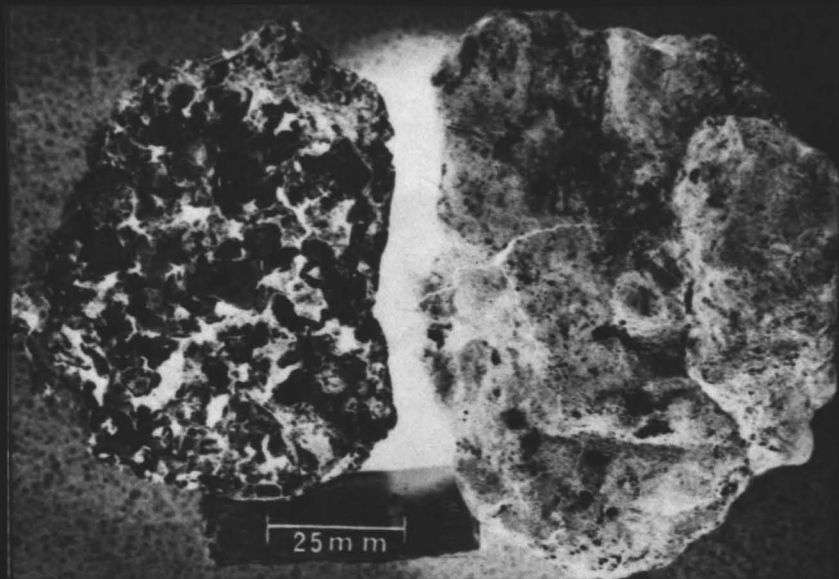


25mm

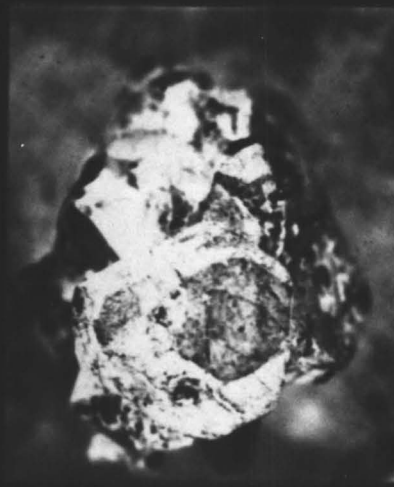
PLATE 24

Plate 25

- A. Sample RC8-D9, the sample on the left is a palagonitized basalt with extensive zeolite crystals coating the fractured networks. Manganese crusts coat the zeolites. The sample on the right is a manganese nodule which contains a high concentration of palagonite. Scale as shown.
- B. Pigeonite crystals which were removed from the palagonite in RC8-D9. They are unusually large and well preserved. Scale as shown.



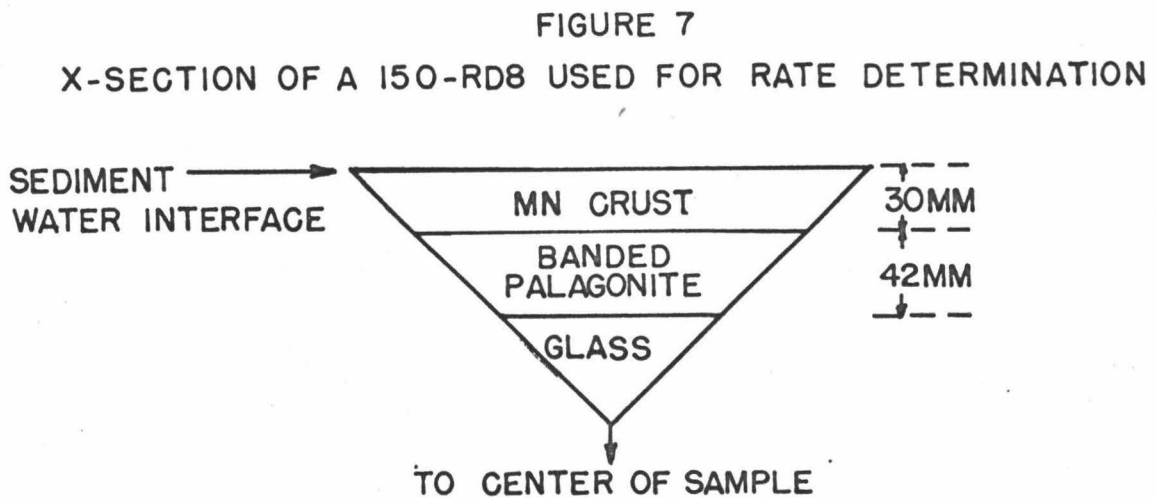
A



B

PLATE 25

Table 8 reports the rates of palagonitization derived from the use of all four rate formulas for the possible ranges in ages of A150-RD8 and for the Japan Sample with a known date of 1,101 years. This data is consistent with the theoretical rates based upon the differences of perlite and palagonite banding. As suggested earlier, palagonitization rates should be more rapid than perlitization rates for similar conditions since the average width of the perlite bands is 20 μ and the average width of the palagonite bands is 50 μ . Marshall (1961) estimated that it is easier to hydrate glasses which are mafic than those which are acidic because the silica, oxygen, and aluminum cross bonds are more numerous in the acidic glasses. Marshall's (1961) conclusion supports the findings here and further suggests that the rate formulas used in this study are genetically consistent with those samples studied. Hydration curves for obsidian and sideromelane are plotted on figure 8



and show the dependence of hydration rates on the effective temperature as well as the general higher rate of palagonite hydration to that of obsidian in both marine and lacustrine environments. The hydration curve for palagonite is drawn parallel to the slope of the obsidian curve. Two data points on the palagonite curve define the position of the curve on the x and y coordinates. The obsidian curve was drawn from data published by Friedman and others (1966) and contains five data points. Both curves should slope evenly since the same process of hydration of glass is shown. The only difference is the rate at which the different glasses hydrate.

Figure 9 shows the rate for palagonitization for all conditions of palagonite thickness. Figure 10 reports the mean rate for palagonitization in the marine environment. Samples from both the Atlantic and Pacific Oceans are plotted on this curve (Figure 10) and their relative ages are interpolated. Those samples from the Bellingshausen Basin are between one and three million years old suggesting that volcanism was probably extensive during the Late Pliocene in that region.

Sample V22-227 is located on the eastern flank of the Mid-Atlantic Ridge. Saito, and others, (1966), have dated samples surrounding V22-227 and have arrived at a Pliocene date for all outcrops in that area. It is therefore, very probably that V22-227 is Pliocene based on foraminiferal dating. Palagonite dating has yielded an age of about 4 my (3.5 to 5.3 my) for this sample. This Pliocene date supports the results obtained

by Saito, and others, (1966).

Sample RC8-D9, from the Muir Seamount in the Atlantic Ocean is shown on Plate 25. It consists of sample of palagonitized basalt coated with manganese. Large 10 mm diameter pigeonite crystals are included in the palagonite. The age of the sample is 2 my (figure 10). During the Pliocene the Muir Seamount erupted. Sea-water reacted with the basaltic glasses on the seamount and formed palagonite crusts which were covered by layers of manganite. The mineralogy and configuration of the alteration materials in the Muir Seamount samples are similar to those samples from the South Pacific. The hydration rates of all these samples are relatively constant since bottom water temperatures do not fluctuate to any great extent in the major oceans.

As with most dating methods this tool is limited by a percentage of possible error both in sampling and in laboratory measuring. The actual size of the sample is a limiting factor in age determination since age is determined by measuring the radius of alteration material. If a sample of only 2 mm were available then the maximum date obtained could only be about 2 my. The palagonite dating method is best used when both palagonite and some portion of the unaltered sideromelane is available in the same sample. It is also advantageous to have a layer of manganese between the palagonite and the sea-water so that the original thickness of palagonite is preserved without any mechanical erosion. All samples studied correspond to these prerequisites.

Table 8

Sample	$R_p = (N-2)Q/T$ Rate Formula	$R_p = NQ/3T$	$R_p = NQ/T$
A150-RD8	286 years/u		
T = 12 MY	3.49u/1,000 years	1.16u/1,000yrs.	3.5u/1,000yrs.
T = 15 MY	358.2 yrs/u 2.79u/1,000yrs	0.92u/1,000yrs.	2.8u/1,000yrs.
T = 18 MY	429.6 yrs/u 2.33u/1,000yrs	0.78u/1,000yrs.	2.33u/1,000yrs.
Salt H ₂ O Temp. 0-10°C			
Mean rate	2.91u/1,000yrs.	0.97u/1,000yrs.	2.92u/1,000yrs.
Lake Motosu Mt. Fuji Japan Fresh H ₂ O Temp. 17°C	7.26u/1,000yrs.	3.67yrs/u 2.62u/1,000yrs.	7.86u/1,000yrs.
Explanation of Rate formula	Rate formula for time greater than 10 ⁶ years.	Rate formula for 1st stage of palagonitization	Rate formula for remaining stages of palagoniti- zation

Hydration Rate for A150-RD8 $[\sum R_h = (N+2)Q/T] =$
356+71 years/u

Hydration rate for Japan = 110 years/u 17°C

FIGURE 8
HYDRATION CURVES FOR
OBSIDIAN AND SIDEROMELANE

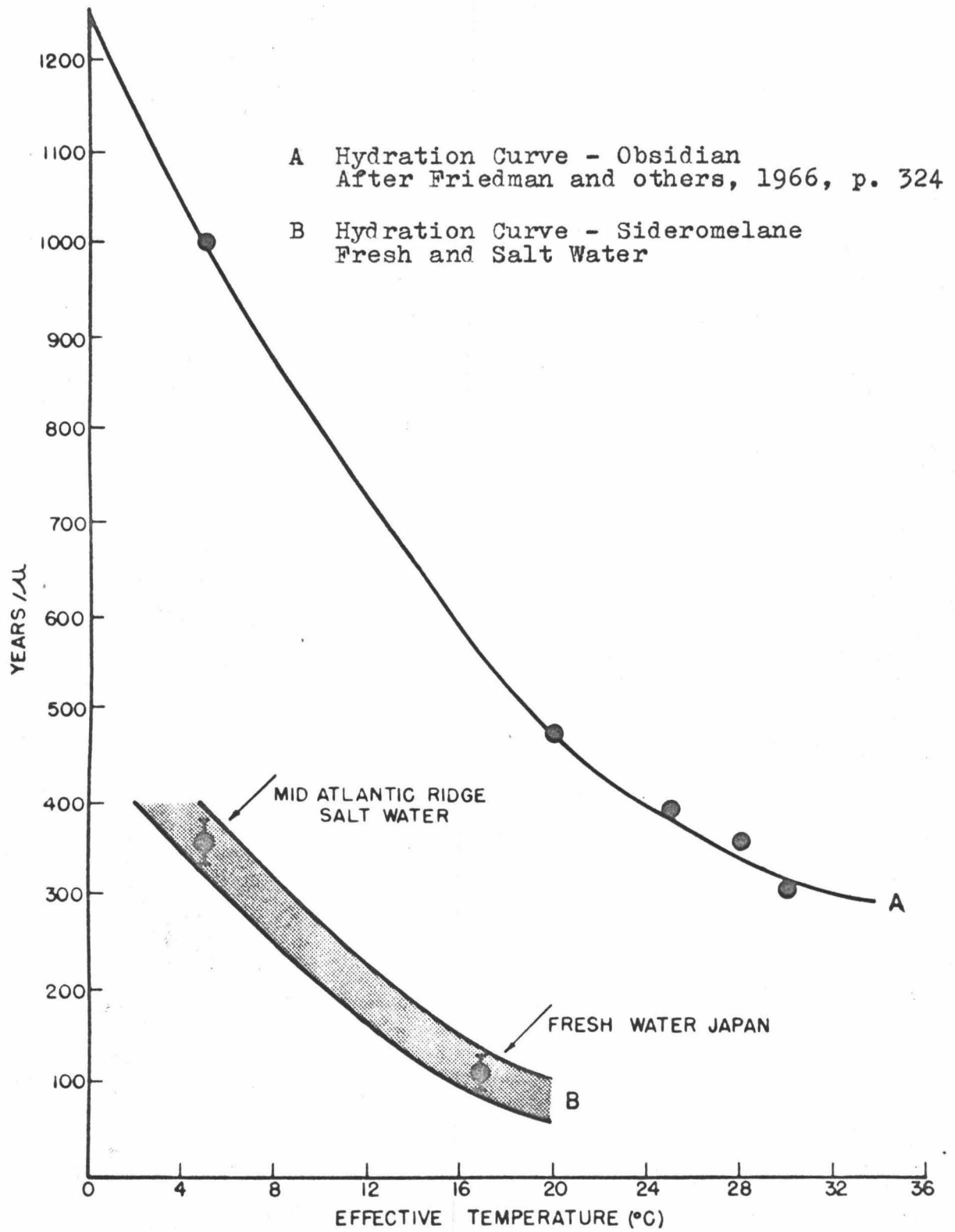


FIGURE 9
 Σ RATE OF PALAGONITIZATION
 FOR N NUMBER OF BANDS IN FRESH AND SALT WATER
 $\Sigma R_p = (N-2)Q/T$ RATE = 2.91 - 0.58 μ / 1000 YEARS

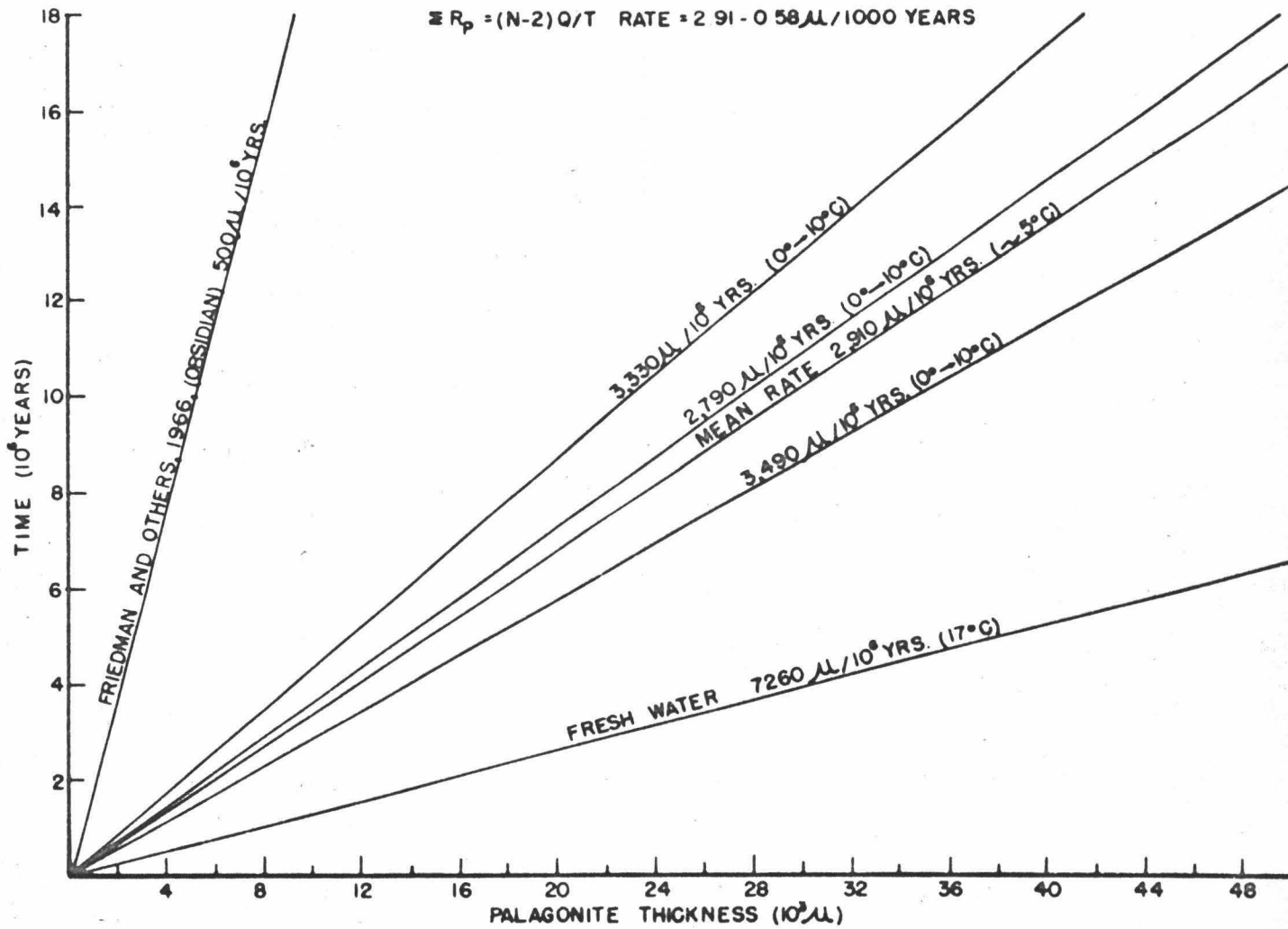
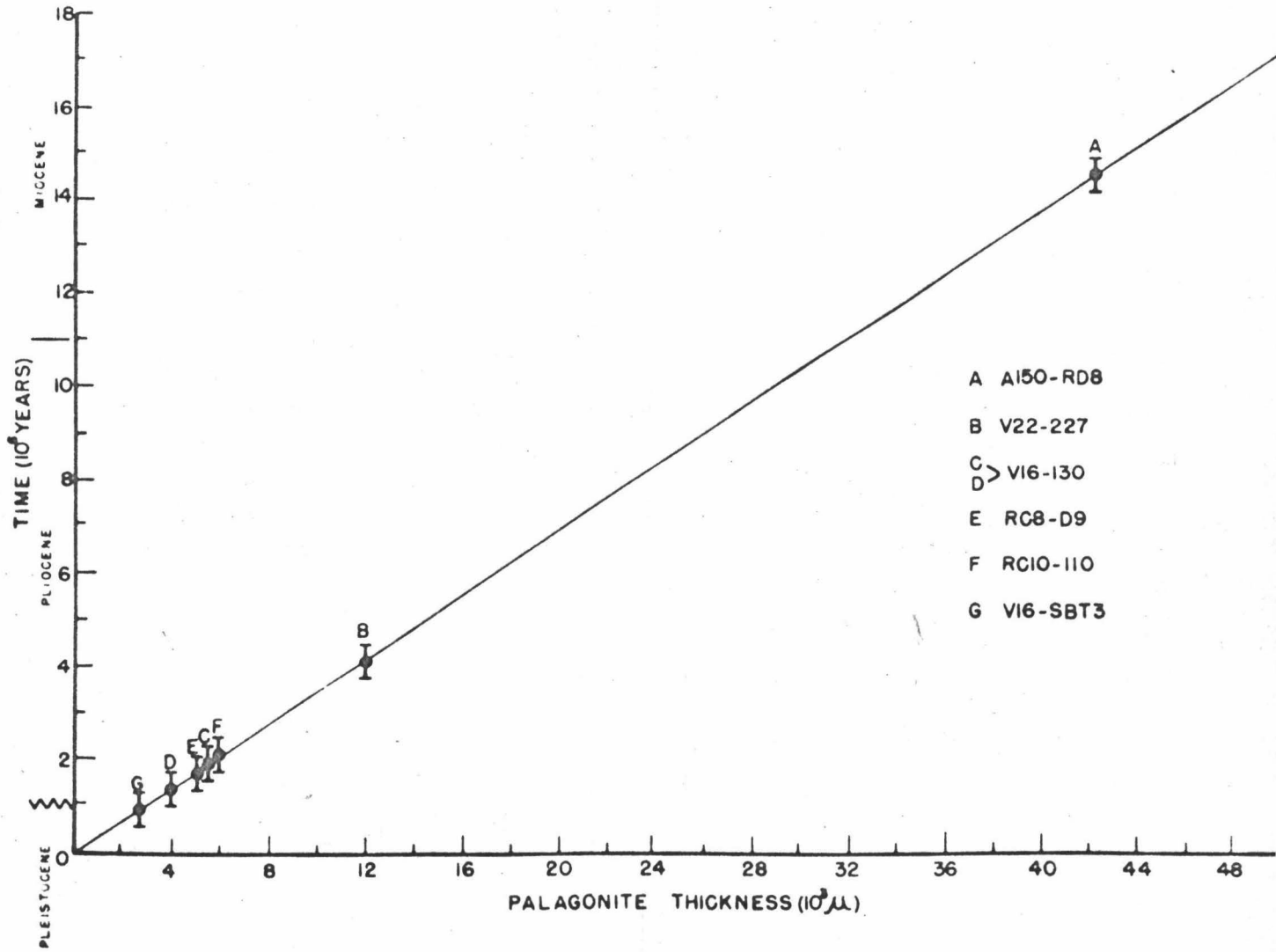


FIGURE 10
 DATES OF VOLCANIC SAMPLES
 FROM THE ATLANTIC AND PACIFIC OCEANS



A traverse of a portion of a thinsection of V22-227 was made from a fracture located in palagonite to the sideromelane border. (Figure 11). The palagonite shows differential mineralization with limonite in the first 135 u. The oldest palagonite borders the fracture, and the youngest is located at the solid solution border. Mean alteration rates are used (Table 8) (0.97 u/1,000 years for the first 50 u and 2.92 u/1,000 years for the remaining palagonite). Based upon these rates, about 195×10^3 years ago the V22-227 sample fractured as shown in the diagram. The first 50 u of palagonite took about 50,850 years to form. A total of 430 u of palagonite formed in about 177,340 years. Since fracturing, 135 u of palagonite have partially crystallized out some limonite (the limonite is amorphous and is intermixed in the remaining palagonite). It would take about 400,000 years longer for the remaining portion of the palagonite to precipitate out an equal portion of limonite through its remaining 280 u length. This is a rate of about 1 u/1,500 years for enough limonite to give the palagonite a distinctive yellow color. It would take substantially longer for all of the palagonite to alter to limonite, smectites and zeolites. The first 135u of palagonite are about 3 times more hydrated than the palagonite which is about 400 u deep into the sample (assuming a constant rate of hydration, the thickness of the limonite rich palagonite is about one third of the entire palagonite thickness).

LINEAR SCAN OF A PHOTOGRAPHIC THINSECTION OF V22-227

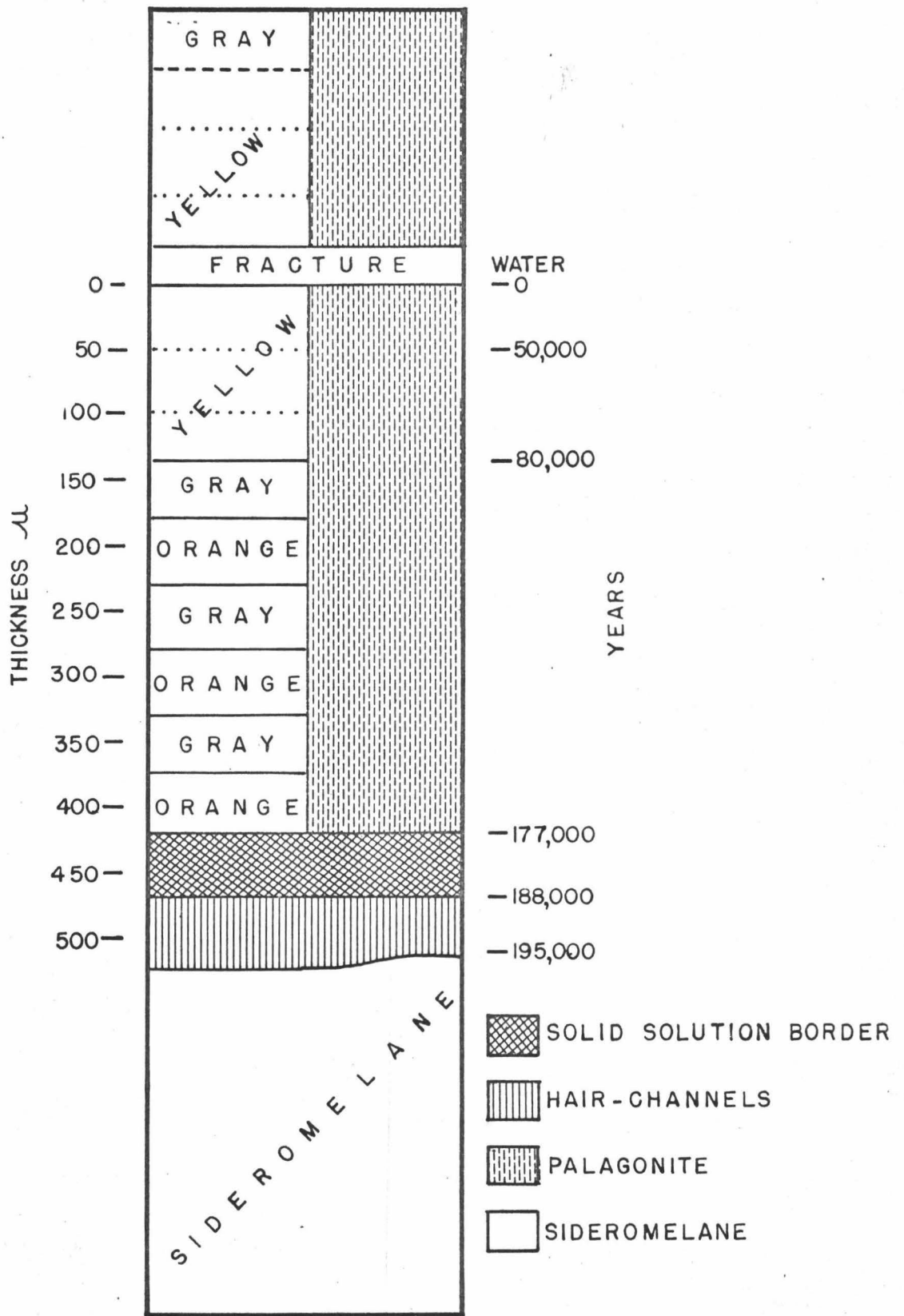
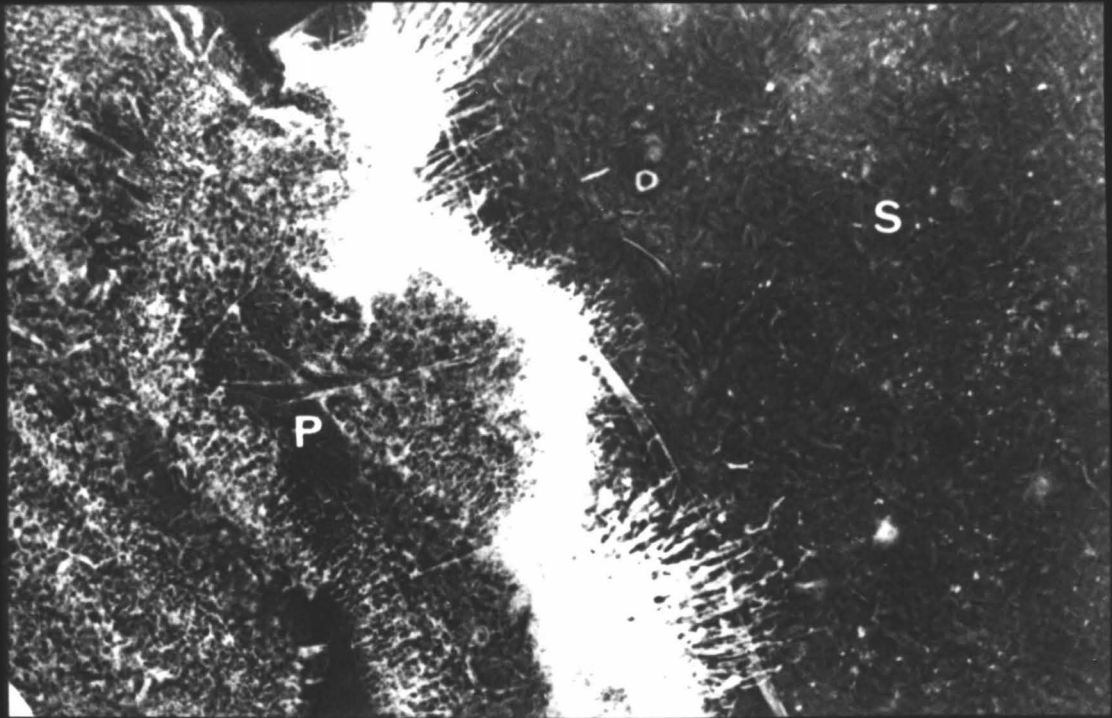


FIGURE 11

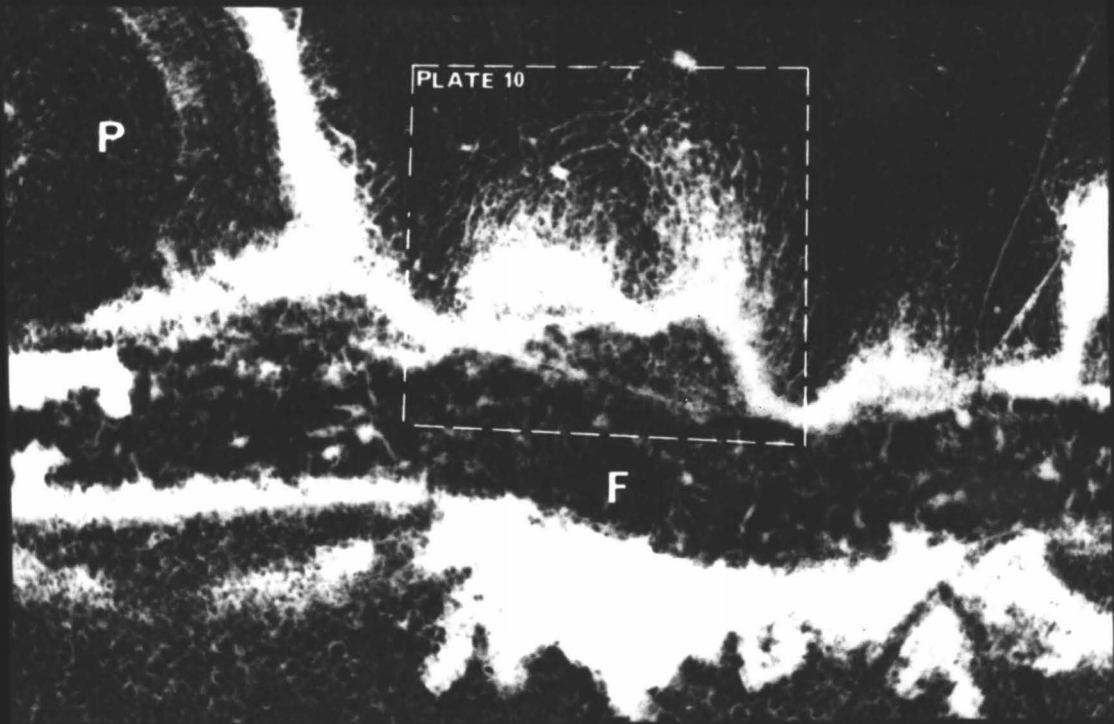
Plate 26

- A. Sideromelane (S) and palagonite (P) are separated by hair-channels and a solid solution border. Remenent hair-channels can be observed in the palagonite bands. Sample V22-227, plane polarized light. Scale as shown.
- B. Hair-channels are growing in sideromelane. A large fracture (F) is filled with zeolite fragments and smectites. Palagonite (P) is also present. The central portion of the photograph is more detailed in plate 10. Sample V22-227, plane polarized light. Scale as shown.



A

100 μ



B

100 μ

PLATE 26

A similar configuration for palagonite alteration is shown in plate 26. The upper photograph shows the unaltered sideromelane on the right and bands of palagonite on the left side. A hair-channel sector and solid-solution border separate the sideromelane from the palagonite. Fossil hair-channels are readily observed in the palagonite banding. In the lower photograph, a fracture is filled with zeolite fragments and smectites. Hair-channels grow perpendicular toward the glass and then curve and interconnect with each other. A more recent small fracture in the upper right portion of the photograph shows a typical orthogonal connection with the larger fracture trending east-west. Typical 50 μ palagonite banding can be seen in the upper left portion of the photograph. Plate 27 shows this banding more clearly. In the central portion of the upper photograph the palagonite bands grow around a plagioclase feldspar lath. The feldspar remains unaltered. The bottom photograph shows the hair-channel sector in more detail. The lower portion of this photograph extends into the solid-solution border zone. As previously mentioned, the hair-channels are the first to form during palagonitization. A fracture extending across a portion of sideromelane has these hair-channels reaching into the glass on either side of the fracture as shown in Figure A of plate 28. The thickness of the hair-channel sector on either side of the fracture is similar (about 50 μ). The rate of palagonite growth on either side of the fracture is therefore equivalent to the rate of

palagonite growth for the typical 50 u bands. The bottom photograph shows the typical cellular configurations which exist during palagonitization. The center of the photograph contains fresh glass. Palagonite alterations circumscribe the glass and grow inward towards its center.

Contribution of Palagonites in Marine Sediments

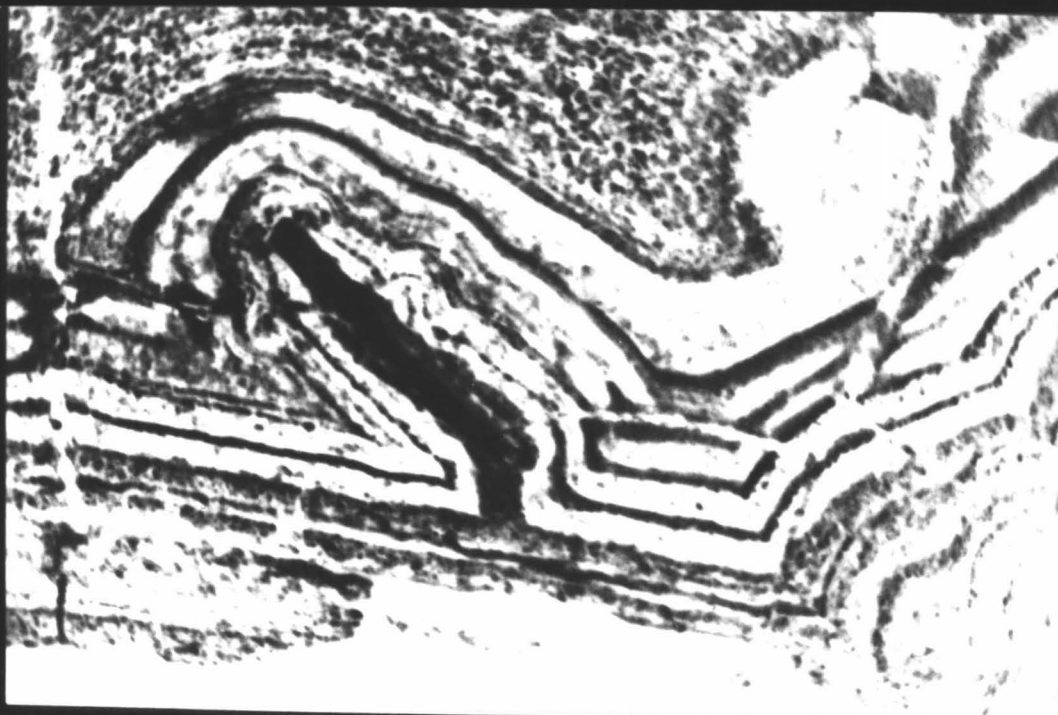
Thus far the concern has been on the chemistry, physics and rate of palagonite formation. The significance of palagonite in deep-sea sediments as well as the possible uses for the new dating tool are also of great importance.

Palagonite Dating Tool

In recent years sediment dating has become of more and more concern because it provides data which deals with such theories as Ocean Floor Spreading, the origin of manganese nodules and the overall rate of sediment accumulation in the ocean basins. Various models have been proposed to explain the origin of manganese nodules. One group suggests that the constituents of manganese nodules² are derived from continental weathering and are precipitated by an inorganic pelagic process. Another group shows that manganese nodules are the products of submarine volcanic eruptives interacting with sea-water. Morgenstein and Felsher (in preparation) have suggested that the process of terrigenous weathering may be combined with the process of oceanic weathering to account for manganese nodule development. We contend that manganese is derived as a product of continental weathering, and then combines with ferruginous

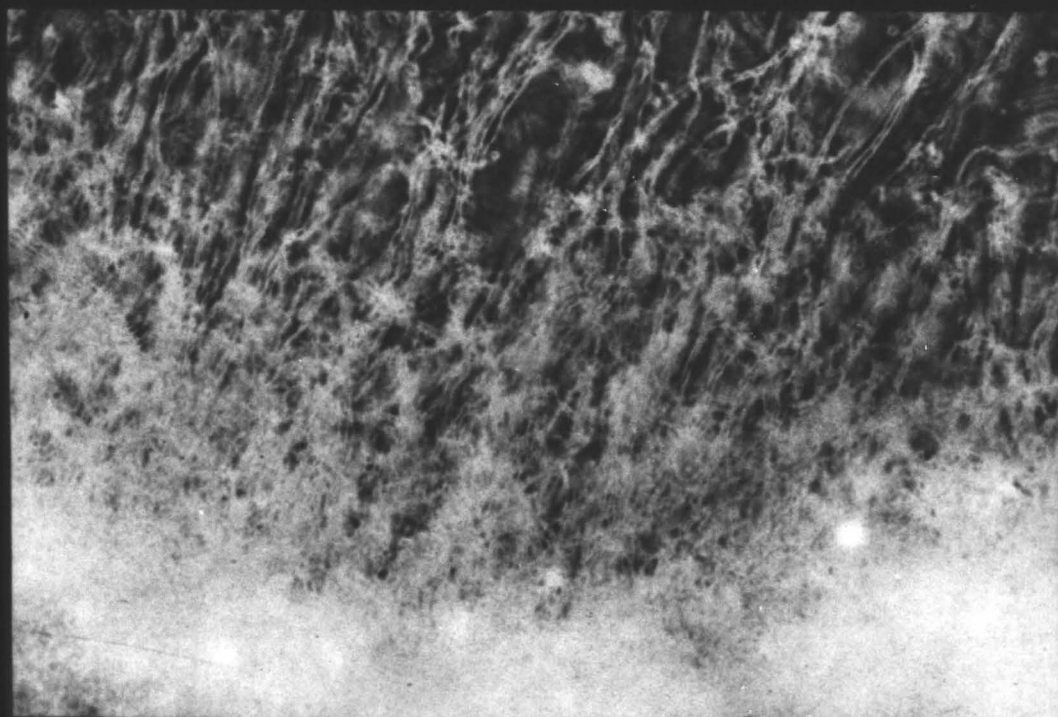
Plate 27

- A. Palagonite banding around a feldspar phenocryst. The bands average 50 μ in width. Sample V16-130, plane polarized light. Scale as shown.
- B. Hair-channels in sideromelane. The bottom of the photograph is the solid solution border. Sample V22-227, plane polarized light. Scale as shown.



A

200 μ



B

25 μ

PLATE 27

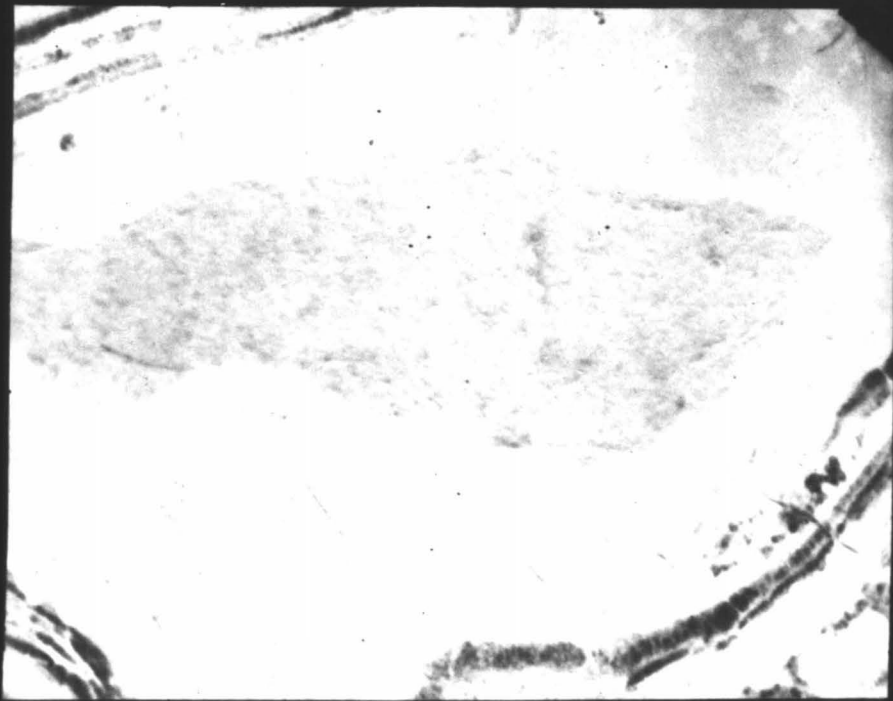
Plate 28

- A. Sideromelane cell with palagonite alterations. A fracture with hair-channels extends across the cell. Sample V25-12-T3, crossed nicols, gypsum plate. Scale as shown.
- B. Typical cellular configuration with a sideromelane center and palagonite circumscribing the glass. Sample V25-13-T3, crossed nicols, gypsum plate. Scale as shown.



A

100 μ



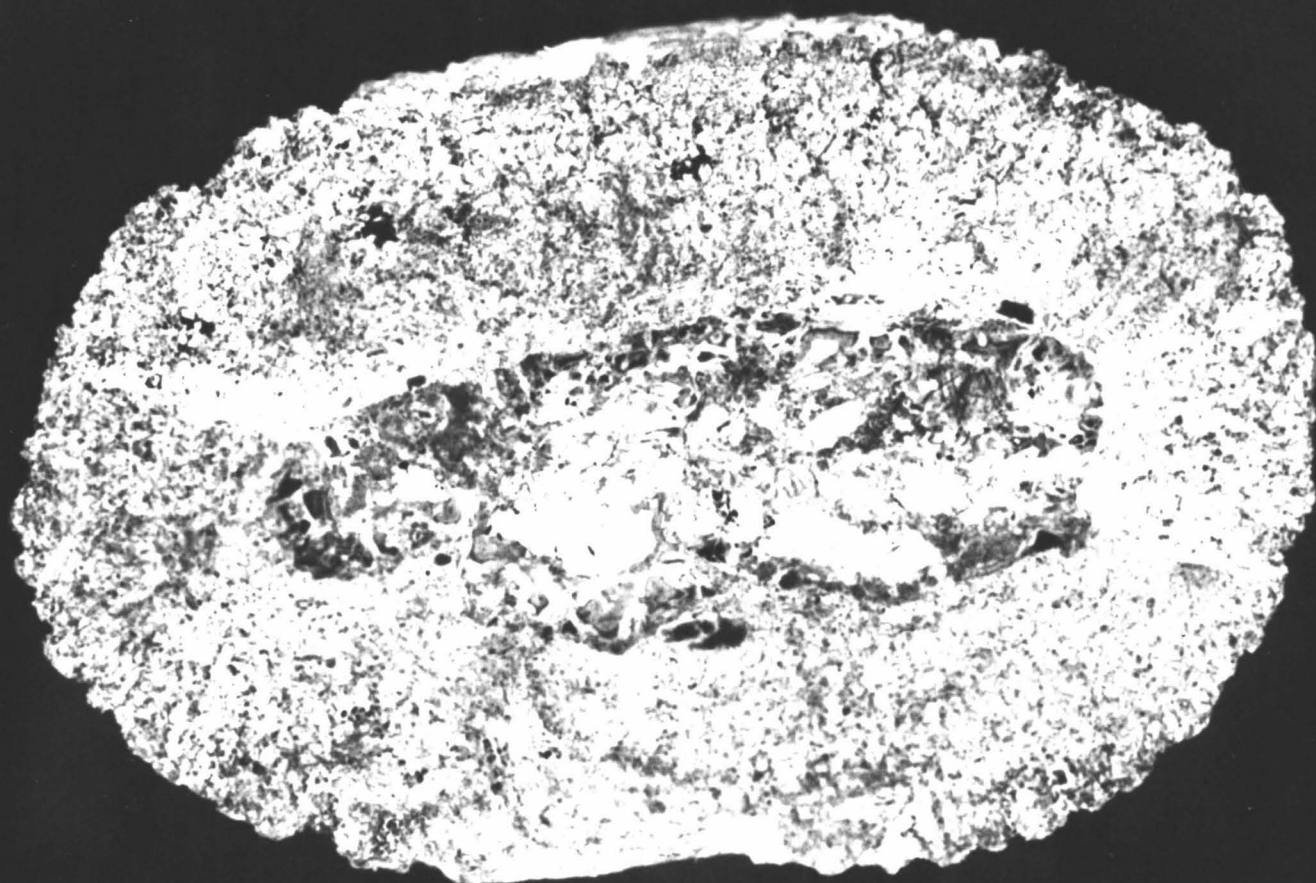
B

100 μ

PLATE 28

and ferromanganiferous complexes produced by the diagenetic alteration of deep-sea palagonites to form manganese nodules. We use the palagonite dating tool, as defined in this paper, to find the ages of deep-sea manganese nodules. The manganese nodules studied, accreted at a rate of 1.7 to 8.7 $\mu/10^3$ years. The rate of accretion decreased with time. This decreasing rate supports the concept that iron catalysts, derived through the solution of palagonite are responsible for accreting manganese nodules. During palagonitization, iron oxides are crystallized out of the palagonite "gel", and then react with manganese ions situated in sea-water, the resultant combination is a manganese nodule. After a period of time, however, all of the iron is used up and the rate of manganese nodule accretion decreases. Plate 29 shows a typical manganese nodule with a sideromelane and palagonite center.

Microprobe analyses were performed on a similar sample (V16-130) from the same locality, in the South Pacific. (Plate 30). A photograph taken of a thin section of this sample shows the manganese-palagonite border. Iron and calcium are concentrated with the manganese of the nodule. There is a higher concentration of silica in the palagonite. A sharp boundary is observed between the manganese and the palagonite in the calcium and manganese displays, indicating that these elements are not derived from the palagonite. Iron and silica displays show a more gradual change in the concentration across the boundary. These elements are derived from the palagonite



25mm

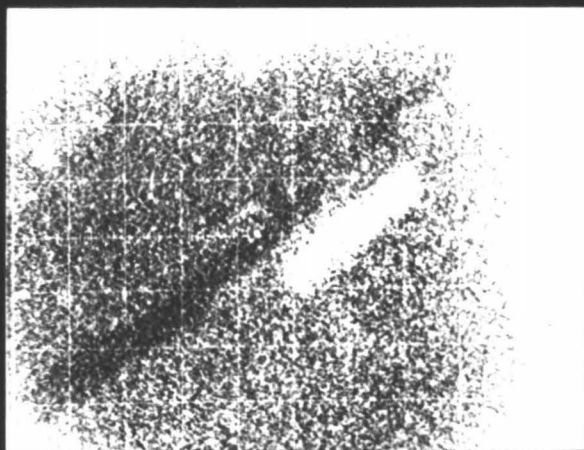
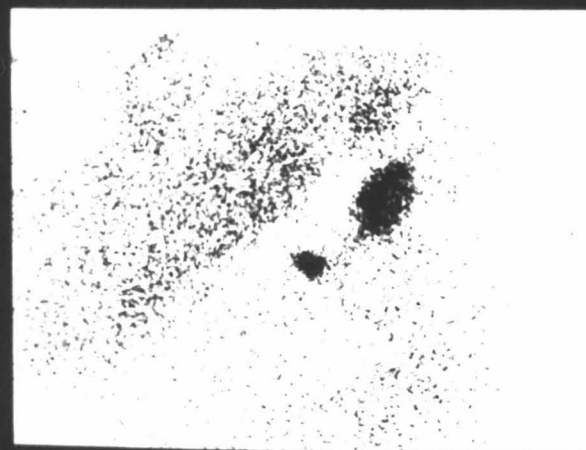
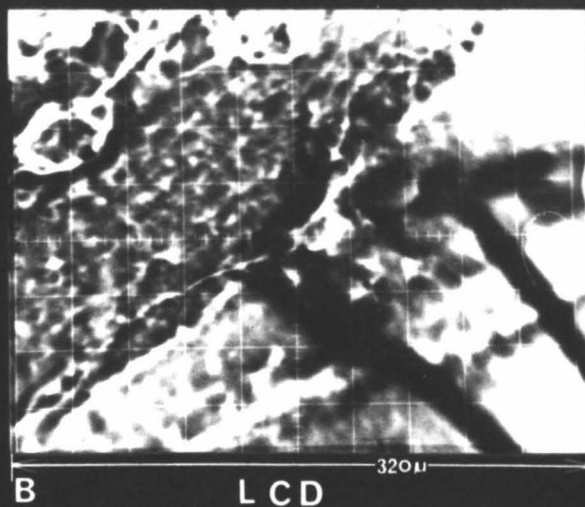
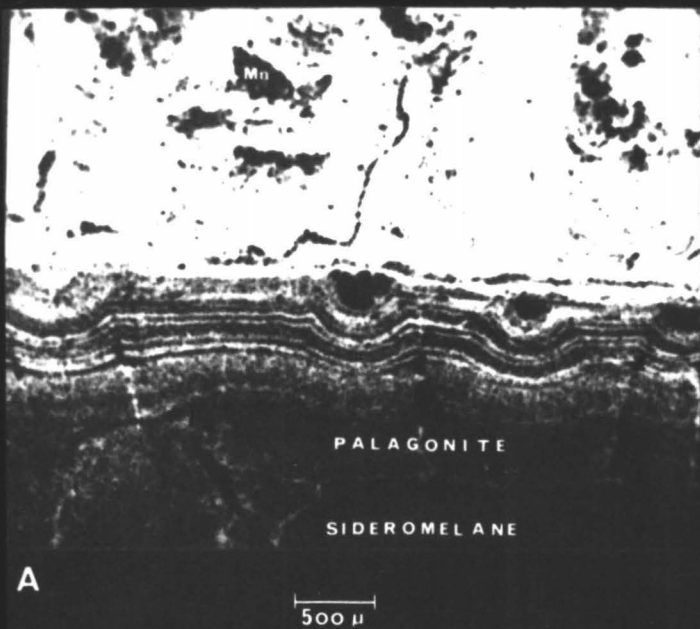
P L A T E 29

Plate 29

Manganese nodules with sideromelane and palagonite center. The sideromelane is in a cellular configuration with palagonite alterations around the center of the cells. Sample V16-130. Scale as shown.

Plate 30

- A. Photograph of a portion of a manganese nodule showing manganese (M), palagonite banding (P) and sideromelane (S). Sample V16-130, plane polarized light. Scale as shown.
- B. Line current display of the same sample showing manganese and palagonite sections. All electron beam scanning photographs in the plate are of 400 diameter magnification and are 320 u along the bottom edge.
- C. Manganese display showing the distribution of this element.
- D. Silica display showing a relatively even distribution of silica in the palagonite and the manganese portion of the nodule.
- E. Calcium display shows a higher concentration of calcium in the manganese portion of the nodule than in the palagonite. The high concentration of calcium in the palagonite is a feldspar lath.
- F. Iron display depicts a sharp boundary line between the manganese and the palagonite. It is however, evenly distributed in both portions of the nodule.



and are deposited in the manganese shell. The above observations support the findings of Morgenstein and Felsher (in preparation) and suggest that iron complexes are derived through the process of palagonite solution and are added to the manganese ions of sea-water (at the sediment-water interface) to accrete manganese nodules.

Authigenic Mineralization of Deep-sea Palagonites

Palagonite is an intermediate product between the deposits of volcanic pyroclastics and the authigenic mineral suites observed in oceanic sediments. Figure 12 shows the relative importance of palagonite to the composition of deep-sea sediments. Most authigenic deep-sea minerals are derived from the solution of palagonite. Feldspars and pyroxenes enter the sediment as residual products from palagonite solution.

Morgenstein (1967) published a review of the alteration stages of mafic pyroclastics in core RC10-110, from the Society Ridge, South Pacific. The following five stages of authigenic mineralization were recognized:

- | | | | |
|-----|----------------|--------------------|---|
| (1) | Basaltic glass | <u>hydration</u> → | Palagonite |
| (2) | Palagonite | <u>hydration</u> → | Montmorillonite + goethite |
| (3) | Palagonite | <u>hydration</u> → | Harmotome + Montmorillonite
+ goethite |
| (4) | Goethite | <u>hydration</u> → | Limonite |
| (5) | Palagonite | <u>hydration</u> → | Harmotome + Montmorillonite
+ Limonite |

Phillipsite was also encountered as a product of palagonite hydration. Essentially, the phillipsite was reported

(Morgenstein, 1967) in sediments which are younger than the alteration layers. A general decrease in harmotome was noted with an increase in phillipsite, although intermediate products of both (eg. calcium-rich-harmotome and Ba-rich-phillipsite) were noted to occur together. These associations demonstrate a continued harmotome-phillipsite series in which the Ba-rich zeolite (harmotome) is produced directly as a consequence of palagonite solution, and phillipsite is produced by the reaction of harmotome with sea-water. Dietrich (1957, p. 221) demonstrates that the oceanic crust contains a higher concentration of barium than does sea-water. It is well recognized that zeolites are capable of ion-exchange, and that an exchange of Ca for Ba would be possible in the hydrous environment of the ocean bottom. Both Ca and Ba are similar in atomic size, further supporting the possibility of an exchange. Microprobe analysis (plate 31) shows an intermediate zeolite which contains both Ba and Ca. It is not known if this zeolite is Ca-rich-harmotome or a Ba-rich-phillipsite. The presence of both Ba and Ca in the same structure is, however, indicative of a continuous series between harmotome and phillipsite.

A similar relationship was also shown to exist between goethite and limonite. Since authigenic mineralization is accomplished by the process of hydration it follows that with increased hydration of palagonite there is increased mobility of ions in the complex structure. Once the ionic-mobility

FIGURE 12

The Contribution of Vulcanism to Deep-sea Sediments

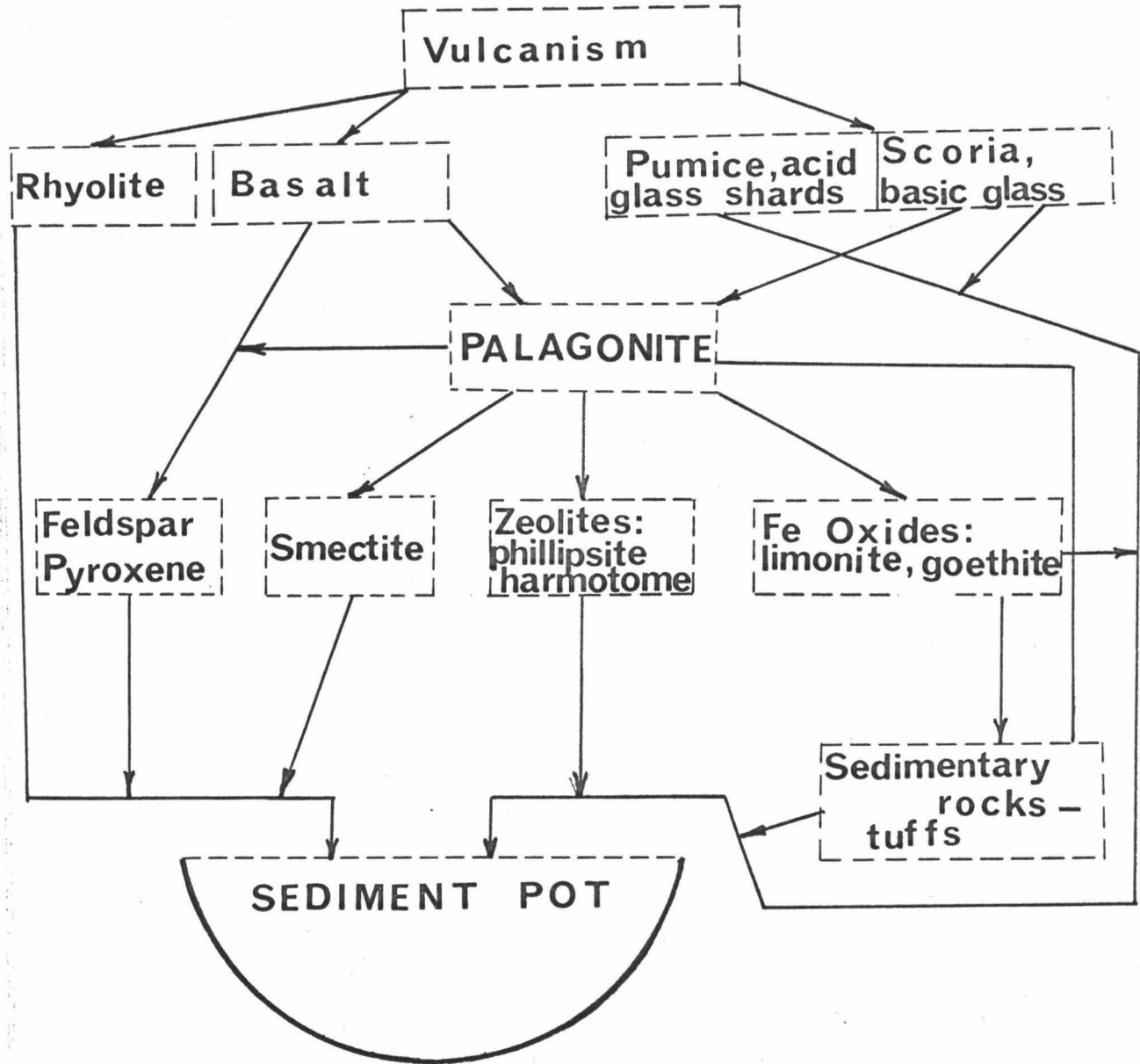
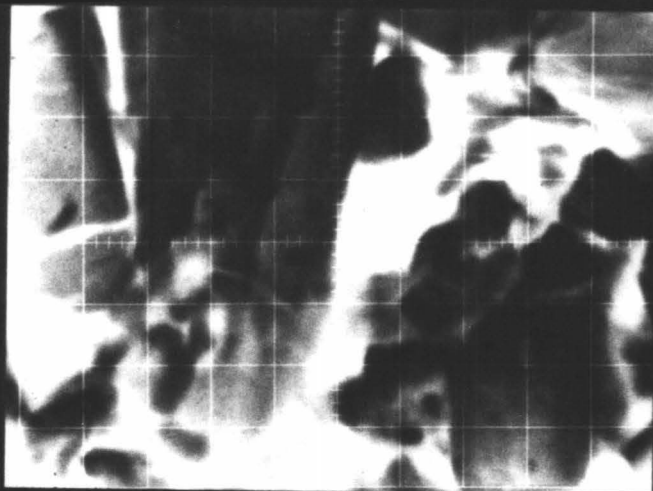


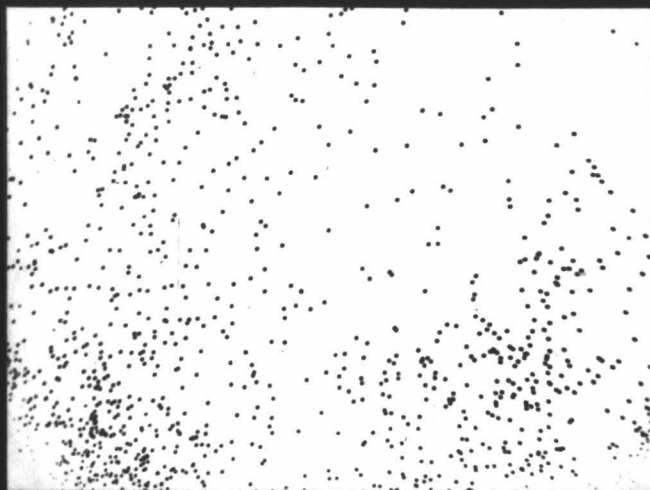
Plate 31

- A. Line current display of zeolite crystals in Sample RC10-110. Bottom length of the photograph is 320 u.
- B. Calcium display showing the concentration of this element in the zeolite structure.
- C. Barium display depicts the concentration of this element in the same zeolite structure.



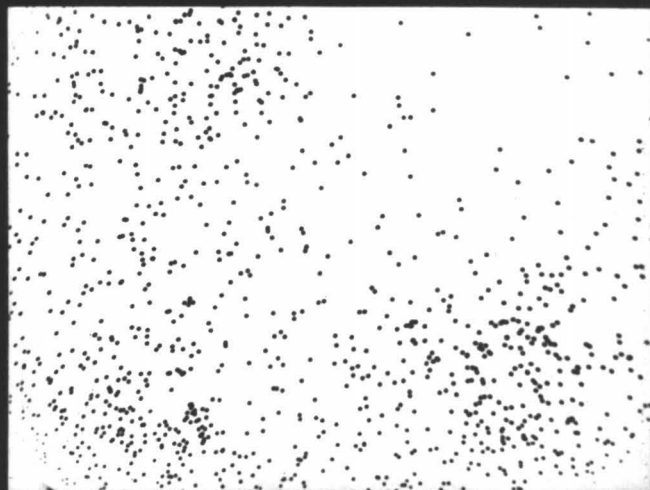
A

LCD



B

Ca_{Kα}



C

Ba_{Kα}

PLATE 31

is great enough goethite crystallizes from the palagonite. Goethite is formed because it is well crystallized and it contains a minimum of attached water molecules. As hydration proceeds the goethite accepts a larger quantity of interstitial water and inverts to the less crystallized state of limonite.

Other authigenic minerals, mostly of the zeolite clan, are also produced during diagenesis. A fine example, previously mentioned, is found in core V22-119, located on the Argentine Seamount, in the South Atlantic. Here clinoptiolite is recognized as a major zeolite associated with phillipsite crystals and palagonite in a turbidite deposit. Clinoptiolite has been reported by Biscaye (1964) and others from deep-sea sediments, however, it is not recognized as a major deep-sea authigenic mineral due to its limited dispersion. The exact origin of this mineral is still uncertain. It probably is a product from the solution of palagonite, but the reason for its crystallization in place of the more commonly occurring zeolites still remains obscure and serves as a topic for future work.

Conclusions

1. During the alteration of basaltic glass to palagonite Na, Mg, Si, Mn, and Ca are lost; K, Ti, Fe and O are gained in the alteration product (palagonite). Aluminum remains relatively constant. These results support the findings of Moore (1966).
2. The chemistry of palagonite formation is relatively constant in the Atlantic and Pacific Oceans.
3. The largest chemical variations occurred between terrestrial and oceanic palagonites. The major difference between oceanic and terrigenous palagonites is the behavior of potassium. Potassium is usually depleted in the alteration material (palagonite) during terrigenous weathering; whereas, it is enriched during halmyrolysis (oceanic weathering). The significant differences in oceanic and terrestrial palagonite chemistry suggests that metamorphosed geosynclinal piles can be shown to have been either oceanic or terrestrial sediments based upon their concentration of potassium.
4. Palagonitization is a process of hydration. Palagonite commonly contains 2 to 3 times more H_2O^- and about 4 to 10 times more H_2O^+ than sideromelane (basaltic glass).
5. The greater the hydration in palagonite, the greater the degree of authigenic mineralization. Authigenic minerals present in deep-sea sediments which are derived from palagonite solution are: Limonite, goethite, smectites,

manganite, harmotome, phillipsite, clinoptilolite and intermediate zeolites of the phillipsite group.

6. Sea-water enters the basaltic glass (sideromelane) through hair-channels which average 50 μ in length. As the hair-channels become more dense with increased hydration, they form a 50 μ thick immobile product layer (solid-solution border). The solid-solution border eventually hydrates to a palagonite band which is 50 μ thick. Palagonitization proceeds as the hair-channels extend into the sideromelane.
7. Most palagonite forms during diagenesis, although there is some syngenetic palagonitization. Palagonites formed during diagenesis have typical 50 μ bands which are representative of hair-channel sector and solid solution border configurations. Palagonites which form syngenetically do not show typical 50 μ banding. Syngenetic palagonitization is too rapid to form by a stage reaction. When basaltic lava enters sea-water there can be an immediate hydration reaction (either during cooling or upon initial contact depending upon the temperature and pressure at which the lava ejects). The result of syngenetic hydration is palagonite rims on outer surfaces of basaltic flows.
8. Sea-water diffusion into mafic volcanic glass does not slow down as the hydrated region (palagonite) becomes thicker. As diffusion proceeds there is greater mobility of reactants due to increased kinetic effects shown by a higher sea-water concentration in the alteration material.

The rate of palagonitization is dependent solely on the initial rate of glass hydration (i.e. the first stage of hair-channel development). Friedman, and others (1966) diffusion constant for a quadratic rate formula cannot be applied to palagonite formation. The rate formula used by Moore (1966) is also not applicable because it uses Friedman's diffusion constant. The use of this constant is based on the incorrect concept that water diffusion in glass slows down as the immobile product layer becomes thicker.

9. Rate formulas for palagonite formation are derived here by studying the geometry of the hair-channel sector, the solid-solution border and the palagonite bands. The average total rate formula for palagonitization is:

$$R_p = (N-2)Q/T$$

where: R_p is the rate of palagonitization, N is the number of palagonite bands, Q is the thickness of each band, and T is the age in years. For the first 50 μ the rate formula is:

$$R_p = NQ/3T$$

For the second and subsequent palagonite bands the rate formula is: $R_p = NQ/T$

When dealing with time in millions of years the expression for the averaged total rate approaches the linear rate

$R_p = NQ/T$. The rate formula for sideromelane hydration is:

$$\sum R_h = (N+2)Q/T$$

where: R_h is equal to the total rate of hydration.

10. During diagenesis the first 50 u of oceanic palagonite forms at an average rate of 0.97 ± 0.19 u/1,000 years. The first 50 u of fresh water palagonite to form during diagenesis does so at the rate of 2.62 u/1,000 years. The average rate of palagonitization after the first 50 u have formed (and including the first 50 u) is: 2.91 \pm 0.58 u/1,000 years. For fresh water palagonite the rate is: 7.26 u/1,000 years.
11. Manganese nodules dated by the palagonite hydration method show that the rate of manganese accretion decreases with time. An iron catalyst supplied through the process of palagonite solution is probably responsible for the accretion of an appreciable amount of the submarine manganese nodules. The rate of manganese accretion observed is between 1.7 and 8.7 u/10³ years. This rate is dependent upon the rate of an iron catalyst evolution into the sediment and therefore, is dependent on the rate of palagonitization.
12. Both diagenetic and syngenetic fracturing exist in sideromelane. Fracture assemblages produced are mostly tensile displacements which are similar to those described by Lachenbruch (1962) for mud cracks. Shear fractures occur during diagenesis and are produced by volume expansion due to the addition of sea-water into the alteration material. Micro-channel fractures (hair-channels) are also produced during diagenesis. Diagenetic

and syngenetic fracturing provides conduits for sea-water entering into sideromelane. Since diagenetic fracturing is dependent upon stresses produced by hydration there is a geometric increase of fracturing as time increases. This mode of fracturing provides increased conduits for sea-water and thus is responsible for an increased volume of alteration material during time. Conchoidal contraction fractures are produced by differential contraction of the glass matrix and its phenocrysts during the quenching of a basaltic magma.

13. Well crystallized and exsolved palagioclase feldspar phenocrysts are not affected by hydration reactions and remain fresh throughout the process of palagonitization. Pyroxene laths such as pigeonite also remain fresh during submarine weathering.

Acknowledgments

This study was performed under the direction and guidance of Murray Felsher, under whose supervision this thesis was written. Samples used for this study came from Lamont-Doherty Geological Observatory. Support for sampling came from the National Science Foundation grant: NSF-GA-1193 and from the Office of Naval Research: TO-4 (N00014-67-A-0108-0004). Thanks are extended to Drs. I. Miyrashero and F. Shido of the Lamont Observatory for wet chemical analysis and to Mr. E. Martin of Philips Electronics for assistance during microprobe analysis. Dr. J. Hays of the Lamont Laboratories provided support and helpful discussions during this investigation. Laura Morgenstein helped in manuscript preparation and drafting. Thanks are also extended to Dr. W. Dean of Syracuse University Geology Department for helpful discussions concerning the geochemistry of sediments and for reading the manuscript.

References

- Arrhenius, G.O.S., 1963, Pelagic sediments. In: M. N. Hill (General Editor), The Sea, Ideas and Observations on Progress in the Study of the Seas: Interscience, New York, N. Y. V. 3, p. 655-718.
- Barnes, V.E. and Russell, R.V., 1966, Devitrification of glass around collapsed bubbles in tektites: *Geochem. et Cosmochim. Acta*, V. 30, p. 143-152.
- Bender, M.L. Ku, Teh-Lung, Broecker, W.S., 1966, Manganese Nodules: their evolution: *Science*, V. 151 (3708), P. 325-328.
- Biscaye, P.E., 1964, Mineralogy and Sedimentation of the Deep-sea Sediment fine Fraction in the Atlantic Ocean and Adjacent Seas and Oceans: Thesis, Yale Univ., New Haven, Conn., pp.189.
- Bonatti, E., 1965, Palagonite, Hyaloclastites and Alteration of Volcanic Glass in the Ocean: *Bull. Volcanologique*, V. 28, p. 1-15.
- Briggs, R. P., 1959, Laterization in east-central Puerto Rico: *Trans. Caribbean Geol. Conf.*, 2nd, Mayaguez, P.R., 1959, p. 103-119.
- Denaeyer, M.E., 1963, Les hyaloclastites de la rive nord du lac Kivu (Congo): *Bull. Volcanologique*, V. 25, p. 201-216.

- Dietrich, G., 1957, General Oceanography. Wiley, New York, N.Y.
p. 221.
- Friedman, I., Smith, R.L., and Long, W.D., 1966, Hydration of
Natural Glass and Formation of Perlite:
Geo. Soc. American Bull., V. 77, p. 323-328.
- Friedman, I., and Evans, C., 1968, Obsidian Dating Revisited:
Science, V. 162 (3855) p. 813-814.
- Fuller, R.E., 1931, The aqueous chilling of basaltic lava on
the Columbia River Plateau: Amer. Jour. of
Science, V. 21, p.281-300.
- Fuller, R.E., 1932, Concerning basaltic glass. Amer. Mineral.,V.
17:104-107.
- Griffith, A.A., 1924, The Theory of Rupture: Proc. (1st)
Intern Congr. Appl. Mech., p. 55-63
- Iijima, A. and Harada, K., 1969, Authigenic zeolites in
zeolitic palagonite tuffs on Oahu, Hawaii:
Amer. Mineral., V. 54, p. 182-197.
- Jost, 1952, Diffusion in Solids, Liquids and Gases: Acad. Press,
New York, N.Y. 558 p.
- Lachenbruch, 1962, Mechanics of Thermal Contraction Cracks and
Ice-Wedge Polygons in Permafrost: Geo. Soc.
America Spec. Paper, 70, p. 40-44.
- Marshall, B.R., 1961, Devitrification on natural glass: Geol.
Soc. America Bull. V. 72, p. 1493-1520.
- Meighan, C.W., Foote, L.J., and Aiello, P.V., 1968, Obsidian
Dating in West Mexican Archeology: Science
V. 160 (3832), p. 1069-1075.

Michels, J.W., 1967, Archeology and Dating by Hydration of
Obsidian: Science, V. 158 (3798) p. 211-214.

Moore, J.G., 1966, Rate of Palagonitization of Submarine Basalt
Adjacent to Hawaii: U.S. Geol. Survey Prof.
Paper, 550 - D, p. 163-171.

Morgenstein, M., 1967, Authigenic Cementation of Scoriaceous
Deep-sea Sediments West of the Society
Ridge, South Pacific: Sedimentology, V. 9,
p. 105-118.

Morgenstein, M. and Felsher, M., (in preparation). The Origin
of Manganese Nodules: A Combined Theory with
Special Reference to Palagonitization.

Murray, J. and Renard, A.F., 1891, Report on Deep-sea deposits
based on specimens collected during the
voyage of H.M.S. "Challenger" in the years
1873 and 1876: "Challenger" Rept. Govt.
Printer, London, 525 pp.

Nayudu, Y.R., 1962, A New Hypothesis for the Origin of Guyots
and Seamount Terraces: Crust of the Pacific
Basin, Geophys. Monograph No. 6, p. 171-180.

Neal, J. T., 1966, Polygonal Sandstone Features in Boundary
Bottle Anticline Area, San Juan County, Utah:
Discussion, Geo. Soc. American, Bull., V.77:
p. 1327-1330.

Nasedkin, V.V., 1963, Volatile components of volcanic glasses:
Izdatel'stvo Akademii Nauk SSSR, Moscow,
V. 98 (chap. 4): p. 118-137.

Peacock, M.A., 1926, The Petrology of Iceland, pt. 1, the basic tuffs: R. Soc. Edimburgh Trans. V. 55, P. 51-76.

Ross, C.S., and Smith, R.L., 1955, Water and other volatiles in volcanic glasses: Amer. Miner., V. 40, p. 1071-1089.

Saito, T., Ewing, M., and Burckle, L., 1966, Tertiary Sediment from the Mid-Atlantic Ridge: Science, V. 151, (3714) p. 1075-1079.

Silvestri, C.S., 1963, Proposal for a genetic classification of hyaloclastites: Bull volcanologique, v. 25, p. 315-321.

Tomkins, J.Q., 1966, Polygonal Sandstone Features in Boundary Batle Anticline Area, San Juan County, Utah: Reply: V. 77, p. 1331-1332.

Biographical Data

Name: Maurice E. Morgenstein

Date and Place of Birth: September 3, 1944, Brooklyn, New York

High School: Rhodes High School, New York, New York
Graduated 1962.

College: Queens College, Flushing, New York, B.A., 1967.

Graduate Work: Syracuse University, Syracuse, New York
(Graduate Teaching Assistant)